CR-54619

DEVELOPMENT OF PROTECTIVE COATINGS FOR CHROMIUM-BASE ALLOYS

by

D. N. Williams, R. H. Ernst, C. A. MacMillan,
J. J. English, and E. S. Bartlett

prepared for

NATIONAL AERONAUTICS AND SPACE ADMINISTRATION

Contract NAS 3-7612

R. E. Oldrieve, Project Manager
S. J. Grisaffe, Research Advisor
NASA Lewis Research Center
Cleveland, Ohio 44135

BATTELLE MEMORIAL INSTITUTE

COLUMBUS LABORATORIES

SUMMARY REPORT

on

DEVELOPMENT OF PROTECTIVE COATINGS FOR CHROMIUM-BASE ALLOYS

by

D. N. Williams, R. H. Ernst, C. A. MacMillan,
J. J. English, and E. S Bartlett

prepared for

NATIONAL AERONAUTICS AND SPACE ADMINISTRATION

March 5, 1968

Contract NAS 3-7612

Technical Management
NASA Lewis Research Center
Cleveland, Ohio
R. E. Oldrieve, Project Manager
S. J. Grisaffe, Research Advisor

BATTELLE MEMORIAL INSTITUTE
Columbus Laboratories
505 King Avenue
Columbus, Ohio 43201

DEVELOPMENT OF PROTECTIVE COATINGS FOR CHROMIUM-BASE ALLOYS

by

D. N. Williams, R. H. Ernst, C. A. MacMillan,
J. J. English, and E. S. Bartlett

ABSTRACT

Metallic cladding systems were applied to a chromium 5 weight percent tungsten alloy by gas-pressure bonding. Resistance to oxidation and nitrogen absorption during cyclic oxidation for up to 600 hours at 2100 and 2300 F were measured. Bend properties after oxidation exposures were determined. Multicomponent cladding systems were examined. The outer oxidation resistant layer consisted of 5 to 10 mils of Ni-30 weight percent Cr or of 5 mils of aluminized (5 weight percent) Ni-30 weight percent Cr or Ni-20 weight percent Cr-20 weight percent W. Barrier layers of W, W-25 weight percent Re, W-1 weight percent ThO_2, and Mo, 0.5 to 2.0 mils thick, were placed between the nickel alloy and the chromium alloy to retard interdiffusion. Compatibility layers of platinum or vanadium foil between the nickel-base alloy and the barrier layer were used in some systems. None of the systems provided adequate protection. Embrittlement of the chromium alloy occurred during cyclic oxidation. Embrittlement was apparently due to metallic contamination at 2100 F and to both metallic and nitrogen contamination at 2300 F, it being noted that at 2300 F edge cracking of the clad specimens occurred. Contamination apparently occurred by diffusion of metallic elements through the barrier or cracks in the barrier layer during cyclic oxidation exposure. Diffusion of nickel into the chromium is suspected. Diffusion of chromium into the cladding material, thereby increasing the tungsten content of the chromium alloy, may also have been a factor. Thermal instability, tentatively attributed to chromium loss and surface enrichment in tungsten, was observed in the chromium alloy heated to 2100 or 2300 F in argon and may also have contributed to poor bend ductility. Studies designed to improve the effectiveness of the barrier layer are recommended.

TABLE OF CONTENTS

	Page
SUMMARY	1
INTRODUCTION	2
SELECTION OF CLADDING SYSTEMS	3
MATERIALS	7
EXPERIMENTAL PROCEDURES	7
Gas-Pressure Bonding	7
Aluminum Modification	11
Evaluation of Oxidation Resistance	15
Measurement of Bend Transition Temperature	16
Metallography and Chemical Analysis	16
RESULTS	16
Selection of Aluminizing Treatment	16
Examination of Cladding Variables	25
Oxidation Resistance at 2100 F	36
Oxidation Resistance at 2300 F	59
Bend Evaluation	72
DISCUSSION OF RESULTS AND CONCLUSIONS	88
SPECIALIZED STUDIES	91
Improved Methods of Sample Preparation	91
Interdiffusion Between Cladding Components	100
Thermal Stability of Chromium-5 Weight Percent Tungsten	121
New Coating System	125
PREPARATION OF EROSION BARS	126
RECOMMENDATIONS	132
REFERENCES	134
APPENDIX	
TABLE A-1	A-1
TABLE A-2	A-4

LIST OF TABLES

Page

TABLE 1. CLADDING SYSTEMS SELECTED FOR STUDY 8
TABLE 2. ANALYSIS AND BEND PROPERTIES OF CHROMIUM-BASE ALLOYS REPORTED BY SUPPLIER 9
TABLE 3. CLADDING MATERIALS. 10
TABLE 4. CLEANING SOLUTIONS FOR COMPONENTS OF CLADDING SYSTEMS 14
TABLE 5. OXIDATION RESISTANCE OF ALUMINIZED NICKEL-BASE ALLOYS 23
TABLE 6. KNOOP HARDNESS OF SYSTEM 4 SAMPLE AFTER VARIOUS PROCESSING STEPS. . 34
TABLE 7. THICKNESS OF BARRIER LAYER AFTER VARIOUS TREATMENTS 35
TABLE 8. OXIDATION RESISTANCE DURING CYCLIC OXIDATION AT 2100 F. 37
TABLE 9. SUMMARY OF WEIGHT CHANGES DURING CYCLIC OXIDATION AT 2100 F 39
TABLE 10. WEIGHT GAIN DURING INTERMEDIATE TEMPERATURE OXIDATION 49
TABLE 11. RESULTS OF METALLOGRAPHIC SURVEY OF SEVERAL SAMPLES OXIDIZED AT 2100 F 51
TABLE 12. KNOOP HARDNESS (100-GRAM LOAD) OF CHROMIUM-5 WEIGHT PERCENT TUNGSTEN ALLOY AFTER CYCLIC OXIDATION (2-HOUR CYCLES) FOR 100 HOURS AT 2100 F 58
TABLE 13. OXIDATION BEHAVIOR DURING CYCLIC OXIDATION AT 2300 F. 61
TABLE 14. SUMMARY OF WEIGHT CHANGES DURING CYCLIC OXIDATION AT 2300 F 63
TABLE 15. RESULTS OF METALLOGRAPHIC SURVEY OF SEVERAL SAMPLES OXIDIZED AT 2300 F 68
TABLE 16. BEND PROPERTIES OF CHROMIUM-5 WEIGHT PERCENT TUNGSTEN ALLOY 79
TABLE 17. OXIDATION BEHAVIOR OF BEND SAMPLES OXIDIZED AT 2100 F USING 20-HOUR CYCLES. 80
TABLE 18. BEND TEST RESULTS FOR SAMPLES CYCLICALLY OXIDIZED AT 2100 F 81
TABLE 19. OXIDATION BEHAVIOR OF BEND SAMPLES OXIDIZED AT 2300 F USING 20-HOUR CYCLES. 86
TABLE 20. BEND TEST RESULTS FOR SAMPLES CYCLICALLY OXIDIZED AT 2300 F 87
TABLE 21. ELECTROPOLISHING BATH USED TO PREPARE CHROMIUM ALLOY SAMPLES. . . . 93
TABLE 22. BEND PROPERTIES OF ELECTROPOLISHED CHROMIUM-5 WEIGHT PERCENT TUNGSTEN ALLOY FROM LOT 67-100. 94
TABLE 23. BEND PROPERTIES OF SYSTEM 1b-CLAD SAMPLES PREPARED BY THE WRAP-AROUND TECHNIQUE AFTER CYCLIC OXIDATION FOR 100 HOURS AT 2100 F . 96
TABLE 24. BEND PROPERTIES OF SYSTEM 1b SAMPLES AFTER CYCLIC OXIDATION, DECLADDING, AND REMOVAL OF VARYING AMOUNTS OF CHROMIUM ALLOY. . . 107
TABLE 25. RELATIVE CONTENTS OF INTERDIFFUSING ELEMENTS AT SEVERAL DEPTHS IN DECLAD SYSTEM 1b SAMPLES. 109
TABLE 26. BEND PROPERTIES OF THREE CLADDING SYSTEMS AFTER EXPOSURE AT 2100 F. 111
TABLE 27. KNOOP HARDNESS OF SYSTEM 14 SAMPLE AFTER 100-HOUR CYCLIC OXIDATION AT 2100 F 117
TABLE 28. BEND PROPERTIES OF THERMALLY CYCLED CHROMIUM-5 WEIGHT PERCENT TUNGSTEN ALLOY. 122
TABLE 29. BEND PROPERTIES OF THERMALLY CYCLED CHROMIUM ALLOY SAMPLES AFTER REMOVAL OF SURFACE MATERIAL 123
TABLE A-1. WEIGHT GAIN DURING ALUMINIZING TREATMENTS A-1
TABLE A-2. SUMMARY OF SAMPLES PREPARED FOR STUDY A-4

LIST OF FIGURES

FIGURE 1. THE Ni-Cr-Al PHASE DIAGRAM 5
FIGURE 2. Ni-Cr-W AND Ni-Cr-W-Al PHASE DIAGRAMS. 6
FIGURE 3. SECTION THROUGH A PACK ASSEMBLY--NOT TO SCALE. 12
FIGURE 4. COMPONENTS FOR PREPARING A 1/16 x 3/4 x 3-1/2-INCH CLAD SAMPLE . . 13

LIST OF FIGURES (continued) Page

FIGURE 5. ALUMINUM WEIGHT GAIN OF Ni-30Cr SAMPLES AS A FUNCTION OF RETORT LOCATION 18
FIGURE 6. AVERAGE WEIGHT GAIN AS A FUNCTION OF ALUMINIZING TEMPERATURE . . 19
FIGURE 7. MICROSTRUCTURE OF TWO NICKEL-BASE CLADDING ALLOYS AFTER ALUMINIZING AT 1750 F. 20
FIGURE 8. MICROSTRUCTURE OF TWO NICKEL-BASE CLADDING ALLOYS AFTER ALUMINIZING AT 1750 F AND HOMOGENIZING FOR 25 HOURS AT 2100 F. 21
FIGURE 9. MICROSTRUCTURE OF ALUMINIZED Ni-20 WEIGHT PERCENT Cr-20 WEIGHT PERCENT W SAMPLE (4.5 WEIGHT PERCENT ALUMINUM) AFTER 100-HOUR CYCLIC OXIDATION AT 2300 F 24
FIGURE 10. MICROSTRUCTURE OF ALUMINIZED NICKEL-BASE ALLOYS (4.5 WEIGHT PERCENT ALUMINUM) AFTER OXIDATION FOR 24 HOURS AT 2300 F . . . 26
FIGURE 11. WEIGHT CHANGE DURING CYCLIC OXIDATION AT 2400 F. 27
FIGURE 12. MICROSTRUCTURE OF ALUMINIZED Ni-20 WEIGHT PERCENT Cr-20 WEIGHT PERCENT W (4.5 WEIGHT PERCENT ALUMINUM) AFTER 24-HOUR OXIDATION AT 2400 F. 28
FIGURE 13. MICROSTRUCTURE OF SYSTEM 4 SAMPLE (IV-4) AFTER ALUMINIZING AND AFTER HOMOGENIZING 30
FIGURE 14. MICROSTRUCTURE OF SYSTEMS 1a (NO Pt LAYER) AND 2a (1/2-MIL PT "COMPATIBILITY LAYER") SAMPLES AFTER ALUMINIZING AND HOMOGENIZING. 31
FIGURE 15. MICROSTRUCTURES OF SYSTEMS 7 AND 8 SAMPLES AS HOMOGENIZED. . . . 32
FIGURE 16. MICROSTRUCTURES OF SYSTEMS 5 AND 6 SAMPLES AS HOMOGENIZED . . . 33
FIGURE 17. APPEARANCE OF OXIDATION SAMPLES AFTER 100-HOUR CYCLIC EXPOSURE AT 2100 F WITH 2-HOUR CYCLES 40
FIGURE 18. MICROSTRUCTURE OF TWO CLAD CHROMIUM SAMPLES AFTER CYCLIC OXIDATION EXPOSURE FOR 200 HOURS AT 2100 F 43
FIGURE 19. MICROSTRUCTURE OF TWO CLAD CHROMIUM ALLOYS AFTER CYCLIC EXPOSURE FOR 100 HOURS AT 2100 F. 44
FIGURE 20. APPEARANCE OF THE TUNGSTEN INTERFACIAL AREA OF SAMPLE IV-1, SYSTEM 4, AFTER 100 HOURS' CYCLIC OXIDATION EXPOSURE. 45
FIGURE 21. APPEARANCE OF BARRIER LAYER IN TWO SAMPLES AFTER CYCLIC OXIDATION AT 2100 F. 46
FIGURE 22. APPEARANCE OF W-1 WEIGHT PERCENT ThO_2 BARRIER IN SAMPLE XII-4, SYSTEM 12, AFTER 100 HOURS' CYCLIC OXIDATION AT 2100 F 47
FIGURE 23. APPEARANCE OF SYSTEM 1b SAMPLE AFTER OXIDATION AT 2100 F FOR 100 HOURS, 1400 F FOR 100 HOURS, AND 2100 F FOR 60 HOURS . . . 50
FIGURE 24. MICROSTRUCTURE OF SYSTEM 1b SAMPLE (I-19) AFTER CYCLIC OXIDATION FOR 600 HOURS AT 2100 F (20-HOUR CYCLES) 52
FIGURE 25. MICROSTRUCTURE OF SYSTEM 2b SAMPLE (II-20) AFTER CYCLIC OXIDATION FOR 600 HOURS AT 2100 F (20-HOUR CYCLES) 53
FIGURE 26. DEPENDENCE OF DEPTH OF PITTING AND CONTAMINATION ON TIME OF OXIDATION AT 2100 F 54
FIGURE 27. MICROPROBE TRAVERSE IN A SOUND REGION NEXT TO A CRACK IN THE TUNGSTEN BARRIER OF SAMPLE I-5, SYSTEM 1a. 56
FIGURE 28. MICROPROBE TRAVERSE THROUGH THE DISCONTINUITY IN THE BARRIER LAYER OF SAMPLE I-5, SYSTEM 1a 57
FIGURE 29. APPEARANCE OF THE SURFACE OF A SAMPLE FROM SYSTEM 4 (IV-11) AFTER 50 HOURS' OXIDATION AT 2100 F. 60
FIGURE 30. APPEARANCE OF OXIDATION SAMPLES AFTER 100-HOUR CYCLIC EXPOSURE AT 2300 F WITH 2-HOUR CYCLES (UNLESS NOTED OTHERWISE). 64
FIGURE 31. MICROSTRUCTURE OF SYSTEM 1b SAMPLE AFTER CYCLIC OXIDATION FOR 240 HOURS AT 2300 F USING 20-HOUR CYCLES (I-20). 67

LIST OF FIGURES (continued)

		Page
FIGURE 32.	DEPENDENCE OF DEPTH OF PITTING AND CONTAMINATION ON TIME OF OXIDATION AT 2300 F	69
FIGURE 33.	APPEARANCE OF SAMPLES AFTER CYCLIC OXIDATION AT 2300 F FOR 100 HOURS USING 2-HOUR CYCLES	70
FIGURE 34.	SOLUTION OF W-25 WEIGHT PERCENT Re BARRIER IN A SYSTEM 5 SAMPLE CYCLICALLY OXIDIZED FOR 10 HOURS AT 2300 F	73
FIGURE 35.	SOLUTION OF 0.5 MIL TUNGSTEN BARRIER DURING CYCLIC OXIDATION AT 2300 F	74
FIGURE 36.	NITRIDING OF A SYSTEM 1b SAMPLE CYCLICALLY OXIDIZED 40 HOURS AT 2300 F (I-22)	75
FIGURE 37.	NITRIDING IN A SYSTEM 1b SAMPLE CYCLICALLY OXIDIZED 40 HOURS AT 2300 F	76
FIGURE 38.	TYPICAL LOAD-DEFLECTION CURVES	77
FIGURE 39.	MICROSTRUCTURE OF BEND SAMPLE II-14	82
FIGURE 40.	STRUCTURE OF TENSION SIDE OF BEND SAMPLE	83
FIGURE 41.	CHANGE IN BEND TRANSITION TEMPERATURE AS A FUNCTION OF TIME OF OXIDATION EXPOSURE AT 2100 F	85
FIGURE 42.	PHOTOGRAPH OF SEVERAL BEND SAMPLES AFTER TESTING	89
FIGURE 43.	ILLUSTRATION OF THE WRAP-AROUND CLADDING TECHNIQUE	95
FIGURE 44.	MICROSTRUCTURE OF SYSTEM 1b SAMPLE PREPARED BY THE WRAP-AROUND TECHNIQUE (SAMPLE 1b-3)	98
FIGURE 45.	APPEARANCE OF SYSTEM 1b SAMPLE PREPARED BY WRAP-AROUND TECHNIQUE AND CYCLICALLY OXIDIZED FOR 100 HOURS AT 2100 F	99
FIGURE 46.	VARIATION OF COMPOSITION IN TUNGSTEN BARRIER OF SYSTEM 1b SAMPLE AFTER CYCLIC OXIDATION AT 2100 F	101
FIGURE 47.	SURFACE APPEARANCE OF SYSTEM 1b SAMPLE AFTER CYCLIC OXIDATION AT 2100 F AND DECLADDING	103
FIGURE 48.	SURFACE APPEARANCE OF SYSTEM 2b SAMPLE AFTER CYCLIC OXIDATION AND DECLADDING	104
FIGURE 49.	SURFACE APPEARANCE OF SYSTEM 11 SAMPLE AFTER CYCLIC OXIDATION AT 2300 F AND DECLADDING	105
FIGURE 50.	EFFECT OF METHOD OF YOKE REMOVAL ON EDGE CRACKING	106
FIGURE 51.	SURFACE APPEARANCE OF SYSTEM 15 SAMPLE AFTER CYCLIC OXIDATION AT 2100 F AND DECLADDING	112
FIGURE 52.	MICROSTRUCTURE OF SYSTEM 13 SAMPLES	114
FIGURE 53.	MICROSTRUCTURE OF SYSTEM 14, AS CLAD	115
FIGURE 54.	MICROSTRUCTURE OF SYSTEM 14 SAMPLE AFTER 100-HOUR CYCLIC OXIDATION AT 2100 F	116
FIGURE 55.	MICROSTRUCTURE OF SYSTEM 15, AS CLAD	118
FIGURE 56.	MICROSTRUCTURE OF SYSTEM 15 AFTER 100-HOUR CONTINUOUS OXIDATION AT 2100 F	119
FIGURE 57.	MICROSTRUCTURE OF SYSTEM 15 SAMPLE AFTER 100-HOUR CYCLIC OXIDATION AT 2100 F	120
FIGURE 58.	MICROSTRUCTURE OF CHROMIUM-TUNGSTEN ALLOY AFTER THERMAL EXPOSURE IN ARGON (2-HOUR CYCLES)	124
FIGURE 59.	BONDING FIXTURE AND SELECTED COMPONENTS USED TO FABRICATE A PROTOTYPE EROSION BAR	127
FIGURE 60.	BONDING CONTAINER SHOWING SELECTIVE COLLAPSE OF THIN COVER	129
FIGURE 61.	METALLOGRAPHIC SECTION SHOWING GOOD COVERAGE AND BONDING OF 1-1/2-MIL W AND 5-MIL Ni-20Cr-20W CLADDING FOILS	130
FIGURE 62.	EROSION BAR TEST SAMPLE	131

DEVELOPMENT OF PROTECTIVE COATINGS FOR CHROMIUM-BASE ALLOYS

by

D. N. Williams, R. H. Ernst, C. A. MacMillan,
J. J. English, and E. S. Bartlett

Battelle Memorial Institute
Columbus Laboratories

SUMMARY

A study of metal cladding as a means of protecting a chromium-5 tungsten* alloy from oxidation and contamination during cyclic exposure at 2100 and 2300 F was performed. A number of cladding systems were examined, all of which were applied by gas-pressure bonding of the desired metal foils to the chromium alloy.

Three outer cladding layers were examined, aluminized Ni-30Cr, aluminized Ni-20Cr-20W, and Ni-30Cr. Aluminum was added after gas-pressure bonding by a pack cementation process followed by a homogenization heat treatment. Approximately 5 percent aluminum was added to the nickel-base alloys. All three outer cladding layers were adequately oxidation resistant at 2100 F. For oxidation at 2300 F, aluminizing permitted a 5-mil cladding layer to be used, while a 10-mil layer of nonaluminized Ni-30Cr was needed.

To prevent rapid interdiffussion of nickel and chromium, a barrier layer was placed between the chromium alloy and the outer cladding layer. Barrier layers examined included tungsten, tungsten-25 rhenium, tungsten-1 thoria, and molybdenum. The barrier layer thickness ranged from 0.5 to 2.0 mils. Molybdenum and tungsten-25 rhenium were not useful, the former due to compound formation and fragmentation during cycling and the latter due to rapid solution in the cladding alloy. Some solution of unalloyed tungsten was also observed. Both the tungsten and tungsten-1 thoria developed cracks during the cyclic oxidation, apparently as a result of thermal fatigue. Contamination of the base metal appears to occur predominantly at such cracks.

Several of the systems included compatibility layers between the nickel-base alloy and the barrier layer. Platinum was used most frequently, although vanadium was also included in one system. Platinum had no beneficial effect. Moreover, it appeared to increase the solution rate of tungsten barriers. Vanadium was extremely detrimental in that its presence resulted in the formation of a liquid oxide at 2300 F and rapid cladding failure.

None of the systems allowed full retention of bend ductility after exposure at either 2100 or 2300 F. After 100 hours cyclic oxidation at 2300 F, nitrides were present throughout the chromium-5 tungsten sample thickness (~60 mils) and

*Alloy compositions are reported in weight percent throughout this report. For example, Cr-5W indicates a chromium-base alloy containing 5 weight percent tungsten.

metallic contamination was evident to a depth of about 7 mils below the cladding layer. Nitrification of the substrate after 2300 F exposure may be due, in whole or in part, to mechanical failure of the cladding at the edges of the test specimens. After 100 hours at 2100 F, no nitrides were present, but metallic contamination extended to a depth of 2 mils. Samples exposed at 2300 F were brittle in bend tests at 1600 F, and none of the samples exposed at 2100 F showed ductility below 1000 F. The chromium alloy was found to lose ductility during cyclic exposure in argon and this factor may also have contributed to the loss in bend properties during cyclic oxidation.

The failure of the cladding systems to result in retention of substrate ductility was most probably due to diffusion of contaminating material through the barrier layer. Both diffusion of nickel into the chromium alloy from the cladding and chromium into the cladding from the alloy are indicated by the experimental measurements and appear to be contributing to poor bend ductility. If so, it may be possible to design improved systems resistant to this failure mechanism. The barrier layer appears to be the critical component in a successful system. Additional studies to improve the effectiveness of the barrier layer are recommended.

The most promising of the systems examined contained an aluminized (5 percent) Ni-20Cr-20W cladding layer 5 mils thick and a 1.5-mil-thick unalloyed tungsten barrier layer. This cladding system was applied to chromium-5 tungsten erosion bars for testing by NASA-Lewis Research Center.

INTRODUCTION

Chromium-base alloys are considered promising for use as vane and blade materials in advanced air-breathing, gas-turbine engines. The strength of chromium-base alloys is adequate for application at temperatures as high as 2400 F, considerably above the upper service temperature limit of superalloys. Although the strength of chromium-base alloys is not maintained to as high a temperature as the strength of tungsten, molybdenum, tantalum, and columbium alloys, chromium alloys are not subject to catastrophic oxidation or rapid embrittlement by oxygen contamination which plague those refractory metals.

While the chromium-base alloys show resistance to catastrophic oxidation, their oxidation resistance is not sufficient to permit their use at temperatures as high as 2400 F, unprotected. Also, absorption of nitrogen occurs quite rapidly at elevated temperatures, and nitrogen contamination can lead to embrittlement. Although it is concluded that a protective coating will be required for chromium-base alloys exposed to temperatures approaching 2400 F, defects in the coating are not expected to result in catastrophic oxidation. Therefore, the development of a useful coating system for chromium-base alloys should be less difficult than for other refractory metal alloys.

Vanes and blades operating in gas-turbine engines are subject to severe thermal shock, impact and erosion by high-velocity particles, and to complex stresses. A ductile coating is expected to best withstand these service conditions. Ductility at room temperature would also facilitate assembly during manufacture. The desirability of maintaining good ductility in an oxidation resistant coating suggests that metallic cladding is the most promising method for

protecting chromium-base alloys in the gas-turbine environment. A bonded overlayer of a protective cladding may also allow rough handling of what may be otherwise a notch-sensitive substrate material.

The objective of the present program was to develop a metallic cladding system which would protect chromium-base alloys from oxidation and contamination at elevated temperatures. Protection for up to 600 hours at temperatures to 2400 F under cyclic temperature conditions is desired.

The bulk of the studies described in this report were conducted during the period from June 22, 1965, through April 21, 1967. The program was extended through December 31, 1967, to permit further definition of cladding problems discovered in the primary investigation. The results of this additional work are appended to the present report as a section entitled Specialized Studies which begins on page 91 .

SELECTION OF CLADDING SYSTEMS

A cladding system capable of protecting chromium from both oxidation and nitrogen absorption during service at temperatures up to 2400 F was sought. It was desired that the cladding system also be ductile over the temperature range from 75 to 2400 F. These requirements limited the useful cladding alloys to certain oxidation-resistant platinum-group metals, iron-chromium-aluminum alloys, and nickel-chromium alloys.

The usefulness of platinum-group metals as cladding materials for refractory metals was under investigation elsewhere[1,2,3] and was, therefore, not examined in the present program. It was considered that if the results of the cited studies proved sufficiently attractive the information could be readily adapted to the development of cladding systems for chromium. The iron-chromium-aluminum alloys possess excellent oxidation resistance at 2400 F[4], but they are susceptible to embrittlement during oxidation at high temperatures. This tendency toward embrittlement suggested that these alloys were of questionable use when ductility after oxidation exposure was required. Nickel-chromium alloys have excellent oxidation resistance up to 2300 F and are not susceptible to embrittlement during oxidation. They show greatly reduced oxidation resistance between 2300 and 2400 F, however[5]. Despite their poor oxidation resistance at 2400 F, it was concluded that oxidation resistance could be improved by minor alloy modification and that the nickel-chromium alloys showed the most promise for meeting the program objectives. Two nickel-chromium alloys were selected for study in this program. The first was a commercial alloy, Tophet 30, which is basically Ni-30Cr. This alloy is considered to be one of the most oxidation resistant binary nickel-chromium alloys. The second alloy selected was an experimental Ni-20Cr-20W alloy developed in an earlier program at Battelle[6]. It has relatively good oxidation resistance, and it was probable that this alloy, as a result of the presence of tungsten, would also show lower thermal expansion and lower permeability by interstitials than other nickel-chromium alloys.

Prospective use of nickel-base alloys as cladding materials at 2400 F prompted improvement of their oxidation resistance. Since aluminum is known to significantly improve the oxidation resistance of nickel-chromium alloys[5,7,9], addition of aluminum to the nickel-chromium or nickel-chromium-tungsten alloys appeared desirable.

The nickel-chromium-aluminum phase relationships at 2100 F are shown in Figure 1[8,9]. About 8 percent aluminum is soluble in Ni-30Cr at 2100 F. At 1560 F, the solubility is only about 5 percent. Sections from the Ni-W-Cr-Al quaternary diagram and the Ni-Cr-W ternary diagram are shown in Figure 2[10,11]. It is seen that the Ni-20Cr-20W alloy is single phase above about 1800 F. The addition of about 7 percent aluminum to Ni-20Cr-20W reduces the solubility of tungsten in the matrix phase, leading to the presence of tungsten phase ($\alpha 2$) in the alloy at 2010 F. However, the phase diagram suggests that intermetallic nickel-aluminum phase would not be present in a Ni-20Cr-20W-7 (or less) Al alloy.

It was concluded from the published phase relationships that as much as 5 percent aluminum could be added to both Ni-30Cr and Ni-20Cr-20W without formation of an embrittling second phase. It was hoped that this addition would benefit oxidation resistance sufficiently to make the alloys useful at 2400 F. In order to avoid fabrication problems, and also to develop a somewhat higher aluminum content near the surface, vapor phase deposition of the aluminum on the clad component followed by a homogenization anneal to diffuse the aluminum into the nickel-base cladding alloy was considered the most attractive procedure. Preliminary studies showed that as much as 5 percent aluminum could be readily alloyed in Ni-30Cr or Ni-20Cr-20W by this procedure.

At elevated temperatures, nickel and chromium have high mutual solubilities, and extensive interdiffusion might be anticipated. The diffusion coefficient of chromium in a Ni-20Cr alloy at 2300 F has been determined as 7×10^{-9} cm^2/sec[12]. Chromium diffusion into the Ni-base alloys could be quite extensive, and presumably, nickel diffusion into the chromium-base alloy would be relatively rapid also. This suggested the need for a diffusion barrier between the chromium alloy and the cladding alloy. The most promising diffusion barrier material was considered to be tungsten. It has been reported that at 3100 F (1700 C) the interdiffusion zone between tungsten and chromium was only 7 mils thick after 1 hour exposure[13], suggesting that diffusion of tungsten in chromium may be relatively low at 2400 F and below. No porosity was formed at the interface, which suggested that the interdiffusion rates of chromium and tungsten were similar. Furthermore, slight tungsten diffusion should not be detrimental since the chromium-base alloy of primary interest contains 5 percent tungsten.

The diffusion of tungsten into the Ni-30Cr or Ni-20Cr-20W was considered a potentially greater problem than its diffusion into chromium. In this case, little was known about diffusion kinetics. As tungsten diffused into either alloy, a second phase would be stabilized, and embrittlement might be developed. Thermal expansion differences between the tungsten barrier layer and the nickel-base cladding alloy also appeared to be a potential source of trouble. Altering the interface region between the tungsten barrier and the nickel cladding alloy by providing a layer of platinum was considered as a possible method of overcoming these problems because of (1) supression of the tendencies to form intermetallic phases during service, and (2) thermal expansion (of platinum) intermediate between chromium (or tungsten) and the nickel alloy clad. This platinum layer is referred to as a compatibility layer. The usefulness of vanadium as a compatibility layer was also examined briefly.

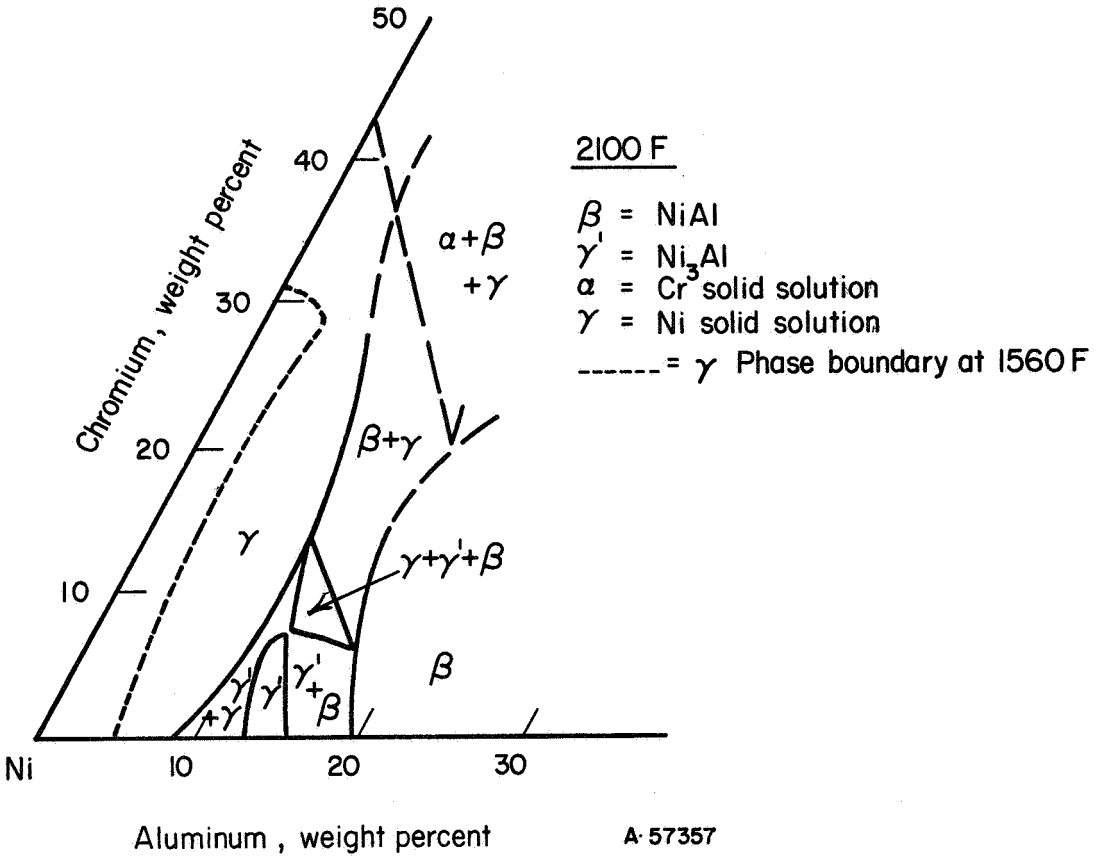

FIGURE 1. THE Ni-Cr-Al PHASE DIAGRAM[8, 9]

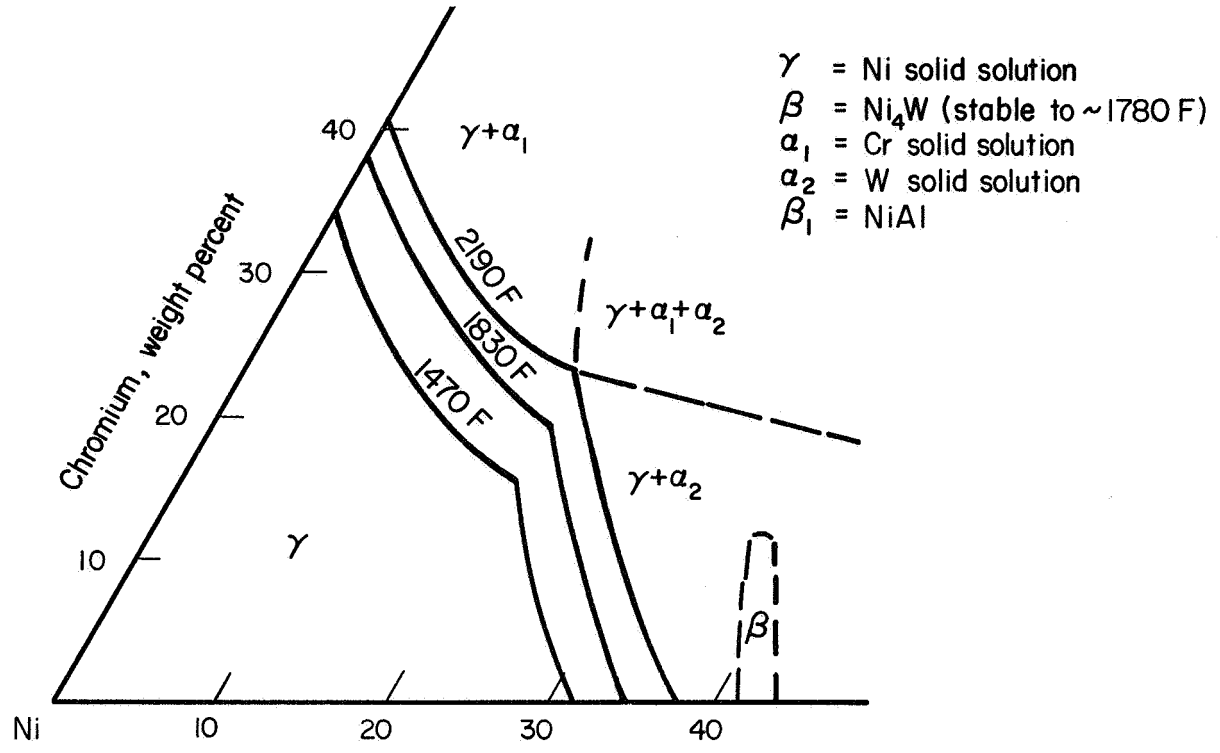

a. Tungsten, weight percent

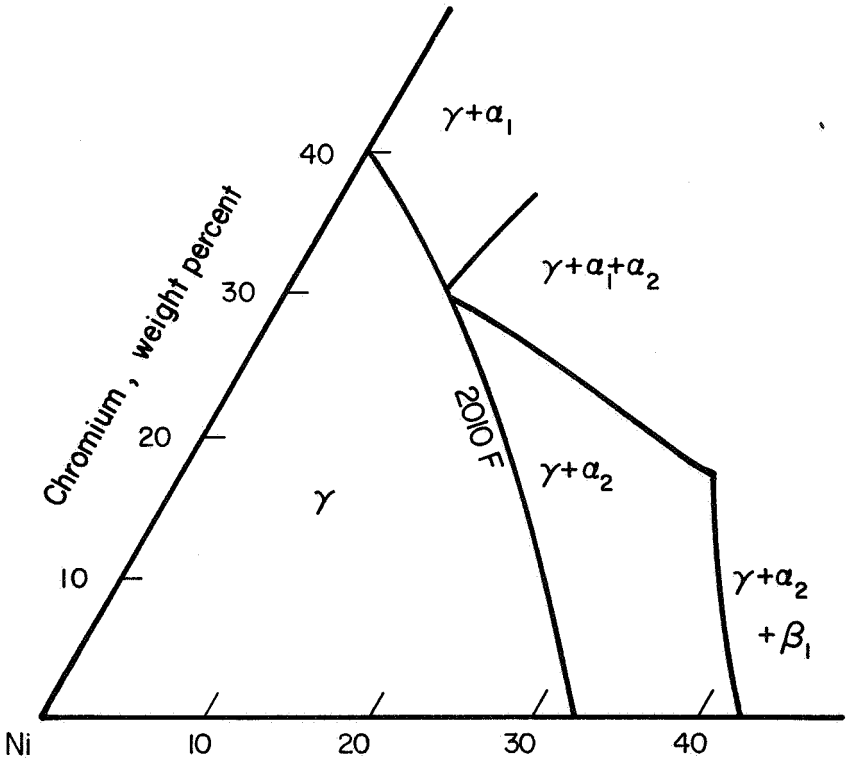

b. Tungsten Plus Aluminum, weight percent
(W:Al ratio = 3:1) A-57358

FIGURE 2. Ni-Cr-W AND Ni-Cr-W-Al PHASE DIAGRAMS[10, 11]

Although unalloyed tungsten was initially considered as the most promising barrier material, alternate materials were briefly evaluated on the basis of early results. These included two tungsten alloys, W-25Re and W-1ThO_2, and unalloyed molybdenum.

A summary of the cladding systems selected for study is given in Table 1. All systems were evaluated on a Cr-5W-0.1Y alloy base.

MATERIALS

The Cr-5W-0.1Y alloy used in this investigation was prepared by the General Electric Company, Refractory Metals Plant, Cleveland, Ohio, as part of a separate NASA-supported program[14]. Analyses of the three lots of material provided for this study are given in Table 2. The sheet from Lot 58-100 proved to be extremely difficult to handle since it cracked quite readily during sample preparation. As a result, very little of this material was used in the program. Lot 64-100 was used most extensively, and unless stated otherwise, all samples described in this report were prepared from sheet from Lot 64-100.

With the exception of the Ni-20Cr-20W alloy, which was arc melted and fabricated to sheet at Battelle, the cladding materials were purchased from commercial suppliers. The materials used in preparing the clad samples are described in Table 3.

EXPERIMENTAL PROCEDURES

Gas-Pressure Bonding

Samples for evaluation were prepared by assembly of the various components and gas-pressure bonding.

Chromium alloy sample sizes before cladding were either 1/16 x 1 x 1 inch, 1/16 x 1 x 2 inches, or 1/16 x 3/4 x 3-1/2 inches. Machining of the 1/16-inch chromium alloy sheet presented a major problem. Initial attempts to edge grind the sheet to size produced some edge cracks. Edge cracking was especially severe in material from Lot 58-100. Cracking was minimized by first rough cutting the sheet samples to size using a soft cut-off wheel followed by careful grinding to finish dimensions. The samples were edge ground in packs of about fifteen samples with mild steel shims between each sample. To prevent microcracking, it was found that only 0.0002-inch per pass could be removed using a silicon carbide grinding wheel and water coolant. This procedure eliminated most edge cracks as shown by dye penetrant inspection and microscopic examination. Only completely crack-free bend samples were used. The major surfaces were also ground to provide a uniform ground finish. The grinding direction in the 3/4 x 3-1/2-inch samples was longitudinal to minimize scratch effects.

TABLE 1. CLADDING SYSTEMS SELECTED FOR STUDY

System	Barrier Layer[5]	Compatibility Layer	Cladding Layer[5]	Aluminized[1]
1a	0.5 mil W	None	5 mil Ni-20Cr-20W	Yes
1b	1.5 mil W	None	5 mil Ni-20Cr-20W	Yes
2a	0.5 mil W	0.5 mil Pt	5 mil Ni-20Cr-20W	Yes
2b	1.5 mil W	0.5 mil Pt	5 mil Ni-20Cr-20W	Yes
2c	1.0 mil W[3]	1.0 mil Pt[3]	5 mil Ni-20Cr-20W	Yes
3	0.5 mil W	0.5 mil Pt	5 or 10 mil Ni-30Cr[2]	No
4	0.5 mil W	0.5 mil Pt	5 mil Ni-30Cr	Yes
5	1.0 mil W-25Re	0.5 mil Pt	5 mil Ni-30Cr	Yes
6	1.0 mil W-25Re	None	5 mil Ni-30Cr	Yes
7	1.0 mil W[3]	0.5 mil Pt	5 mil Ni-30Cr	Yes
8	0.5 mil W	1.0 mil Pt[3]	5 mil Ni-30Cr	Yes
9	1.5 mil W	1.0 mil V	5 mil Ni-20Cr-20W	Yes
10	2.0 mil Mo	0.5 mil Pt	5 mil Ni-20Cr-20W	Yes
11	1.5 mil W	None	10 mil Ni-30Cr[4]	No
12	2.0 mil W-1ThO_2	0.5 mil Pt	5 mil Ni-20Cr-20W	Yes

(1) From 3 to 5 percent by weight aluminum was added to the cladding by pack aluminizing and subsequent annealing to homogenize the aluminum distribution.

(2) 5-mil cladding used for 2100 F oxidation exposure, two 5-mil layers used for 2300 F oxidation exposure.

(3) Two 0.5-mil layers were used to give a total thickness of 1.0 mil.

(4) Two 5-mil layers.

(5) All alloy compositions in weight percent.

TABLE 2. ANALYSIS AND BEND PROPERTIES OF CHROMIUM-BASE ALLOYS REPORTED BY SUPPLIER[14]

Lot No.	58-100	64-100	67-100
Form	1/16-inch sheet	1/16-inch sheet	1/16-inch sheet
Analysis, wt. percent			
Tungsten	4.86	4.82	4.90
Yttrium	0.07	0.11	0.12
Sulfur	0.0020	0.0050	0.0070
Phosphorus	<0.0010	0.0010	0.0020
Carbon	0.0080	0.0080	<0.0010
Oxygen	0.0080	0.0050	0.0041
Nitrogen	0.0045	0.0035	0.0030
Hydrogen	0.0001	0.0008	0.0005
4T Bend Transition Temp., F			
Longitudinal	985	435	300
Transverse	1065	480	615

TABLE 3. CLADDING MATERIALS

Material(1)	Thickness	Source
	Barrier Layers	
Tungsten	0.5 mil	Henry Cross Metals
	1.5 mil	Wah Chang Corporation and Henry Cross Metals
W-25Re	1 mil	Chase Brass & Copper Company
W-1ThO_2	2 mil	Henry Cross Metals
Molybdenum	2 mil	Fansteel
	Compatibility Layers	
Vanadium	1 mil	Vanadium Corp. of America
Platinum	0.5 mil	Baker Platinum Division, Engelhard Industries, Inc.
	Cladding Layers	
Tophet 30 (Ni-30Cr)	5 mil	Wilber B. Driver Company
Ni-20Cr-20W	5 mil	Battelle Memorial Institute

(1) All compositions in weight percent.

Edge protection of the chromium samples was provided by a picture frame of Ni-30Cr alloy which was machined to fit the chromium sample and to provide 1/8-inch edge protection on all four edges of each sample. This procedure was selected to avoid the problems involved in uniformly cladding all surfaces of the specimens during the preliminary evaluation stage of the program and was subsequently used throughout the program except for the work reported as specialized study. The major surfaces of the samples were clad with the components listed in Table 1. In the first samples prepared, a barrier layer of tungsten was not placed between the edges and the Ni-30Cr picture frame. However, this resulted in excessive edge diffusion and cladding failures over the substrate-picture frame junctures. A tungsten barrier was used to protect the edges of specimens subsequently prepared. A section through a typical pack assembly is shown in Figure 3. As shown in this figure, the nickel-base cladding alloy was cut to fit over the picture frame. The barrier layer, and compatibility layer when present, were cut to the size of the chromium alloy sample. The entire assembly was enclosed in a steel container for gas-pressure bonding. A molybdenum foil barrier layer was used between the nickel-base cladding alloy and the steel can to prevent iron and carbon contamination of the cladding during gas-pressure bonding. Figure 4 is a photograph showing the components of a typical 1/16 x 3/4 x 3-1/2-inch sample assembly.

Prior to assembly, the components were chemically cleaned in the solutions listed in Table 4, degreased in methyl-ethyl-ketone, and rinsed in acetone and alcohol. To avoid shifting in the pack assembly, the barrier and compatibility layers were tack welded to the chromium alloy sample before assembly.

After assembly, the steel can was welded shut in a vacuum chamber. The welded assembly was then gas-pressure bonded at 2150 F using a 10,000 psi isostatic pressure for 2 hours. The steel can and molybdenum barrier layer were removed after bonding by leaching in a nitric acid solution. The edges of the picture frame were then ground to a uniform radius.

Aluminum Modification

In order to improve the oxidation resistance of the nickel-base cladding alloys by adding 4 to 6 percent aluminum while retaining room temperature ductility, a pack aluminizing-cementation process was selected. Cementation techniques were developed using 10-mil samples of the cladding alloy, adding aluminum from both sides. This procedure simulated that anticipated in subsequent aluminizing of the 5-mil cladding alloy from one side.

Aluminizing procedures used in these studies were as follows:

(1) Acid clean the sample in 50 volume percent HNO_3 aqueous solution, rinse in water, acetone, and hot trichloroethylene vapor.

(2) Place sample in a graphite box containing a mixture of 1 weight percent -200 mesh aluminum powder, 1 weight percent NaCl, and 98 weight percent Al_2O_3 (-100, +200 mesh).

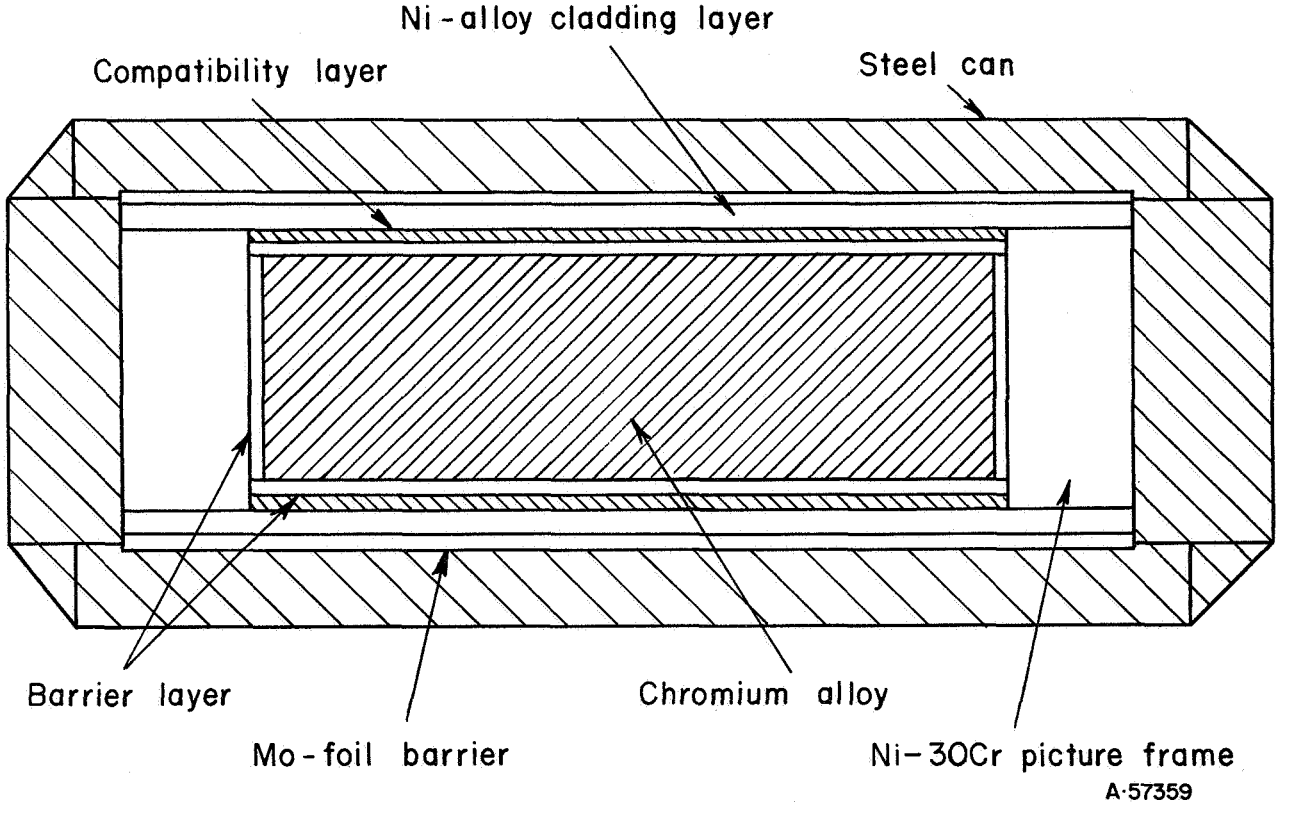

FIGURE 3. SECTION THROUGH A PACK ASSEMBLY - NOT TO SCALE

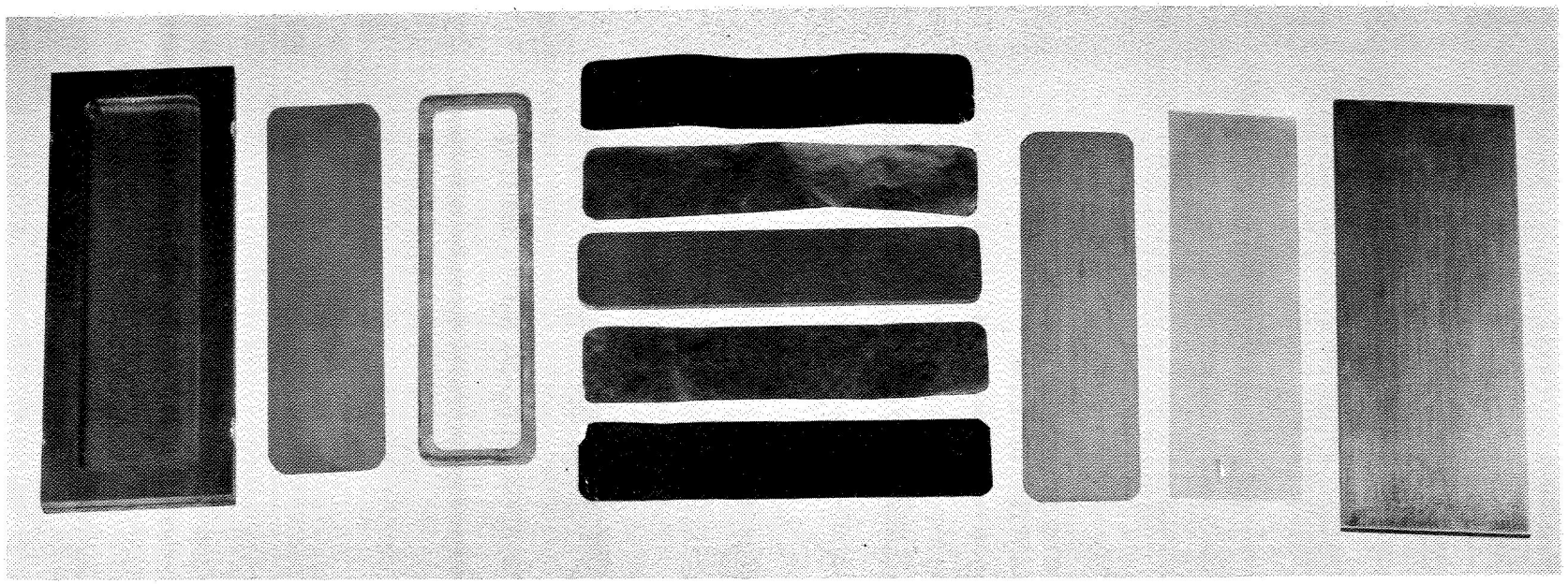

~1/2X 31983

Steel bottom plate and yoke with Mo barrier in position | 5-mil Ni-base cladding | 1/16-inch-thick Ni-30Cr yoke | Pt foil
W foil
Cr-5W sheet
W foil
Pt foil | 5-mil Ni-base cladding | 3-mil Mo barrier | Steel cover plate

FIGURE 4. COMPONENTS FOR PREPARING A 1/16 x 3/4 x 3-1/2-INCH CLAD SAMPLE

TABLE 4. CLEANING SOLUTIONS FOR COMPONENTS OF CLADDING SYSTEMS

Material, weight percent	Solution, volume percent	Temp., F
W	45 HF-20 HNO_3-35 H_2O	75
W-25Re	Ditto	"
W-1ThO_2	"	"
Mo	Organic solvent only	-
Pt	Ditto	-
V	"	-
Ni-30Cr	33HF-33 HNO_3-34 H_2O	Boiling
Ni-30Cr-20W	Ditto	"
Cr-5W	33 HF-33 HNO_3-34 H_2O	Boiling

(3) Place the graphite box in a cold Inconel-lined muffle furnace and heat to the aluminizing temperature in a flowing argon atmosphere, hold at the aluminizing temperature for 12 hours (in a few cases, 18 hours), and cool in the furnace to below 700 F. Remove the box from the furnace and open. Preliminary experimentation resulted in the selection of a temperature of 1750 F for aluminizing.

After aluminizing, the samples were homogenized to distribute the aluminum content more uniformly. The standard homogenization treatment was to anneal for 4 hours at 2100 F plus 16 hours at 2200 F in argon followed by an air cool.

A tabulation of the amount of aluminum added to each sample prepared in this program is given in the Appendix, Table A-1.

Evaluation of Oxidation Resistance

Because of the rapid failure observed with aluminized and nonaluminized nickel alloys during oxidation at 2400 F, it was decided to limit oxidation studies on clad chromium alloys to temperatures of 2300 F. To simulate the type of exposures observed in gas-turbine engines, cyclic oxidation tests were necessary. In these tests, samples were furnace heated in air to the oxidation temperature, held a pre-selected time, and cooled in air to room temperature. After each cycle of exposure, the samples were weighed and examined for evidence of spalling or thermal fatigue cracks. After completion of the prescribed number of cyclic exposures, or after premature sample failure, specimens were sectioned for metallographic examination. Oxidation studies were normally performed on either 1 x 1 or 1 x 2-inch clad samples.

Temperatures for cyclic oxidation tests were either 2300 or 2100 F. A 200-hour exposure time at temperature was used as a standard screening exposure. During the first 100 hours, the samples were cooled to room temperature every two hours. During the second 100-hour exposure period, a 20-hour cycle was used. The samples were exposed on an alumina rack in a static air atmosphere. The most promising systems as determined from the 200-hour cyclic oxidation tests were exposed to 600-hour cyclic tests at 2100 or 2300 F. 20-hour cycles were used in these tests.

Several of the clad samples were intentionally defected before oxidation exposure by cutting a 30-mil-wide groove into the cladding surface to a depth of 5, 7, or 10 mils. The purpose of these tests was to determine the resistance of the samples to defects in the cladding layer.

Several of the systems were also oxidation tested using two or three continuous exposure periods at two different temperatures. Test procedures used were:

(1) 2100 F for 100 hours, 1400 F for 100 hours, and air cool.

(2) 2100 F for 100 hours, 1400 F for 100 hours, 2100 F for 60 hours, and air cool.

These studies were selected to determine if oxidation exposure at lower temperatures destroyed the effectiveness of the cladding system as has been observed in certain other coating systems.

Measurement of Bend Transition Temperature

The bend transition temperature was determined in accordance with the Standard Materials Advisory Board recommended procedures[15]. Bend samples measured 5/8 x 3-1/2 x 1/6 inch. Only longitudinal bend samples (the 3-1/2-inch dimension parallel to the rolling direction) were prepared. Samples were bent over a 4T bend mandrel using three-point loading, the end loading points being 1.5 inches apart. The rate of mandrel movement was one inch per minute. The bend equipment was contained in an electrically heated furnace capable of heating the samples to 1600 F. Thermocouples were attached to the sample and to the bend mandrels to measure the sample and mandrel temperatures. The temperature difference between the sample and mandrel at the time of test was always <50 F.

Bend tests were performed on bare Cr-5W, clad samples, and clad samples after cyclic oxidation exposure at 2100 or 2300 F. The Ni-30Cr picture frame used to protect the edges of the sample from oxidation during cyclic exposures was removed and the edges radiused by grinding through 600-grit paper before bend tests were run.

Metallography and Chemical Analysis

Clad samples were examined as prepared after oxidation exposure and after bend testing to determine the microstructural characteristics of the cladding layer and to examine the presence and extent of interdiffusion. The metallographic samples were examined both as polished and after etching. Etching solutions used included 30 volume percent lactic-20 volume percent nitric-15 volume percent HF, Murakami's reagent (10g ferricyanide and 10g potassium hydroxide in 100 ml water), 5 volume percent chromic acid (electrolytic), or 10 volume percent oxalic acid (electrolytic) depending upon the structural feature being studied (structure of Ni cladding, structure of W barrier, diffusion of compatibility layer, or structure of Cr alloy, respectively). Microhardness measurements using the Knoop indentor with a 100-gram load were also used to examine for interdiffusion.

Several studies of the extent of interdiffusion were made using electron microprobe analysis for the major elements present. Analyses for nitrogen contamination were made using the micro-Kjeldahl technique.

RESULTS*

Selection of Aluminizing Treatment

The aluminizing variables investigated included aluminizing temperature, nickel alloy composition, nickel alloy thickness, and sample location in the retort. Aluminizing procedures were presented in the previous section of this report.

---

*A tabulation of all samples prepared in this program showing their composite, size, and disposition is given in the Appendix, Table A-2.

These studies showed that with equivalent aluminizing treatments, neither alloy content (Ni-30Cr versus Ni-20Cr-20W) nor sample thickness (10 mils versus >50 mils) affected the amount of aluminum picked up by the material during pack aluminizing. Sample location in the retort was a more significant variable. Samples near the front of the retort gained slightly more weight. The results of a detailed study of the effect of sample location, using 30 samples of 10-mil-thick (3/4 x 1 inch) Ni-30Cr are shown in Figure 5. The samples were placed in a vertical position in the retort with the 3/4 x 1 inch surfaces parallel to the front of the retort. Samples were arranged in two vertical layers in the 2-1/2 x 5 x 8-inch graphite box (top and bottom) and in two horizontal rows (left and right). The samples were spaced 1 inch apart in each row and the row position was adjusted so that the sample position in adjacent rows was 1/2 inch from that above or across from it. As shown in Figure 5, about ±10 percent variation in weight gain was obtained as a result of sample location.

The weight gain observed as a function of aluminizing temperature is shown in Figure 6. Except for the run at 2000 F, the results show a linear relationship on an Arrhenius plot. Thus, weight gain can be controlled quite readily by controlling the aluminizing temperature. The somewhat low aluminum adsorption at 2000 F probably resulted from aluminum depletion of the pack mixture. Assuming a sample thickness of 10 mils aluminized on both sides (or 5 mils aluminized on one side) and alloy densities of 8.3 gm/cc for Ni-30Cr and 9.5 gm/cc for Ni-20Cr-20W an aluminum addition of 5 weight percent would necessitate a weight gain during aluminizing of 5.5 mg/cm^2 for Ni-30Cr and 6.4 mg/cm^2 for Ni-20Cr-20W.

The microstructure of the two alloy samples after aluminizing at 1750 F is shown in Figure 7. The surface is seen to consist of intermetallic phases, probably based on the compounds Ni_2Al_3, NiAl, and Ni_3Al. The average hardness of the surface layer was 600 Knoop as compared to about 300 Knoop for the nickel-base alloy. The thickness of the compound layer varied as follows with temperature:

	Coating Thickness, mils	
Temperature	Ni-30Cr	Ni-20Cr-20W
1600	0.5	0.7
1700	1.2	1.1
1750	1.2-1.3	1.5
2000	4-6	3.3-3.5

After aluminizing, these initial samples were homogenized for 25 hours at 2100 F in an argon atmosphere to distribute the aluminum content more uniformly. The structure of two samples after homogenization is shown in Figure 8. Considerable diffusion occurred, and some subsurface porosity was developed. The aluminum content in these samples was approximately 5 percent. As predicted by the phase diagrams shown previously (Figure 3) , aluminizing appeared to increase the amount of tungsten phase in the Ni-20Cr-20W alloy. The homogenized samples successfully withstood bending over a 1/32-inch die at room temperature (about 3T) indicating that aluminizing did not result in embrittlement. As apparent in Figure 8, remnants of aluminide phases remained on the cladding surface. A subsequently developed homogenization treatment of 4 hours at 2100 F plus 16 hours at 2200 F eliminated the aluminide-phase remnants and resulted in uniform microstructure throughout the cladding thickness. Subsurface porosity, however, remained.

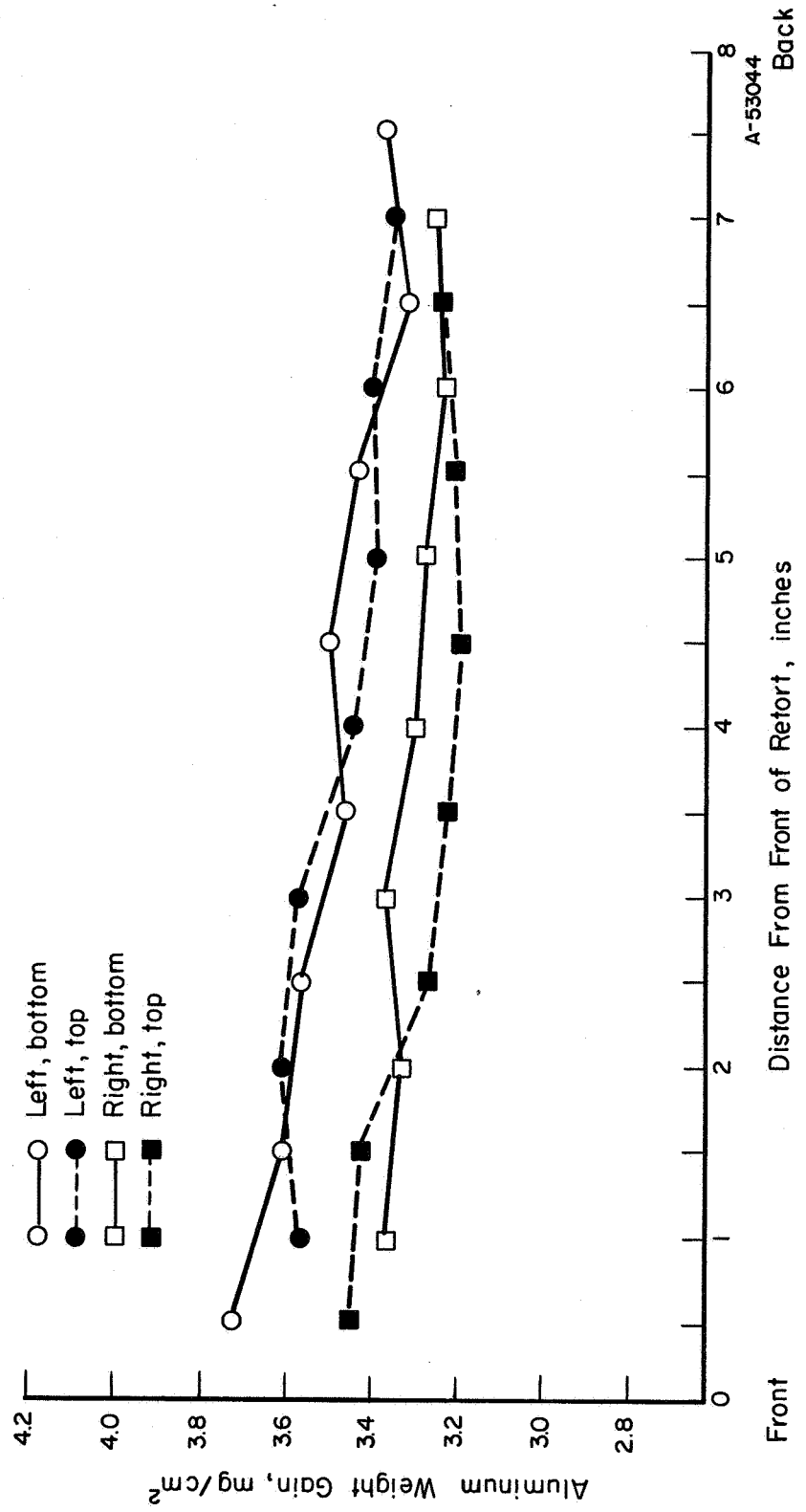

FIGURE 5. ALUMINUM WEIGHT GAIN OF Ni-30Cr SAMPLES AS A FUNCTION OF RETORT LOCATION

Samples were aluminized at 1700 F for 12 hours.

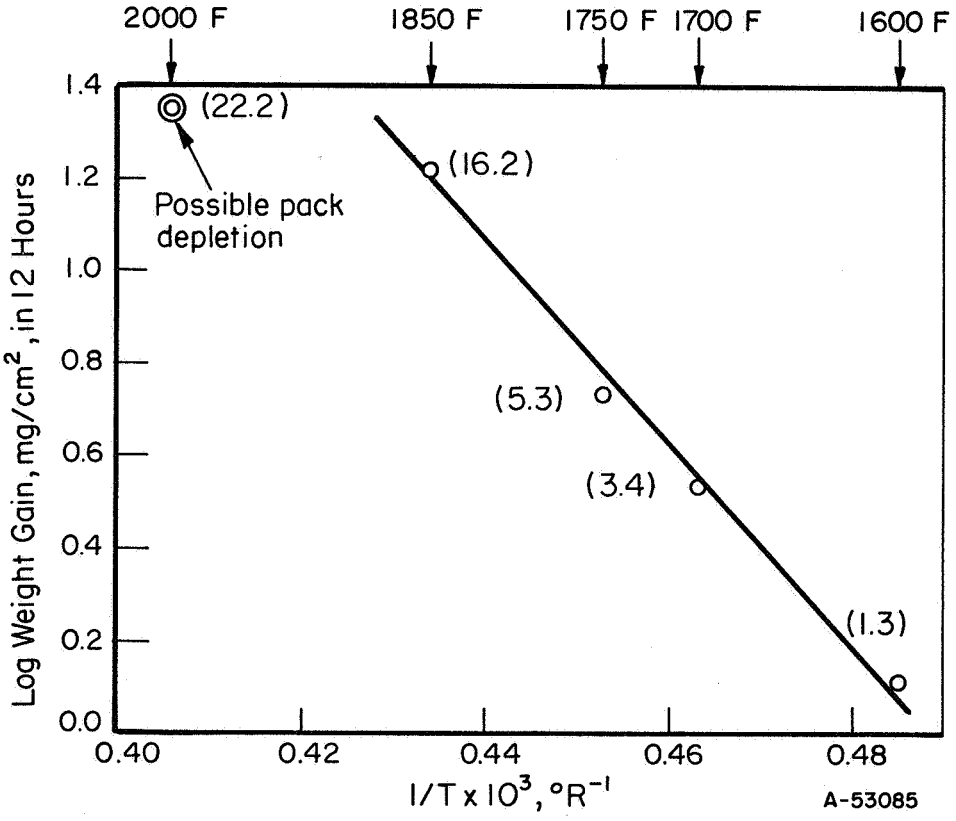

FIGURE 6. AVERAGE WEIGHT GAIN AS A FUNCTION OF ALUMINIZING TEMPERATURE

All samples aluminized for 12 hours. Numbers in parentheses are aluminum weight gain in mg/cm^2.

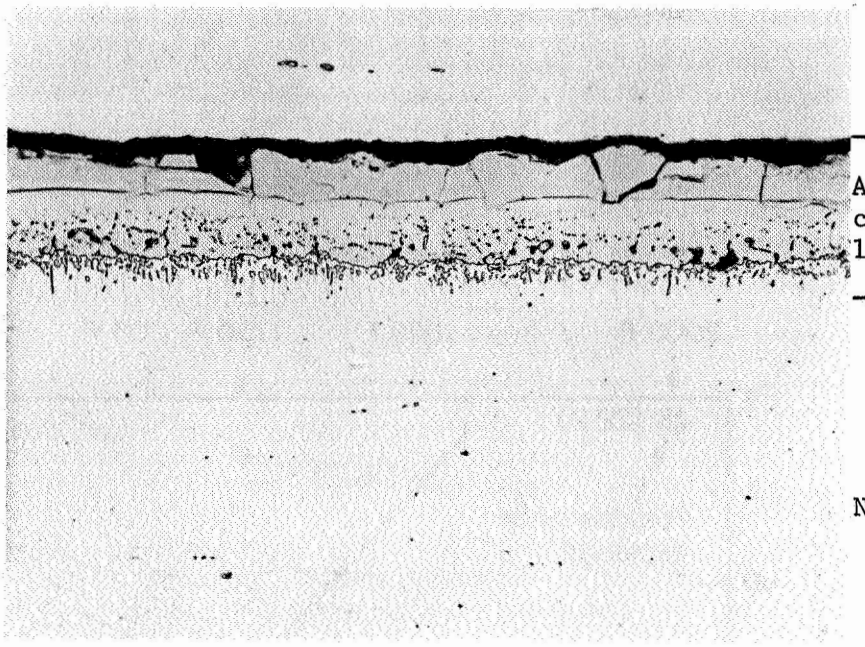

500X 28593

(a) Ni-30 weight percent Cr

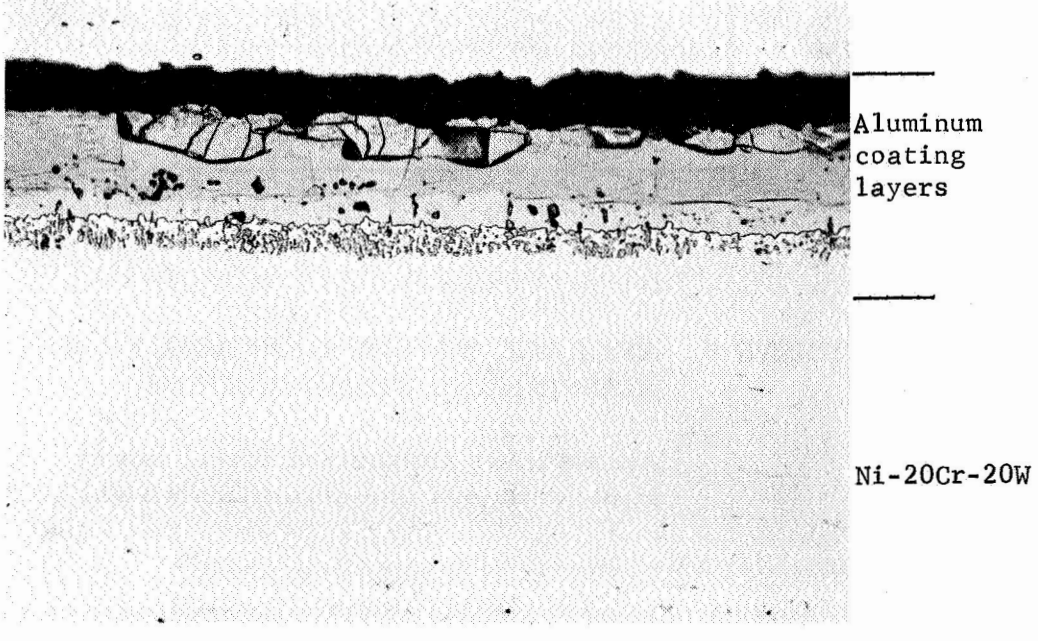

500X 28594

(b) Ni-20 weight percent Cr-20 weight percent W

FIGURE 7. MICROSTRUCTURE OF TWO NICKEL-BASE CLADDING ALLOYS AFTER ALUMINIZING AT 1750 F

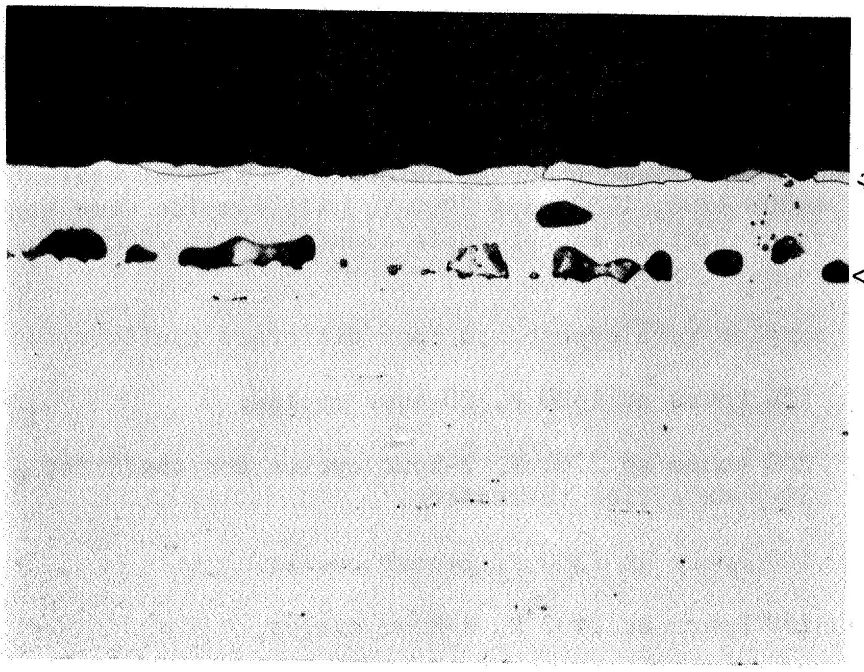

500X 28592

(a) Ni-30 weight percent Cr

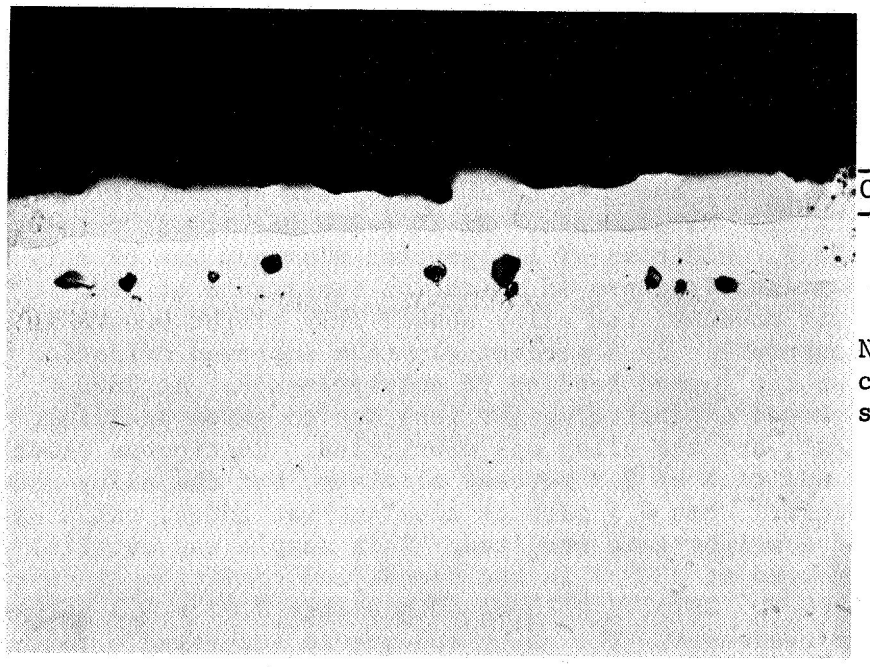

500X 28595

(b) Ni-20 weight percent Cr-20 weight percent W

FIGURE 8. MICROSTRUCTURE OF TWO NICKEL-BASE CLADDING ALLOYS AFTER ALUMINIZING AT 1750 F AND HOMOGENIZING FOR 25 HOURS AT 2100 F

Samples of 10-mil-thick Ni-30Cr and Ni-20Cr-20W were processed to provide several different final aluminum contents and were then evaluated for oxidation resistance to determine whether the aluminum content was beneficial. After the oxidation treatment, the samples were bend tested at 75 F over a 1/32-inch radius to detect embrittlement during oxidation. Samples evaluated included those aluminized at 1600, 1700, 1750, and 2000 F. All samples were homogenized 25 hours at 2100 F before evaluation except those aluminized at 2000 F which were evaluated as aluminized.

The samples were exposed to four different cyclic oxidation treatments:

(1) 100 hours at 1600 F, 20-hour cycles.

(2) 200 hours at 2100 F, 2-hour cycles for the first 100 hours, 20-hour cycles thereafter.

(3) 100 hours at 2300 F, 2-hour cycles.

(4) 100 hours at 2400 F, 2-hour cycles.

The results of the first three tests are summarized in Table 5. All samples showed a small weight gain at 1600 F. Some intermetallic phase precipitated during the exposure. This was sufficient to partially embrittle the Ni-20Cr-20W sample containing 4.5 percent aluminum. Both alloys were sufficiently oxidation resistant at 1600 F to be useful as a 5-mil cladding alloy without aluminum modification. At 2100 F, the unaluminized Ni-30Cr alloy had good oxidation resistance, showing a slight weight loss in 200 hours due to a small amount of oxide spalling. About 0.5 mil of surface material was lost per side. Adding 1.1 percent aluminum was quite detrimental, but 2.9 percent aluminum halted the oxide spalling noted on unaluminized Ni-30Cr. 16.5 percent aluminum, mostly present as surface intermetallics, resulted in failure by thermal fatigue during cyclic oxidation. In contrast to Ni-30Cr, the Ni-20Cr-20W alloy was not oxidation resistant at 2100 F without aluminizing. Nonaluminized Ni-20Cr-20W was almost completely oxidized in 80 hours at 2100 F. Addition of 1.1 percent aluminum was of only minor benefit, but 2.9 aluminum greatly improved oxidation resistance at 2100 F. When 2.9 percent aluminum was present, the alloy showed only slight weight gain and remained ductile after exposure. 16.5 percent aluminum improved oxidation resistance, but intermetallic phases formed leading to embrittlement. At 2300 F, the unmodified Ni-30Cr alloy showed extensive weight loss due to oxide spalling. One to two mils per side was lost, and the alloy was embrittled. Continuous oxide spalling also occurred after addition of 2.9 percent aluminum, but the alloy showed some ductility after exposure. When 4.5 percent aluminum was added, oxide spalling was largely eliminated, and a weight gain resulted. This sample was ductile. The Ni-20Cr-20W alloy was not tested at 2300 F in the unmodified condition since severe oxidation was noted at 2100 F. Samples alloyed with either 2.9 or 4.5 percent aluminum were quite oxidation resistant. The oxide appearance suggested a molten oxide was present, perhaps a mixture of Al_2O_3 and WO_3. The $2Al_2O_3 \cdot 5WO_3$ oxide melts at 2250 F[16] Partial embrittlement resulting from oxide penetration up to 3 mils in certain areas occurred in the sample containing 2.9 aluminum. The sample containing 4.5 percent aluminum was ductile, however. The microstructure of this sample after oxidation is shown in Figure 9. It is seen that the oxide is largely restricted to the surface region.

TABLE 5. OXIDATION RESISTANCE OF ALUMINIZED NICKEL-BASE ALLOYS

Approximate Al Content, weight percent	Ni-30Cr Samples		Ni-20Cr-20W Samples	
	Weight Gain, mg/cm^2	Bend Results	Weight Gain, mg/cm^2	Bend Results
	Oxidized at 1600 F for 100 hours, 20-hour cycles			
0	0.2	Ductile	-	-
2.9	0.3	Ductile	0.1	Ductile
4.5	0.3	Ductile	0.1	Partially Ductile
	Oxidized at 2100 F for 200 hours, 2-hour cycles for 100 hours, 20-hour cycles thereafter			
0	-1.0	Ductile	>8(2)	Brittle
1.1	-6.9	Brittle	11	Brittle
2.9	1.7	Ductile	1.4	Ductile
16.5	(1)	-	-3.6	Brittle
	Oxidized at 2300 F for 100 hours, 2-hour cycles			
0	-10	Brittle	-	-
2.9	-10	Partially Ductile	1.3	Partially Ductile
4.5	3.2	Ductile	-0.7	Ductile

(1) Sample failed in 60 hours by thermal fatigue.

(2) Test halted after 80 hours.

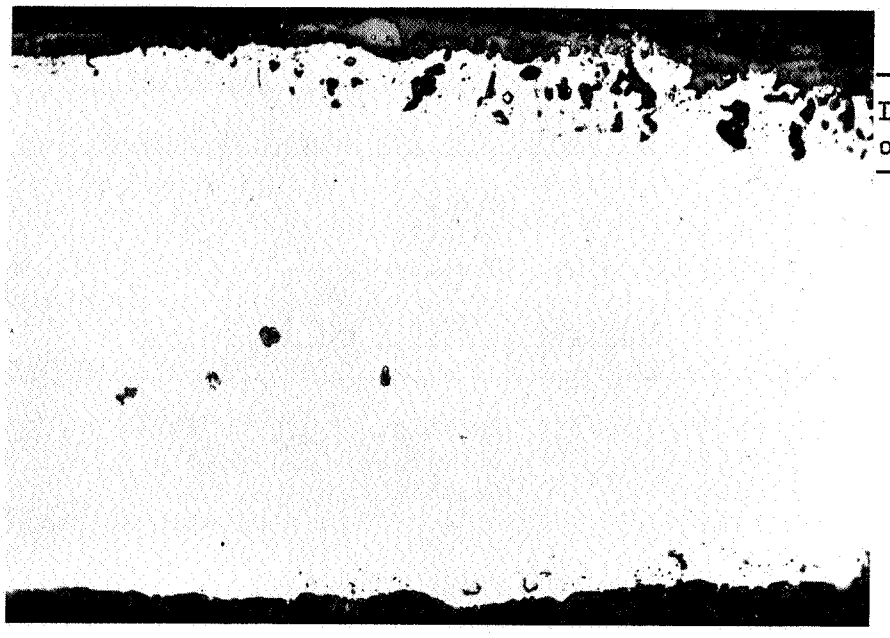

300X 28585

FIGURE 9. MICROSTRUCTURE OF ALUMINIZED Ni-20 WEIGHT PERCENT Cr-20 WEIGHT PERCENT W SAMPLE (4.5 WEIGHT PERCENT ALUMINUM) AFTER 100-HOUR CYCLIC OXIDATION AT 2300 F

Continuous weight measurements were made during static oxidation of samples aluminized to give about 4.5 percent aluminum. After 24 hours at 2300 F, both alloys showed about the same weight gain and were oxidizing in a parabolic manner. The microstructure of the two alloys after oxidation for 24 hours at 2300 F is shown in Figure 10. The surface appeared more irregular on the Ni-30Cr alloy, and a small amount of internal oxide was present. The Ni-20Cr-20W alloy showed evidence of tungsten depletion near the surface and appeared to show more uniform attack. No internal oxidation was apparent.

The weight change observed in samples oxidized at 2400 F is shown in Figure 11. Both nickel-base alloys showed poor oxidation resistance at 2400 F. Modification with 1.1 or 2.9 percent aluminum improved oxidation resistance somewhat, but not sufficiently to make the alloys useful at 2400 F. Samples containing 16.5 aluminum were completely embrittled after the first cyclic exposure at 2400 F.

Samples containing 4.5 percent aluminum were exposed to constant temperature oxidation for 24 hours at 2400 F. The Ni-30Cr alloy showed severe oxidation and some evidence of melting. In contrast, the Ni-20Cr-20W showed relatively little damage during this test. Considerable tungsten depletion throughout the sample thickness was evident, however, as shown in Figure 12.

After oxidation exposures of all thin cladding materials at 2300 and 2400 F, the samples were severely warped and distorted. This condition is more severe than would be expected when the materials are backed with the thick substrate. Although excessive oxide spalling may be linked to this distortion, the general indications of these studies are believed valid.

The results described above suggest that the Ni-30Cr alloy is sufficiently oxidation resistant to be used in the unmodified condition at 2100 F. At 2300 F, aluminum modification is necessary. At 2300 F, aluminized Ni-20Cr-20W alloys appear superior to aluminized Ni-30Cr alloys. Neither system appeared sufficiently oxidation resistant for service at 2400 F. It was concluded from these studies that modification with 4.5 percent aluminum (1750 F aluminizing treatment) was about optinum, and this treatment was selected for use in preparing clad chromium samples. Some study of unmodified Ni-30Cr-clad samples also appeared justified.

Examination of Cladding Variables

Several of the cladding systems were examined to determine the effects of gas-pressure bonding, aluminizing, and homogenizing on the structure of the interfacial region. These systems were 1a, 2a, 4, 5, 6, 7, and 8.*

Gas-pressure bonding for 2 hours at 2150 F using 10,000 psi pressure resulted in good bonding between the chromium alloy and the barrier layer and between the barrier layer and cladding layer. Some porosity was apparent between the two 0.5-mil tungsten foils used to provide the 1-mil barrier layer in System 7, but this tended to be eliminated during homogenization (see Figure 15 for an illustration of the porosity present after homogenization).

*To facilitate discussion, the various cladding systems are referred to by system number throughout this report. Systems are identified in Table 1, page 8.

400X 29591

(a) Aluminized Ni-30 weight percent Cr

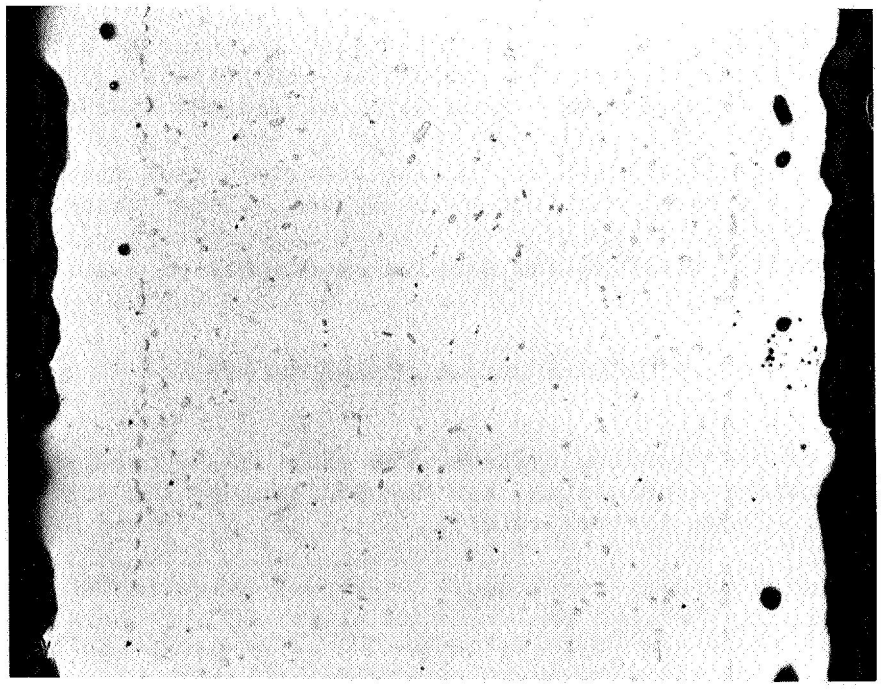

400X 29587

(b) Aluminized Ni-20 weight percent Cr-20 weight percent W

FIGURE 10. MICROSTRUCTURE OF ALUMINIZED NICKEL-BASE ALLOYS (4.5 WEIGHT PERCENT ALUMINUM) AFTER OXIDATION FOR 24 HOURS AT 2300 F

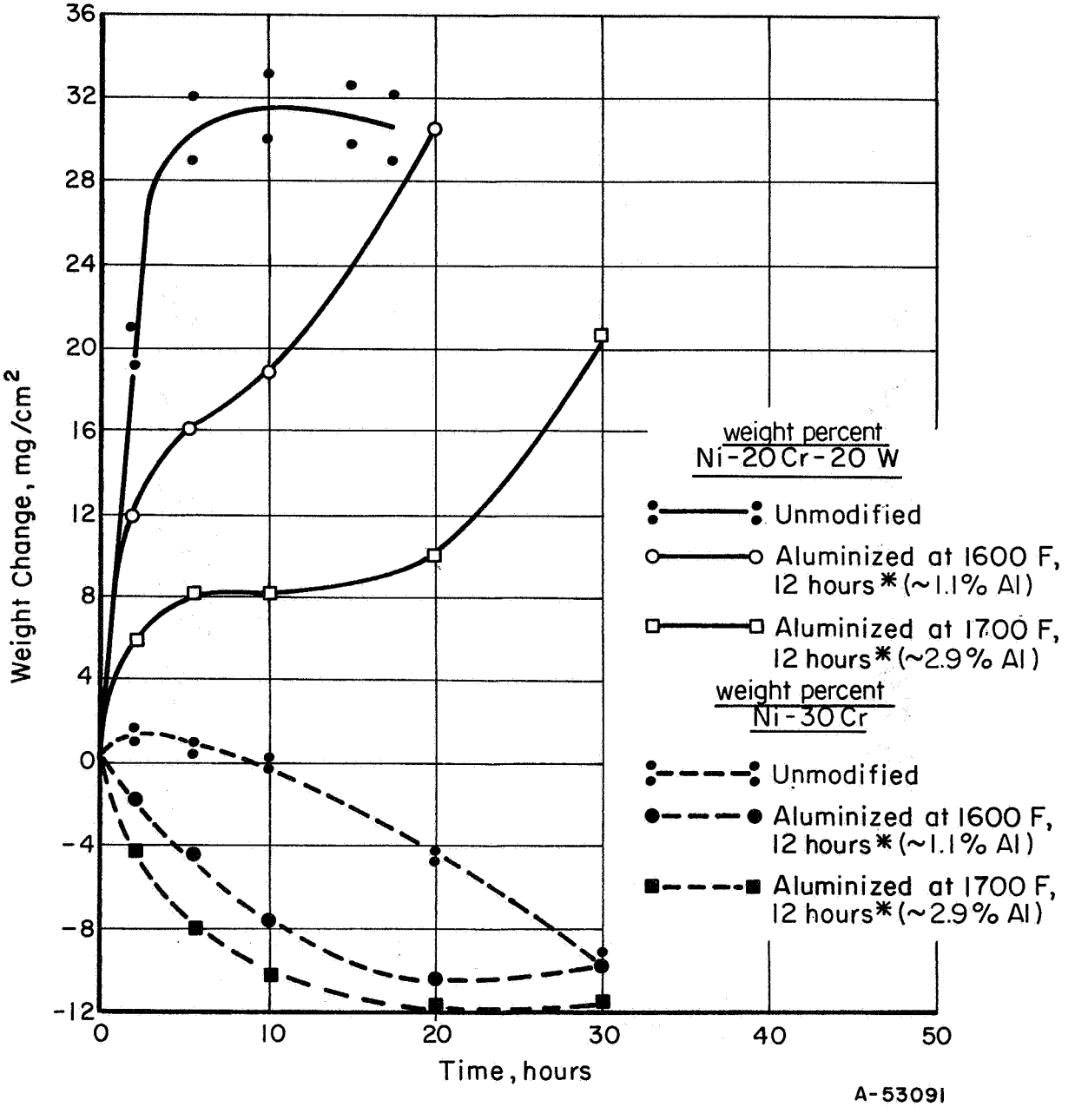

FIGURE 11. WEIGHT CHANGE DURING CYCLIC OXIDATION AT 2400 F

*Samples were homogenized at 2100 F for 25 hours.

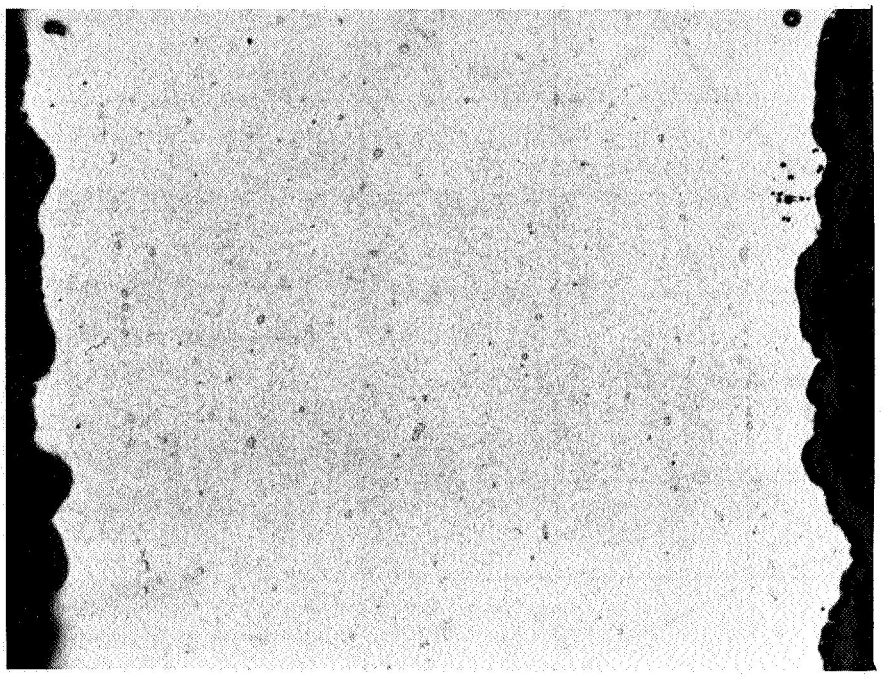

400X 29589

FIGURE 12. MICROSTRUCTURE OF ALUMINIZED Ni-20 WEIGHT PERCENT Cr-20 WEIGHT PERCENT W (4.5 WEIGHT PERCENT ALUMINUM) AFTER 24-HOUR OXIDATION AT 2400 F

Aluminum was deposited largely as intermetallic phases during aluminizing. Homogenization for 4 hours at 2100 F followed by 16 hours at 2200 F resulted in diffusion of the aluminum into the cladding layer. This is illustrated for a System 4 sample in Figure 13. Porosity tended to develop near the cladding surface during diffusion. The extent of porosity formation was generally greater during homogenization of aluminized Ni-30Cr claddings than during homogenization of aluminized Ni-20Cr-20W claddings. (This may be seen by comparing Figures 13, 15, and 16 with Figure 14.) The rapid diffusion of the platinum compatibility layer is apparent in these figures. Some diffusion of this layer occurred during gas-pressure bonding. After homogenization, this layer was not easily located.

The variation in hardness observed in the System 4 sample after bonding, after aluminizing, and after homogenizing is shown in Table 6. Diffusion of platinum into the cladding alloy caused a marked increase in hardness near the barrier layer. After homogenization, the hardness had dropped significantly as the platinum concentration was distributed more uniformly. Aluminum diffusion, combined with platinum diffusion during homogenization, increased the hardness of the cladding alloy but not excessively. No hardening of the chromium alloy was apparent throughout the processing schedule.

Measurements of the thickness of the barrier layer after the various processing steps are presented in Table 7. Of the seven systems examined, all but one, System 1a, contained a platinum compatibility layer. This system was the only one not showing significant loss of the barrier material during processing. Also, it was observed that System 8, which contained twice as much platinum as the other platinum-containing systems, showed the greatest loss of barrier material. The appearance of Systems 1a and 2a after homogenization is shown in Figure 14. The difference in the barrier layer thickness is readily apparent. Also, it can be seen that the platinum layer is not visible in System 2a after homogenization. Thus, the original intent of the platinum layer, to provide a region of intermediate thermal expansion between nickel and tungsten alloys and to prevent intermetallic compound formation, was unlikely to be successfully realized. Systems 7 and 8 are compared in Figure 15. These samples are identical except for the relative thicknesses of platinum and tungsten. Initially, System 7 contained 1 mil of tungsten and 0.5 mil of platinum. System 8 contained 0.5 mil of tungsten and 1.0 mil of platinum. Very little barrier layer was left in System 8 after homogenization.

Platinum appeared beneficial when using a W-25Re alloy barrier layer. In System 6, where no platinum was present, the barrier layer showed extensive cracking during homogenization. The System 5 sample did not show fragmentation, presumably due to the presence of platinum. The structures of these two systems are shown in Figure 16. The tungsten-rhenium alloy is apparently not compatible with Ni-30Cr in the absence of platinum. The fairly extensive attack of the barrier layer along the interface between the barrier and cladding in System 5 suggests that it is only marginally compatible when platinum is present.

These evaluations indicated that gas-pressure bonding to produce a composite cladding system was feasible and that a reasonably uniform aluminum addition could be made to the cladding alloy after bonding by vapor phase deposition and homogenization. They also indicated that solution of the barrier layer during prolonged elevated temperature exposure could be expected, and that the presence of platinum accelerated the rate of attack of the barrier. System 6 was shown to be defective after homogenization as a result of incompatibility between W-25Re and aluminized Ni-30Cr.

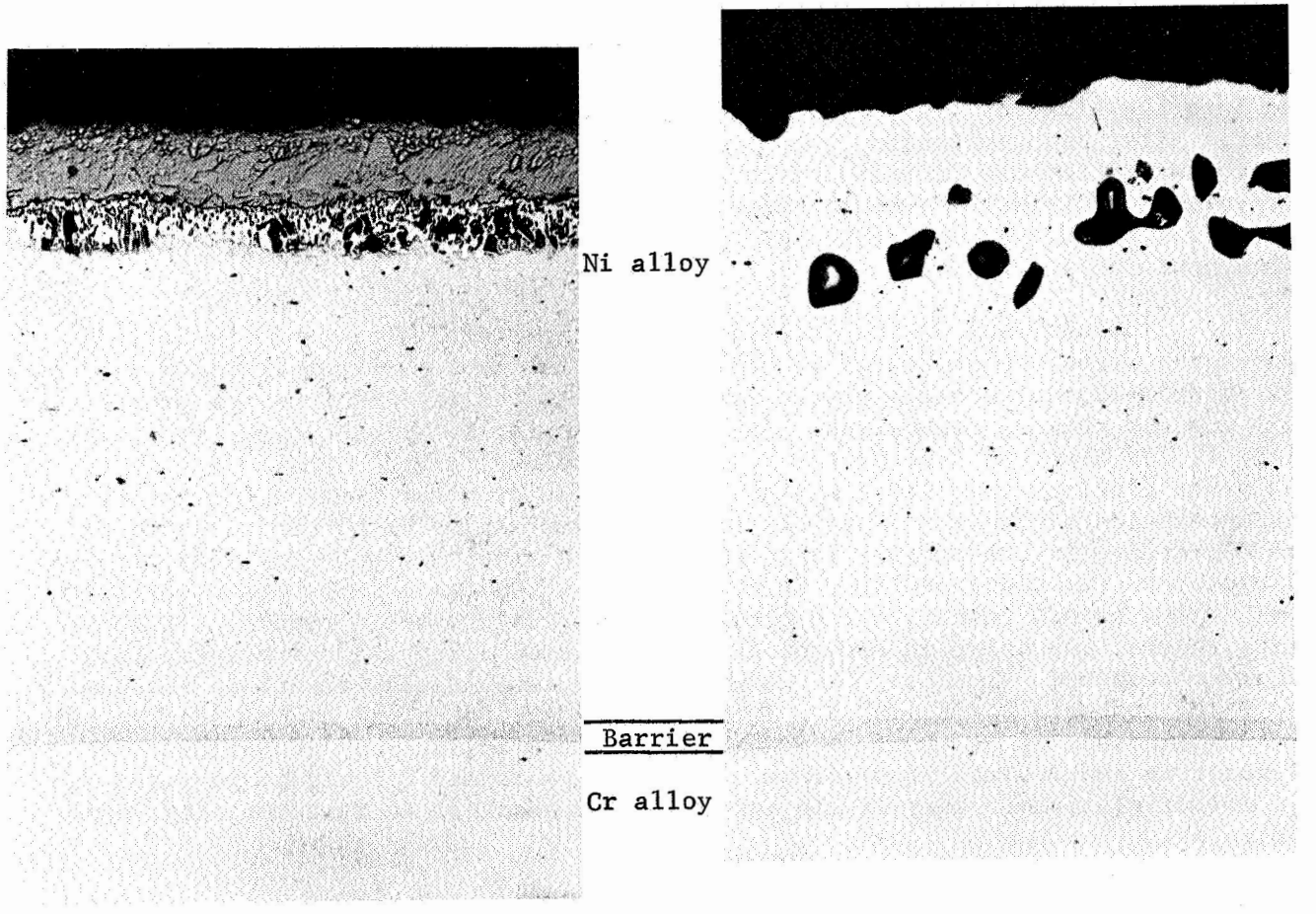

500X As aluminized 1A891

500X As homogenized 1A892

FIGURE 13. MICROSTRUCTURE OF SYSTEM 4 SAMPLE (IV-4) AFTER ALUMINIZING AND AFTER HOMOGENIZING

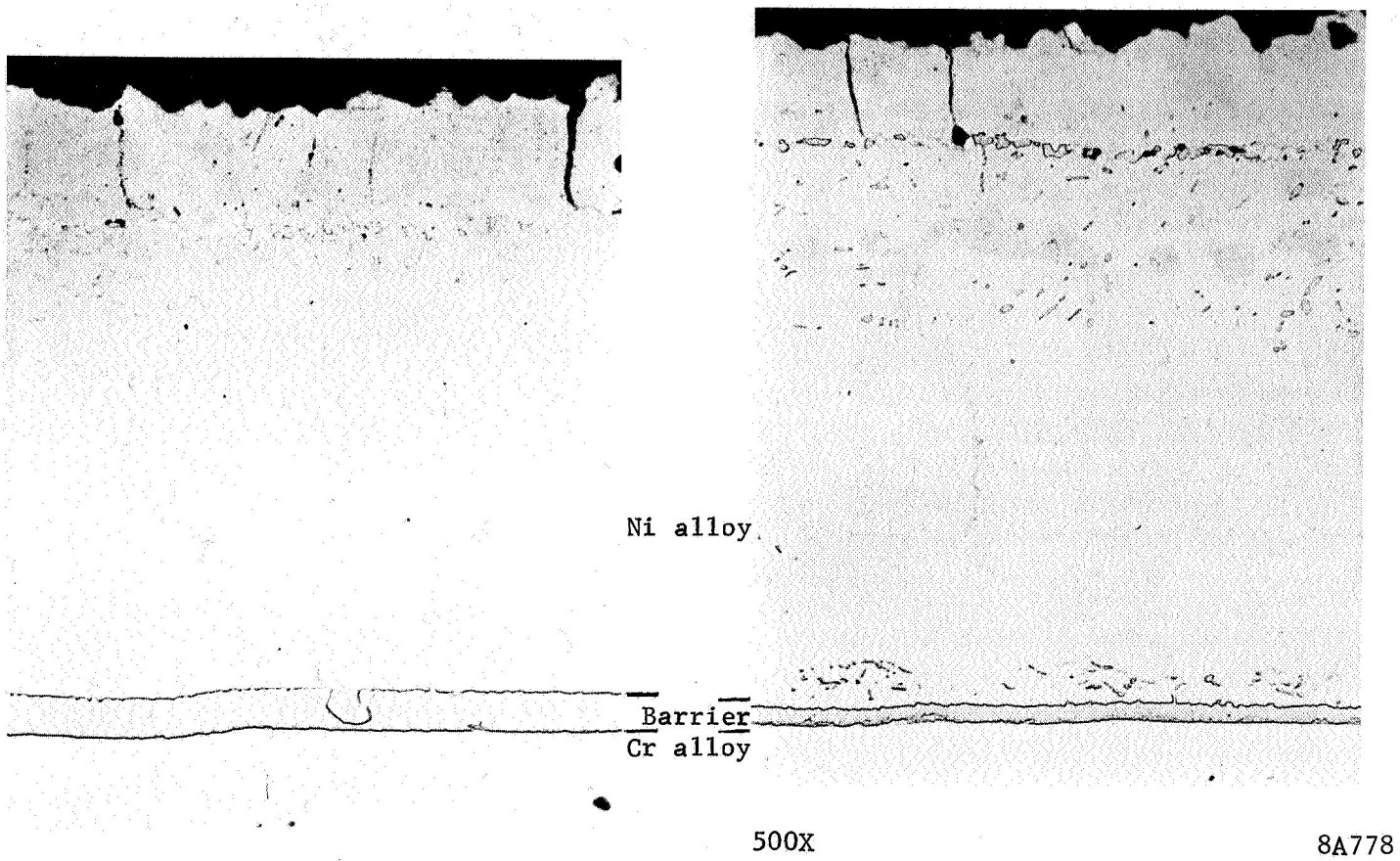

System 2a (II-8)

System 1a (I-9)

FIGURE 14. MICROSTRUCTURE OF SYSTEMS 1a (NO Pt LAYER) AND 2a (1/2-MIL Pt "COMPATIBILITY" LAYER) SAMPLES AFTER ALUMINIZING AND HOMOGENIZING

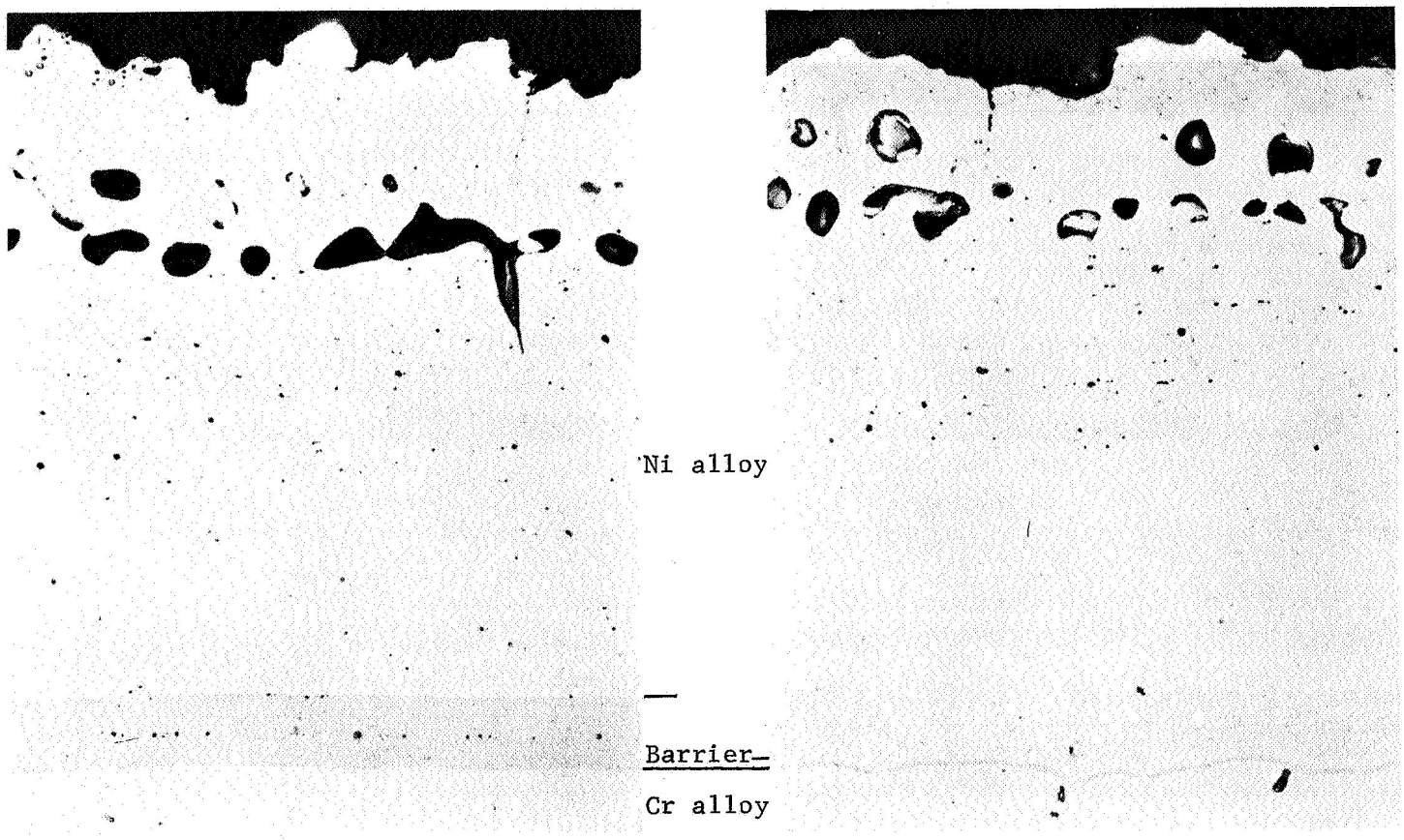

500X System 7 (VII-7) (1 mil W:1/2 mil Pt) 6A049 500X System 8 (VIII-7) (1/2 mil W:1 mil Pt) 6A050

FIGURE 15. MICROSTRUCTURES OF SYSTEMS 7 AND 8 SAMPLES AS HOMOGENIZED

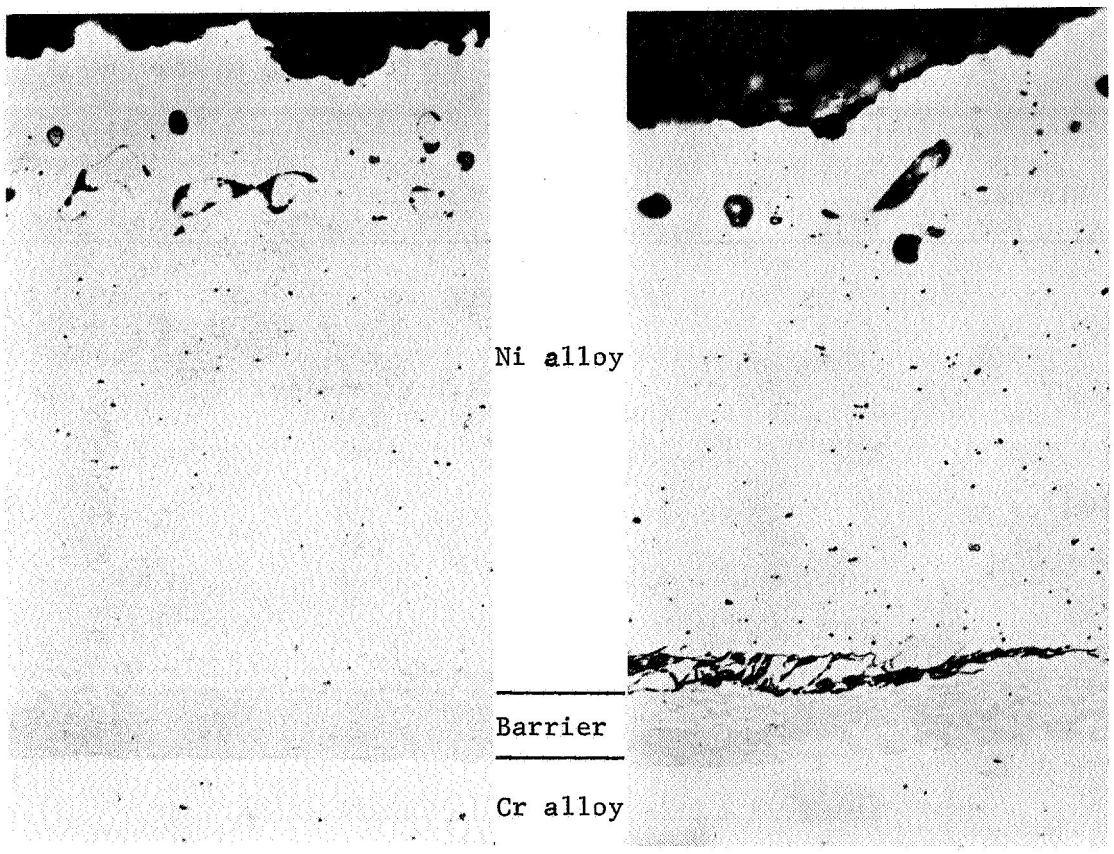

500X System 5 (V-9) (1/2 mil Pt) 6A047

500X System 6 (VI-3) (no Pt) 6A048

FIGURE 16. MICROSTRUCTURES OF SYSTEMS 5 AND 6 SAMPLES AS HOMOGENIZED (W-25 PERCENT Re BARRIER LAYER)

TABLE 6. KNOOP HARDNESS OF SYSTEM 4 SAMPLE AFTER VARIOUS PROCESSING STEPS (100-gram load)

Distance from Tungsten Barrier, mils	As Gas-Pressure Bonded	As Aluminized (5 mg/cm^2)	As Homogenized 4 hr 2100 F + 16 hr 2200 F
	Cladding Layer		
-5.5	-	440 (In aluminide)	(Porous)
-4	180	200	280
-3	170	220	270
-2	-	220	280
-1.5	280	240	-
-1	330	290	270
-0.5	630	680	320 (two phase regions)
	In Tungsten Barrier		
0	370	300	380
	Chromium-5 weight percent Tungsten Alloy		
1	200	220	220
2	200	230	210
3	230	230	210
4	220	240	220
5	240	220	230
10	210	240	240
20	230	240	240
30	230	220	220

TABLE 7. THICKNESS OF BARRIER LAYER AFTER VARIOUS TREATMENTS

System	Sample Number	Thickness of Tungsten Layer, mils			
		Initial	As Gas-Pressure Bonded	As Aluminized	As Homogenized
1a	I-9	~0.5	0.5	0.4	0.4
2a	II-8	~0.5	0.3	0.3	0.2
4	IV-12	~0.5	0.3	0.4	0.3
	IV-4	~0.5	0.5	0.3	0.3
5	V-9	~1.0	0.6	0.6	0.7
6	VI-3	~1.0	0.9	0.6	Extensive fracturing
7	VII-7	~1.0	1.0	0.9	0.7
8	VIII-7	~0.5	0.2	0.2	<0.1

Oxidation Resistance at 2100 F

The behavior of samples exposed to cyclic oxidation at 2100 F is summarized in Table 8, and photographs of a representative oxidation test sample of each system are shown in Figure 17. One would expect the weight gain in cyclic oxidation tests to be determined largely by the composition of the cladding alloy layer. However, diffusion of the barrier or compatibility layer into the cladding layer could alter the oxidation behavior. The weight gains measured in these tests are grouped according to cladding alloy in Table 9. In considering these data, it must be recognized that some inconsistencies are present owing to rupture of the cladding at corners and edges where the substrate contacted the massive picture frame. In Systems 1b, 2b, 9, 10, 11, and 12 and System 1a, Specimens 4 and 5, this localized clad defecting was prevented by including tungsten barrier layers at substrate edges. Notwithstanding, the extent of local clad defecting at 2100 F was considered sufficiently limited so that analyses of weight change data are generally valid. As shown in Table 9, the aluminized Ni-30Cr cladding showed the highest weight gain. A lower weight gain was observed in unaluminized Ni-30Cr and still less with aluminized Ni-20Cr-20W. It is not certain whether this represents differences in amount of oxidation or in the extent of spalling. Within each group of systems having similar surface cladding, some differences were observed. A portion of this difference no doubt is due to differences in amount and distribution of aluminum among the various samples. However, it is apparent that the composition of the barrier and compatibility layers also is significant. An extreme example of this is shown by System 9 which contained a vanadium compatibility layer. Vanadium resulted in rapid deterioration of the sample, apparently causing a molten oxide to form. Platinum appeared to increase the weight gain in samples clad with aluminized Ni-20Cr-20W or Ni-30Cr. In unaluminized Ni-30Cr-clad samples, platinum reduced the weight gain during oxidation. Examination of the surface appearance after oxidation (see Figure 17) shows several differences, as summarized below.

(1) The blistering tendency observed on System 6 was not seen on System 5. Thus, platinum may be beneficial in a Ni-30Cr-clad system where a W-Re barrier is used. System 6 was defective as processed, as pointed out in the previous section.

(2) Increased platinum changed the surface appearance of samples clad with aluminized Ni-30Cr. (The System 8 samples developed a mottled surface during oxidation.)

(3) Platinum had little effect on the surface appearance of samples clad with aluminized Ni-20Cr-20W (System 1a versus 2a, System 1b versus 2b and 2c).

(4) The use of Mo or W-1ThO_2 barrier instead of tungsten had little effect on surface appearance after oxidation.

(5) Vanadium present in the system caused a marked change in surface appearance.

TABLE 8. OXIDATION RESISTANCE DURING CYCLIC OXIDATION AT 2100 F

System	Sample Number	Weight Gain, mg/cm^2 in. 100 hr	200 hr	600 hr	Comments
1a	I-1	1.51	-		Extensive cracking at clad:picture frame junction.(1)
	I-4	0.61	0.61		Sample in excellent condition.
	I-5	0.74	0.71		One corner crack; otherwise in excellent condition.
1b	I-16	0.81	-		Sample appeared in good condition.
	I-19			1.15	All samples in good condition. Gray oxide formed. Some spalling on picture frame.
	I-23			1.19	
	I-24			1.22	
	I-26			1.23	
2a	II-1	1.95	-		Extensive cracking at clad:picture frame junction.(1)
	II-2	0.68	0.69		Samples in good condition except for cracks at corners where cladding joined picture frame.(1)
	II-3	0.84	0.91		
2b	II-17	1.01	-		Sample in good condition.
	II-18			0.93	Spalling on one edge; inadequate aluminizing.
	II-19			1.95	Samples in good condition. Some spalling late in test accounts for weight differences.
	II-20			1.28	
	II-24			1.17	
2c	II-9	1.55	1.86		Sample in excellent condition except for corner cracks.(1)
	II-10	2.63	-		Corners of cladding fracture at interface with picture frame and curled up.(1)
3	III-1	1.17	1.02		Oxide spalling began after about 50 hours. Weight loss occurred from this point. Some separation of cladding:picture frame junction.(1)
	III-2	0.85	-		
	III-3	0.68	0.23		
4	IV-1	2.42	-		Some cracking at cladding:picture frame junction, especially at corners.(1)
	IV-2	2.23	2.83		
	IV-3	1.90	2.49		
5	V-3	1.10	1.34		Samples in good condition. Cracks at one corner at picture frame:cladding junction.(1)
	V-4	1.22	-		
	V-5	1.32	1.62		
6	VI-1	1.02	1.32		Slight cracking at picture frame: cladding interface; otherwise good.(1)
	VI-2	1.08	-		
	VI-4	2.26 in 40 hours			Sample apparently defective.(1)
7	VII-1	1.38	1.69		Some cracking along picture frame: cladding junction.(1)

TABLE 8. (continued)

System	Sample Number	Weight Gain, mg/cm^2 in. 100 hr	200 hr	600 hr	Comments
7 (cont.)	VII-3	1.20 in 50 hours			Sample developed crack in cladding surface.(1)
	VII-4	2.24 in 90 hours			Sample developed crack in cladding surface.(1)
8	VIII-1	2.21	-		Sample in good condition except for cladding cracks over picture frame junction. Few small blisters on surfaces.(1)
	VIII-2	2.45	2.96		
	VIII-3	1.83	2.10		
9	IX-3	3.52 in 10 hours			Oxide melting and rapid attack occurred.
10	X-4	0.94	-		Sample in excellent condition.
11	XI-1	1.56	-		Sample in excellent condition.
12	XII-4	0.82	-		Sample in excellent condition.

(1) No tungsten barrier between picture frame and chromium alloy.

TABLE 9. SUMMARY OF WEIGHT CHANGES DURING CYCLIC OXIDATION AT 2100 F

System	Cladding Layer(1)	Compatibility Layer	Barrier Layer(1)	Weight Gain, mg/cm^2, after 100 hr	Weight Gain, mg/cm^2, after 200 hr
		Unmodified Ni-30Cr			
11	10 mil Ni-30Cr	-	1.5 mil W	1.56	-
3	5 mil Ni-30Cr	0.5 mil Pt	0.5 mil W	0.90	0.62
		Aluminized Ni-30Cr			
4	5 mil Ni-30Cr:5Al	0.5 mil Pt	0.5 mil W	2.18	2.66
7	Ditto	Ditto	1.0 mil W	1.38	1.69
8	"	1.0 mil Pt	0.5 mil W	2.16	2.53
6	"	-	1.0 mil W-25Re	1.05	1.32
5	"	0.5 mil Pt	Ditto	1.21	1.48
		Aluminized Ni-20Cr-20W			
1a	5 mil Ni-20Cr-20W:5Al	-	0.5 mil W	0.68	0.66
2a	Ditto	0.5 mil Pt	Ditto	0.77	0.80
1b	"	-	1.5 mil W	0.81	-
2b	"	0.5 mil Pt	Ditto	1.01	-
2c	"	1.0 mil Pt	1.0 mil W	1.55	1.86
12	"	0.5 mil Pt	2 mil W-1ThO_2	0.82	-
10	"	Ditto	2.0 mil Mo	0.94	-
9	"	1 mil V	1.5 mil W	$\gg$3.52	-

(1) Alloy compositions and aluminum additions given in weight percent.

System 1a (I-5)

System 1b (I-16)

System 2a (II-2)

System 2b (II-17)

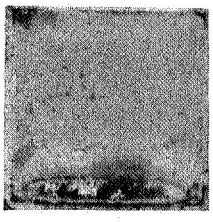

System 2c (II-9)

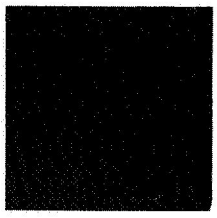

System 3(III-2)

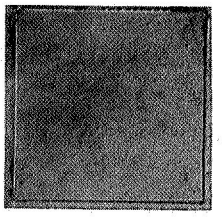

System 4 (IV-1)

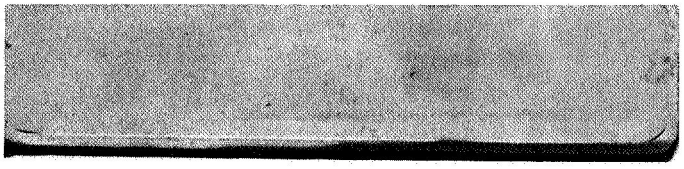

System 5 (V-3)

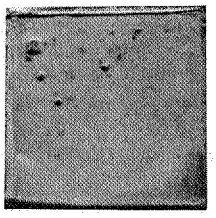

System 6 (VI-2)

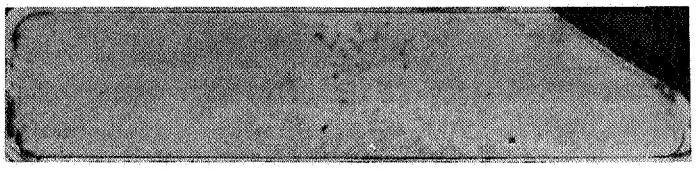

System 7 (VII-1)

FIGURE 17. APPEARANCE OF OXIDATION SAMPLES AFTER 100-HOUR CYCLIC EXPOSURE AT 2100 F WITH 2-HOUR CYCLES [( ) = sample number]

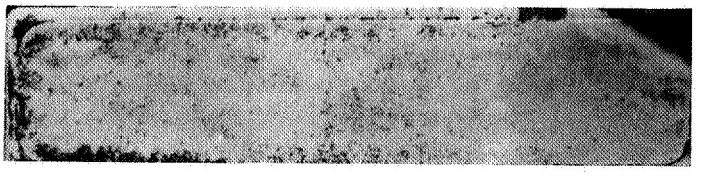

System 8 (VIII-2)

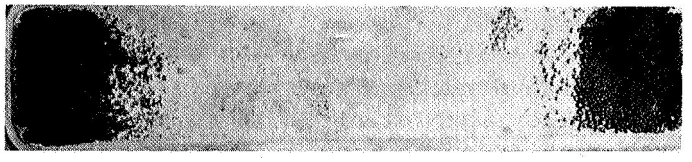

System 9 (IX-3)
(This sample exposed only 10 hours)

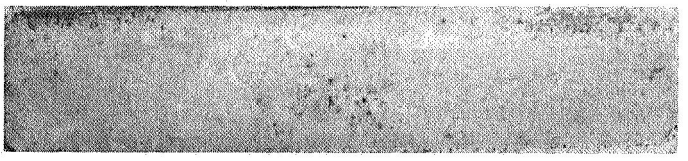

System 10 (X-4)

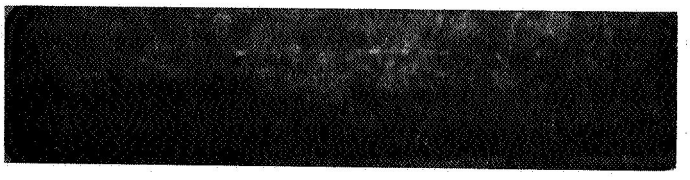

System 11 (XI-1)

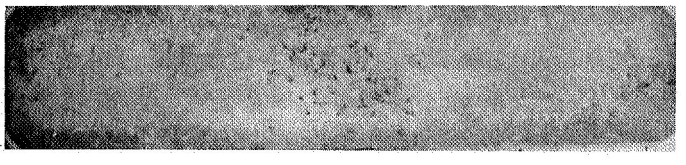

System 12 (XII-4)

FIGURE 17. (continued)

Of much more importance than weight gain or surface appearance is the microstructural changes at the interface between the chromium-base alloy and the cladding layers occurring during cyclic oxidation. The microstructures of two clad samples after cyclic oxidation exposure for 200 hours at 2100 F are shown in Figure 18. Both samples developed a considerable amount of cracking of the tungsten barrier layer. Pitting of the chromium alloy, apparently as a result of diffusion through the cracked regions in the barrier layer is also apparent. The platinum layer originally present in System 2a is not visible indicating complete solution and diffusion. The severity of break-up of the tungsten layer appeared greater in the platinum-containing system. The cladding layer was in reasonably good shape in both samples.

Figure 19 illustrates the appearance of two samples, one of System 1b and one of System 2b, after cyclic oxidation for 100 hours at 2100 F. An etch designed to develop the chromium grain structure was used. This etch results in appreciable staining of the cladding alloy when platinum is present, which accounts for the unusual appearance of the clad layer in Sample II-17. An obviously different etching response is seen in both samples in the chromium alloy immediately beneath the barrier layer for a depth of one or two grains. This apparently results from diffusion of the cladding alloy. Cracking of the barrier layer is extensive in both samples. However, there is no evidence of nitride contamination in the samples, which would show up as a grain boundary phase and as needles within the grains (see Figure 36, page 75). Extensive separation along the cladding:barrier layer interface on Sample I-16 was observed.

One sample was analyzed to determine if nitrogen contamination occurred during cyclic oxidation at 2100 F. This sample, I-23, a System 1b sample exposed for 600 hours at 2100 F using 20-hour oxidation cycles, contained 180 ppm nitrogen by analysis. The base analysis of the chromium alloy was 50 ppm. Thus, it appears that the cladding system provided quite good protection against nitrogen contamination at 2100 F.

A further illustration of the structure at the interface region is shown in Figure 20. As polished, it appears that some tungsten diffusion into the cladding alloy layer has occurred since a second phase, which resembles tungsten, is seen in the aluminized Ni-30Cr alloy extending about 0.5 mil into the cladding layer. A diffusion region of variable depth is seen in the chromium-base alloy. The depth of this layer is greatest under cracks in the tungsten. Etching in Murakami's etch results in development of the tungsten microstructure (and also solution of the tungsten-rich phase in the cladding alloy near the tungsten:cladding alloy interface).

Measurements of the barrier layer thickness after oxidation exposure indicated that the tungsten barrier tended to dissolve only slightly into alloy or the cladding layer. This was true in both platinum-containing and platinum-free systems. Little change in tungsten thickness occurred beyond that attributable to the homogenization anneal. The solution rate of the W-25Re barrier was much more rapid than that of unalloyed tungsten, and the barrier appeared two-phase after cyclic exposure. The appearance of the W-25Re barrier in System 5 after 200 hours at 2100 F is shown in Figure 21a. In some cases, the tungsten barrier also developed a two-phase appearance when etched in Murakami's etch as shown in Figure 21b. This is believed to be an etch artifact, however. The W-1ThO_2 barrier in System 12 shown in Figure 22 appeared to develop cracks in much the same manner as unalloyed tungsten. The molybdenum barrier was apparently incompatible with the chromium alloy and the cladding alloy as extensive fracturing occurred throughout the molybdenum-rich region during cyclic oxidation.

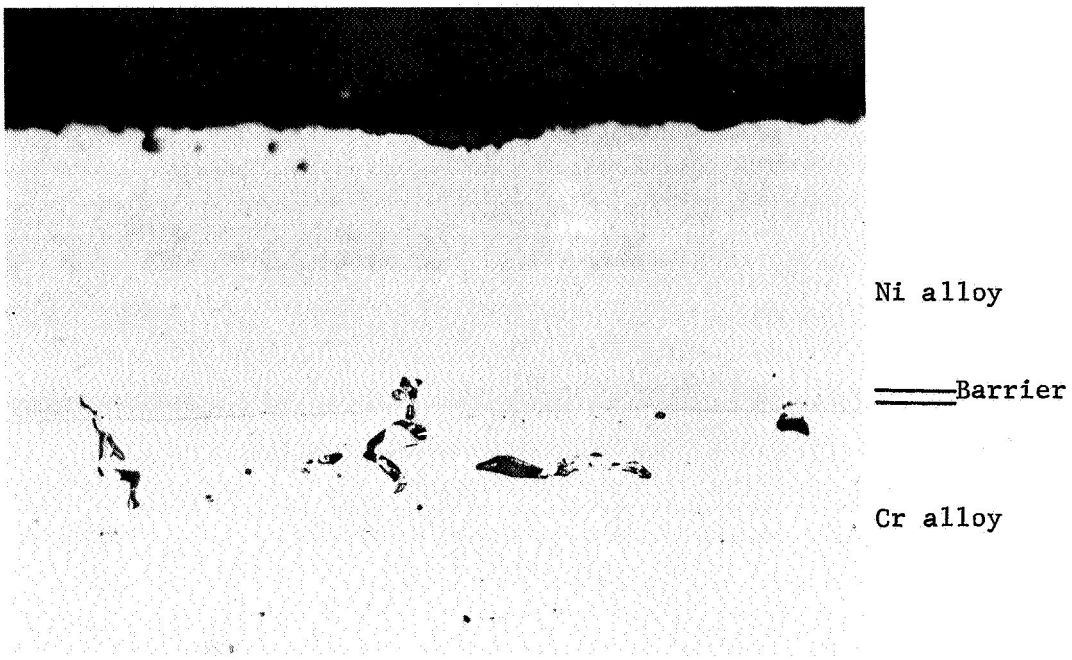

250X System 1a--Sample I-5 (no Pt) 6A694

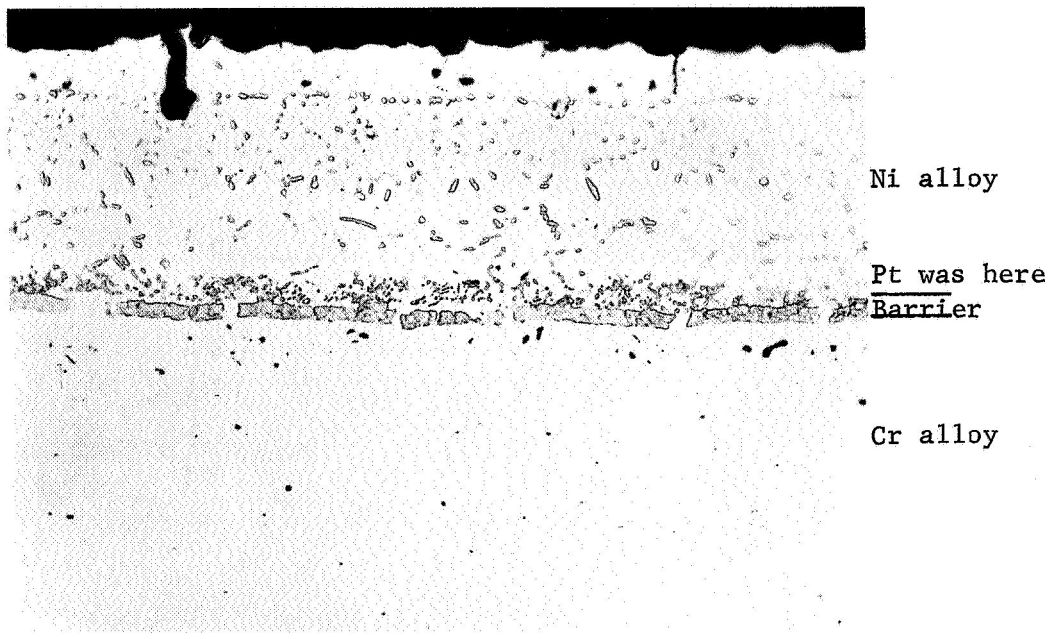

250X System 2a--Sample II-2 (1/2 mil Pt) 6A695

FIGURE 18. MICROSTRUCTURE OF TWO CLAD CHROMIUM SAMPLES AFTER CYCLIC OXIDATION EXPOSURE FOR 200 HOURS AT 2100 F

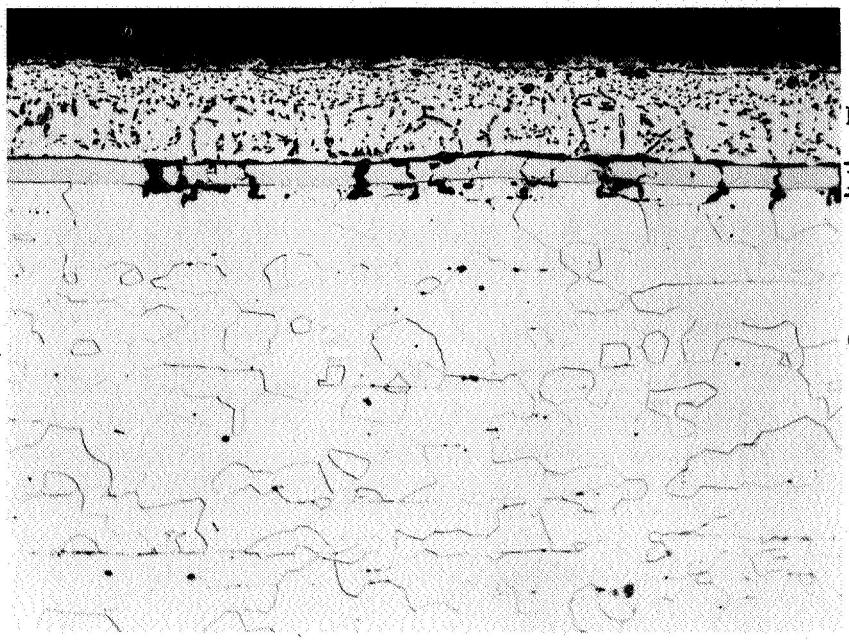

100X System 1b--Sample I-16 (no Pt) 5B215

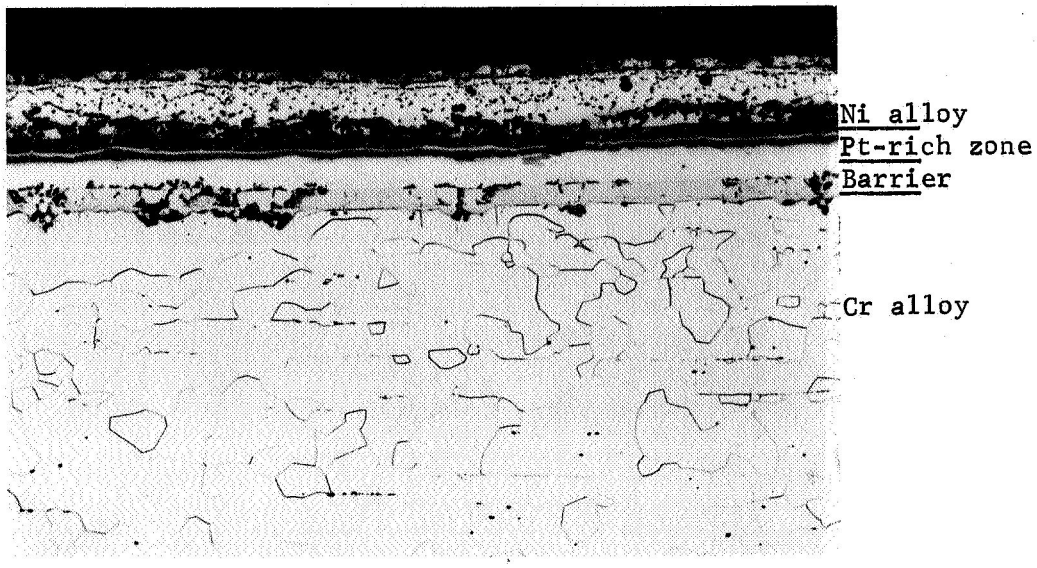

100X System 2b--Sample II-17 (1/2 mil Pt) 5X218

FIGURE 19. MICROSTRUCTURE OF TWO CLAD CHROMIUM ALLOYS AFTER CYCLIC EXPOSURE FOR 100 HOURS AT 2100 F

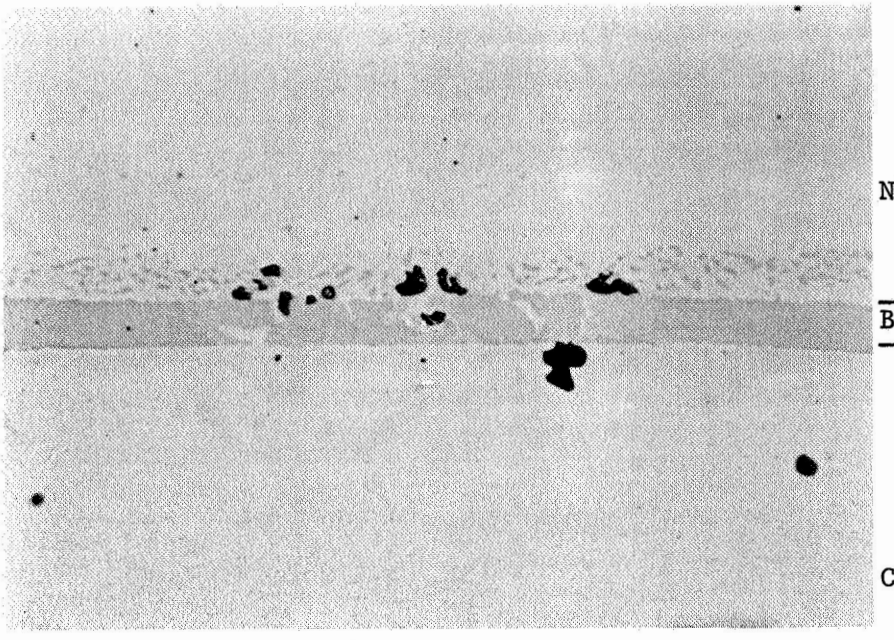

750X (a) As polished 3A435

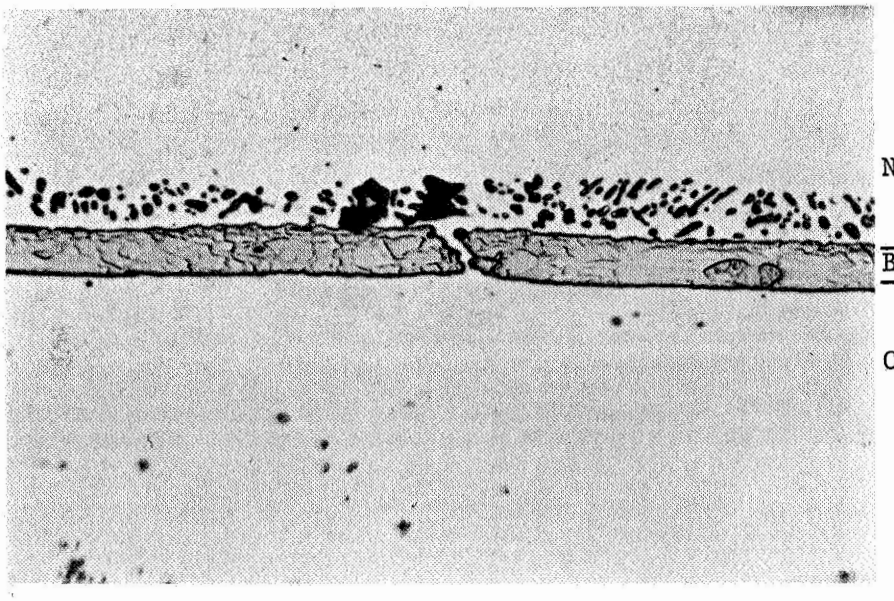

750X (b) Murakami's etchant 3A441

FIGURE 20. APPEARANCE OF THE TUNGSTEN INTERFACIAL AREA OF SAMPLE IV-1, SYSTEM 4 AFTER 100 HOURS CYCLIC OXIDATION EXPOSURE

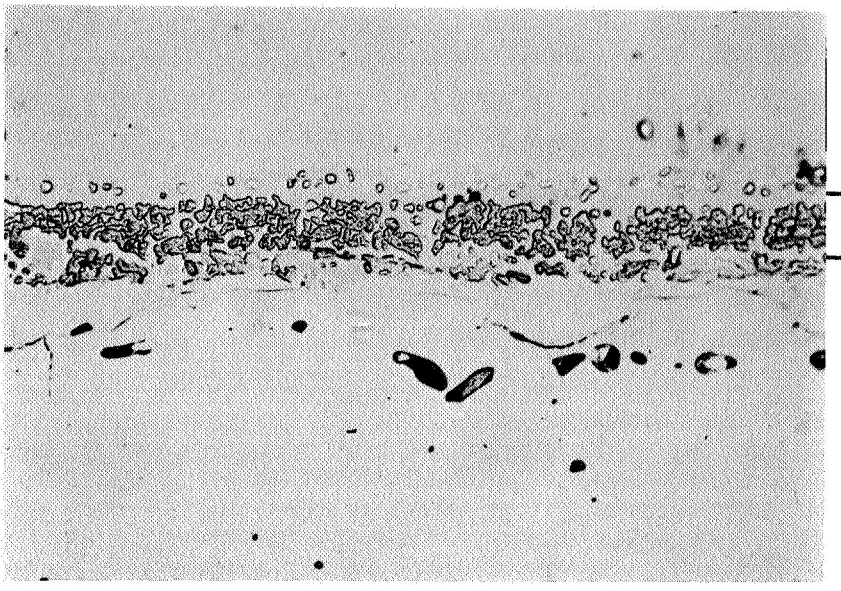

500X 8A773

(a) System 5--Sample V-3 (200 hours)
(W-25 weight percent Re barrier)

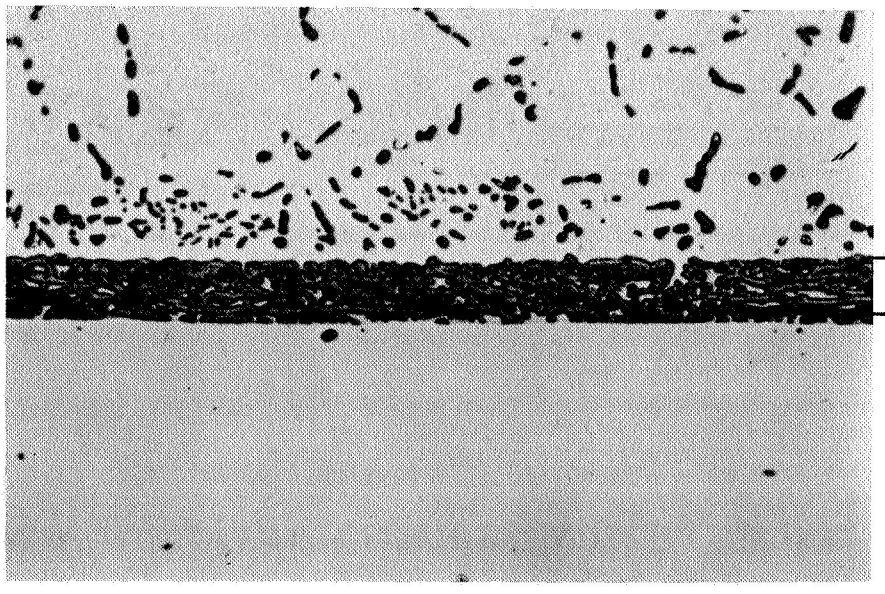

750X 3A440

(b) System 2a--Sample II-1 (100 hours)
(W barrier)

FIGURE 21. APPEARANCE OF BARRIER LAYER IN TWO SAMPLES AFTER CYCLIC OXIDATION AT 2100 F

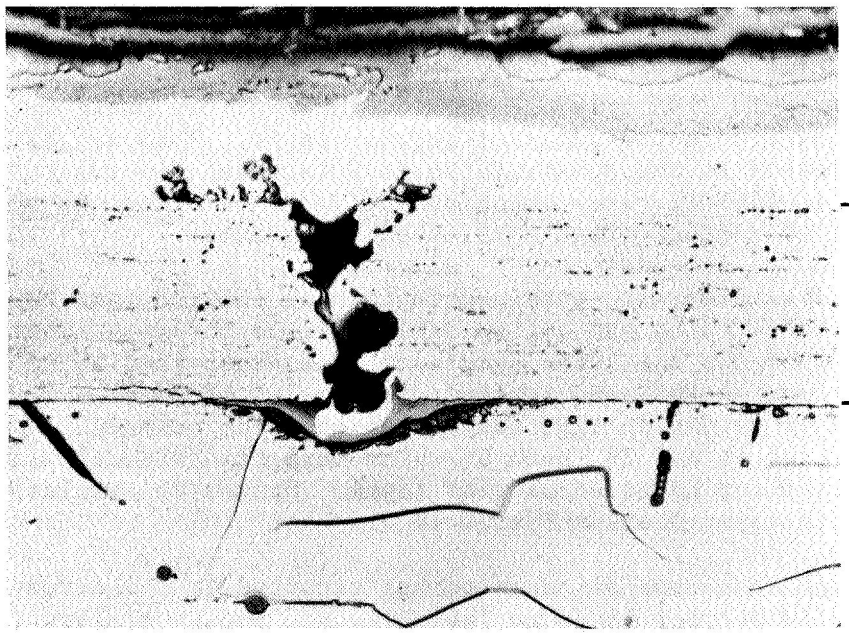

500X 5B227

FIGURE 22. APPEARANCE OF W-1 WEIGHT PERCENT ThO_2 BARRIER IN SAMPLE XII-4, SYSTEM 12, AFTER 100 HOURS CYCLIC OXIDATION AT 2100 F

Samples from two of the systems, 1b and 2b, were oxidized using prolonged exposure at 2100 and 1400 F. One sample of each system was exposed for 100 continuous hours at 2100 F followed by 100 continuous hours at 1400 F. A second sample was exposed 100 continuous hours at 2100 F, then 100 continuous hours at 1400 F, and finally 60 continuous hours at 2100 F. These exposure conditions were designed to show if prolonged intermediate temperature exposure was harmful to the cladding system. The results of these tests are shown in Table 10. All four samples appeared in excellent condition at the completion of the test. The microstructure of the System 1b sample exposed to the 2100 F:1400 F:2100 F sequence is shown in Figure 23. Separation of the cladding at the tungsten: chromium alloy interface is apparent in this figure; however, much of the cladding remained well bonded. This separation may have occurred during sectioning for metallographic examination. Of special interest is the absence of cracks in the tungsten barrier layer irrespective of whether cladding separation had occurred. Apparently, the cracking of tungsten observed during cyclic oxidation testing is the result of thermal cycling. In regions away from the separation shown in Figure 23, no contamination was metallographically apparent. However, the System 1b sample exposed only to 2100 F:1400 F showed a precipitate phase extending about 2 mils beneath the undefected tungsten barrier layer. This suggests that metallic contamination present at the substrate surface exceeded the solubility limit at 1400 F, but not at 2100 F. The companion specimens of System 2b showed metallographic evidence of contamination after both treatments.

Several samples were examined to gain an insight into the factors affecting cracking of the tungsten and contamination of the chromium substrate. These included a number of the oxidation samples already described as well as a few samples prepared primarily for bend testing. These latter samples were included because of the longer oxidation time they received. The primary comparisons were made between Systems 1b and 2b, both of which were clad with aluminized Ni-20Cr-20W and had a 1.5-mil-thick tungsten barrier layer. System 2b samples contained a platinum compatibility layer whereas System 1b did not.

Although some loss of tungsten has occurred as indicated by the thickness measurements of the barrier layer in Table 11, the amount of loss is small at 2100 F. No consistent change with time at 2100 F is apparent suggesting that most of the loss in tungsten occurred during processing of the sample. Chromium pits tended to develop under cracks in the tungsten barrier. The appearance of the pitting and contamination observed in these samples after 600 hours oxidation exposure at 2100 F is shown in Figures 24 and 25. Examination of the data for Systems 1b and 2b in Table 11 suggests that the tendency for cracking of the tungsten and pitting in the chromium is partially related to the number of thermal cycles. (Sample II-20 is believed to have developed separation at the barrier:chromium interface early in the test. A good measurement of pit spacing and depth could not be made.) Thus, the pit spacing is smallest in those samples (I-16 and II-17) having the most number of cycles. The depth of pitting and the depth of contamination appear related to the oxidation time. This is illustrated in Figure 26. The depths of both pitting and contamination appeared to vary with the square root of time ($d \sim t^{1/2}$). Although the differences were slight, System 1b showed slightly less contamination than 2b, suggesting that the presence of platinum may be undesirable.

Considerable interface pitting or separation was also observed in these samples. This was of two types, separation along the cladding:barrier interface and separation along the barrier:chromium interface. These two types of separation are shown in Figures 19 and 23, respectively. Separation along the barrier:

TABLE 10. WEIGHT GAIN DURING INTERMEDIATE TEMPERATURE OXIDATION

System	Sample Number	Weight Gain, mg/cm^2, during static oxidation: 1st Exposure, 100 hr 2100 F	2nd Exposure, 100 hr 1400 F	3rd Exposure, 60 hr 2100 F
1b	I-18	0.8	0.01	-
	I-17	0.6	0.01	0.4
2b	II-23	0.8	0.00	-
	II-21	0.8	0.01	0.3

Note: Samples were air cooled to room temperature after each exposure period.

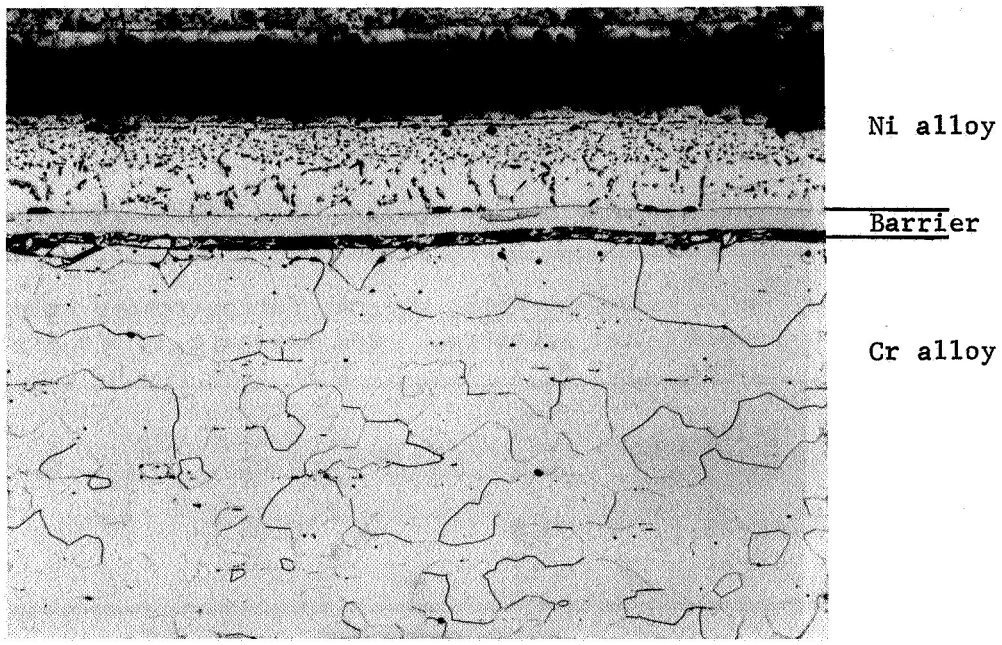

100X 5B232

FIGURE 23. APPEARANCE OF SYSTEM 1b SAMPLE AFTER OXIDATION AT 2100 F FOR 100 HOURS, 1400 F FOR 100 HOURS, AND 2100 F FOR 60 HOURS (I-17)

TABLE 11. RESULTS OF METALLOGRAPHIC SURVEY OF SEVERAL SAMPLES OXIDIZED AT 2100 F

System	Sample Number	Exposure Conditions: Time at 2100 F, hr	Exposure Conditions: No. of Cycles	Thickness, mils, of: Barrier	Thickness, mils, of: Cladding	Chromium Pits, mils: Avg. Depth	Chromium Pits, mils: Avg. Pit Spacing	Depth of Visible Contamination, mils	Interface Separation: Clad:Barrier	Interface Separation: Barrier:Cr
1b	I-18	100	2	1.2	5.9	0	-	2.3	None	None
	I-17	160	3	1.1	5.7	0	-	0	None	Lots
	I-16	100	50	1.2	6.6	1.0	4.0	0.5	Some	None
	I-31(1)	300	15	1.2	5.7	1.3	9.1	3.6	Lots	None
	I-19(1)	600	30	1.4	5.8	2.4	9.6	4.0	Some	Some
2b	II-23	100	2	1.0	6.3	1.0	Variable	3.1	None	None
	II-21	160	3	0.9	6.8	0.8	7.1	2.4	None	None
	II-17	100	50	1.0	5.9	1.0	4.4	3.5	Some	None
	II-33(1)	300	15	1.2	6.4	1.6	8.5	4.5	Lots	Lots
	II-20(1)	600	30	1.2	5.9	-	-	6.2	Some	Lots
11	XI-1	100	50	1.2	9.9	1.2(2)	16.5(2)	0	None	None
12	XII-4	100	50	2.2	6.5	0.7	14.5	2.3	None	None

(1) These are bend samples.

(2) Only one surface of sample showed pits.

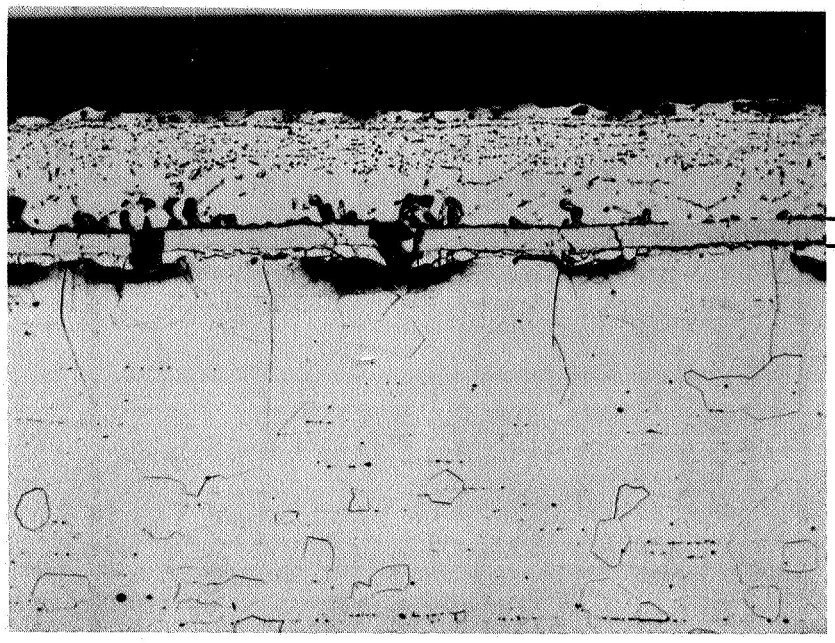

100X 5B234

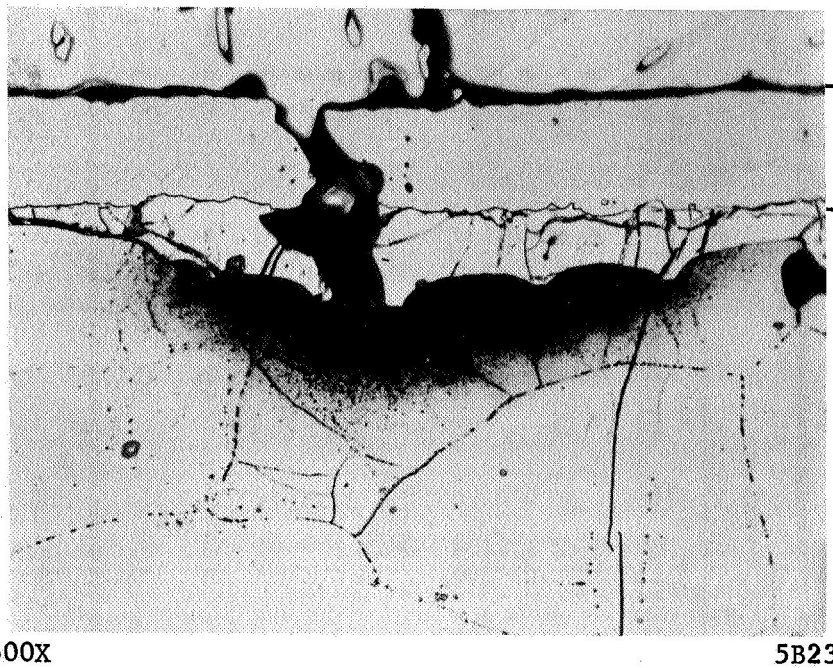

500X 5B235

FIGURE 24. MICROSTRUCTURE OF SYSTEM 1b SAMPLE (I-19 AFTER CYCLIC OXIDATION FOR 600 HOURS AT 2100 F (20-HOUR CYCLES)

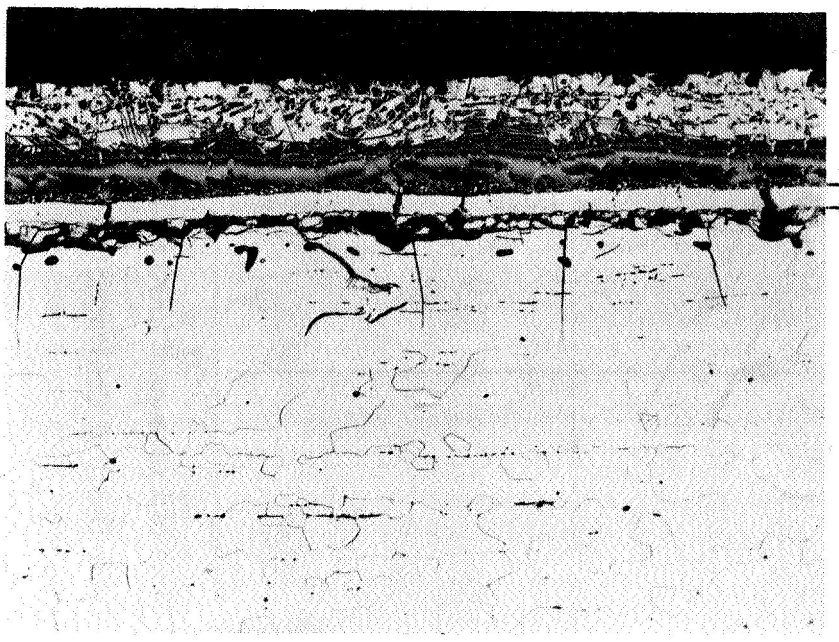

100X 5B236

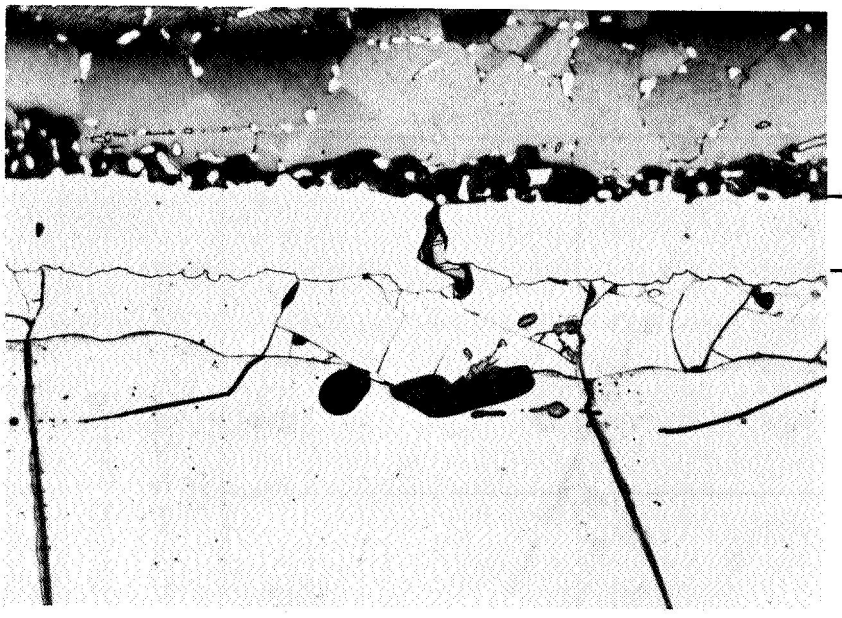

500X 5B237

FIGURE 25. MICROSTRUCTURE OF SYSTEM 2b SAMPLE (II-20) AFTER CYCLIC OXIDATION FOR 600 HOURS AT 2100 F (20-HOUR CYCLES)

Oxalic acid electrolytic etch.

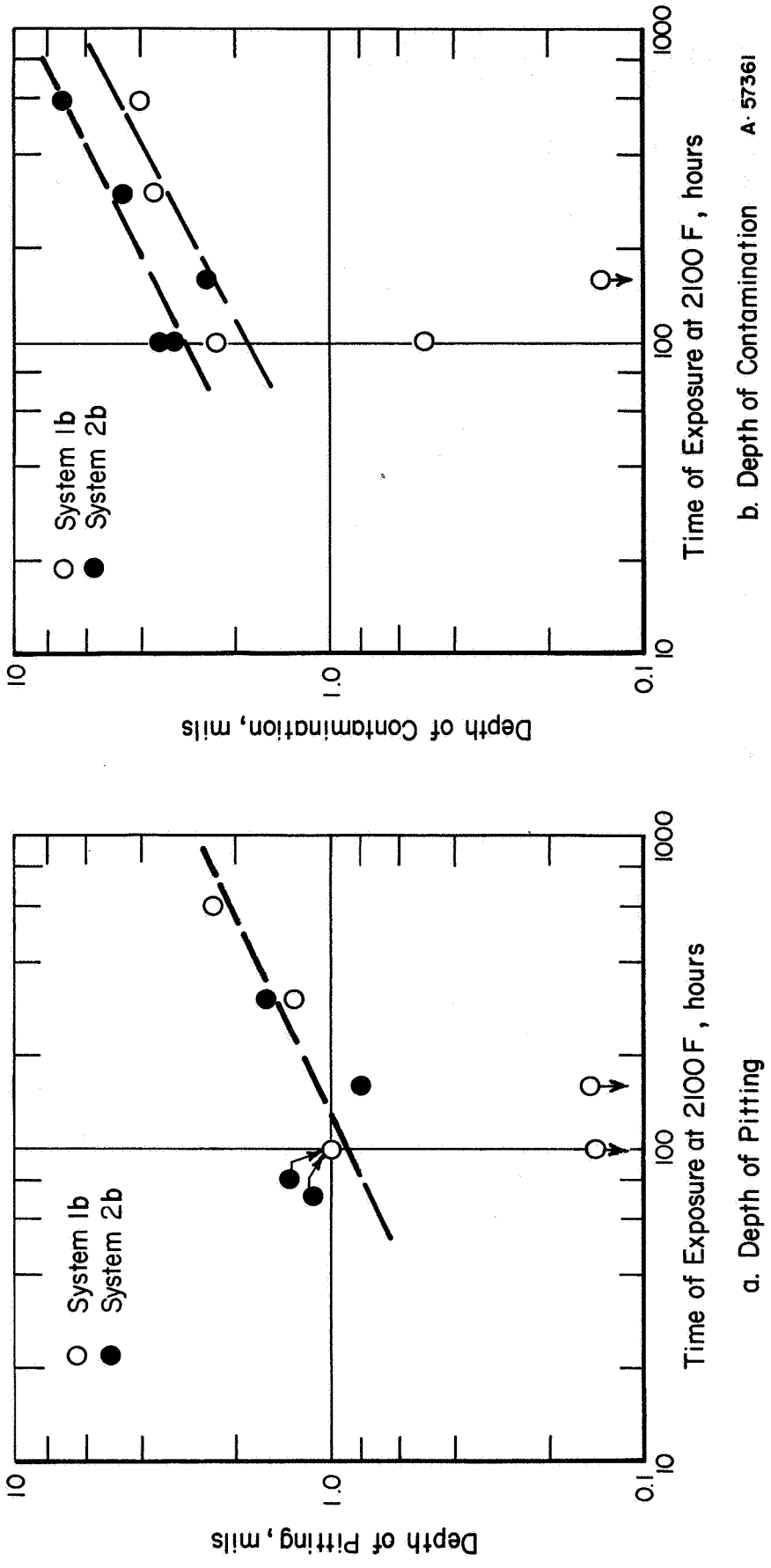

FIGURE 26. DEPENDENCE OF DEPTH OF PITTING AND CONTAMINATION ON TIME OF OXIDATION AT 2100 F

chromium interface may have occurred during sample sectioning for metallographic examination. As shown in Table 11, both types of separation appeared related more to exposure time than to number of cycles. Separation of the barrier:cladding interface was similar in both systems. Barrier:chromium separation was greater in System 2b, again suggesting that platinum may be harmful.

Data for two other systems, 11 and 12, are also given in Table 11. Both appear superior to Systems 1b and 2b from the standpoint of durability of the system under cyclic oxidation conditions at 2100 F. The crack frequency in the barrier layer is less and the depth of visible contamination is less. Neither system was free from barrier layer defects after oxidation exposure, however.

The extensive visual contamination and pitting observed in these samples suggested that significant interdiffusion of cladding and chromium alloy elements was occurring. Electron microprobe analyses were made in the vicinity of a pit in a System 1a sample. The sample examined, I-5, had received 200 hours cyclic oxidation exposure at 2100 F. Figure 27 shows the variation in Ni, Cr, and W near a crack in the tungsten. The cladding layer was aluminized Ni-20Cr-20W, but detection of aluminum was not possible with the particular instrument used. The values indicated are relative intensity, not weight percent. The cladding layer shows the expected alloy variation, with occasional high tungsten areas as second-phase particles are traversed. It appears that chromium content increases as the barrier is approached suggesting diffusion from the chromium alloy into the cladding alloy. The nickel content decreases near the barrier layer. Very little diffusion of tungsten into the cladding alloy is observed. Some nickel and a lesser amount of chromium have apparently diffused into the tungsten barrier. The chromium alloy shows a significant loss of chromium near the barrier layer, and an increase in tungsten and nickel. Tungsten penetration into the alloy was only about 1 mil, but nickel was detected 4 mils below the barrier. A second traverse, made through the discontinuity in the barrier layer, is shown in Figure 28. This traverse is similar to that shown in Figure 27. The principal differences are a greater increase of chromium in the cladding layer and depletion of chromium to a greater depth in the base metal.

The microprobe analyses show major diffusion is occurring across the barrier layer, chromium diffusing into the cladding layer from the alloy and nickel diffusing into the alloy from the cladding layer. Some tungsten diffusion into the alloy from the barrier is also apparent. Although it is felt that diffusion was favored by the discontinuities in the tungsten, microprobe analysis made on a crack-free sample of System 1b (I-17) showed some transfer of material across the barrier layer. The depth of penetration was less, however. Nickel was detected about 1 mil into the chromium alloy. Tungsten was detected to 3/4 mil. Aluminum distribution was also examined using a more sensitive microprobe instrument. Except for trace indications in intermetallic-like inclusions near the cladding surfaces, no aluminum was detected in the cladding alloy. A cyclically oxidized sample of System 11 (XI-1) was also examined using the microprobe. This sample was cracked, but not too severely. The traverse was made in a crack-free area. Nickel was not detected in the chromium alloy (a 1.5-mil barrier layer of tungsten was present) and the chromium depletion near the barrier was small and extended only about 0.5 to 0.75 mils into the alloy.

A further indication of the contamination occurring in the substrate through the barrier layer and its relationship to cracks in the barrier is shown by the microhardness data given in Table 12. Two traverses were made for each sample, one below a crack in the barrier layer and one below a crack-free region

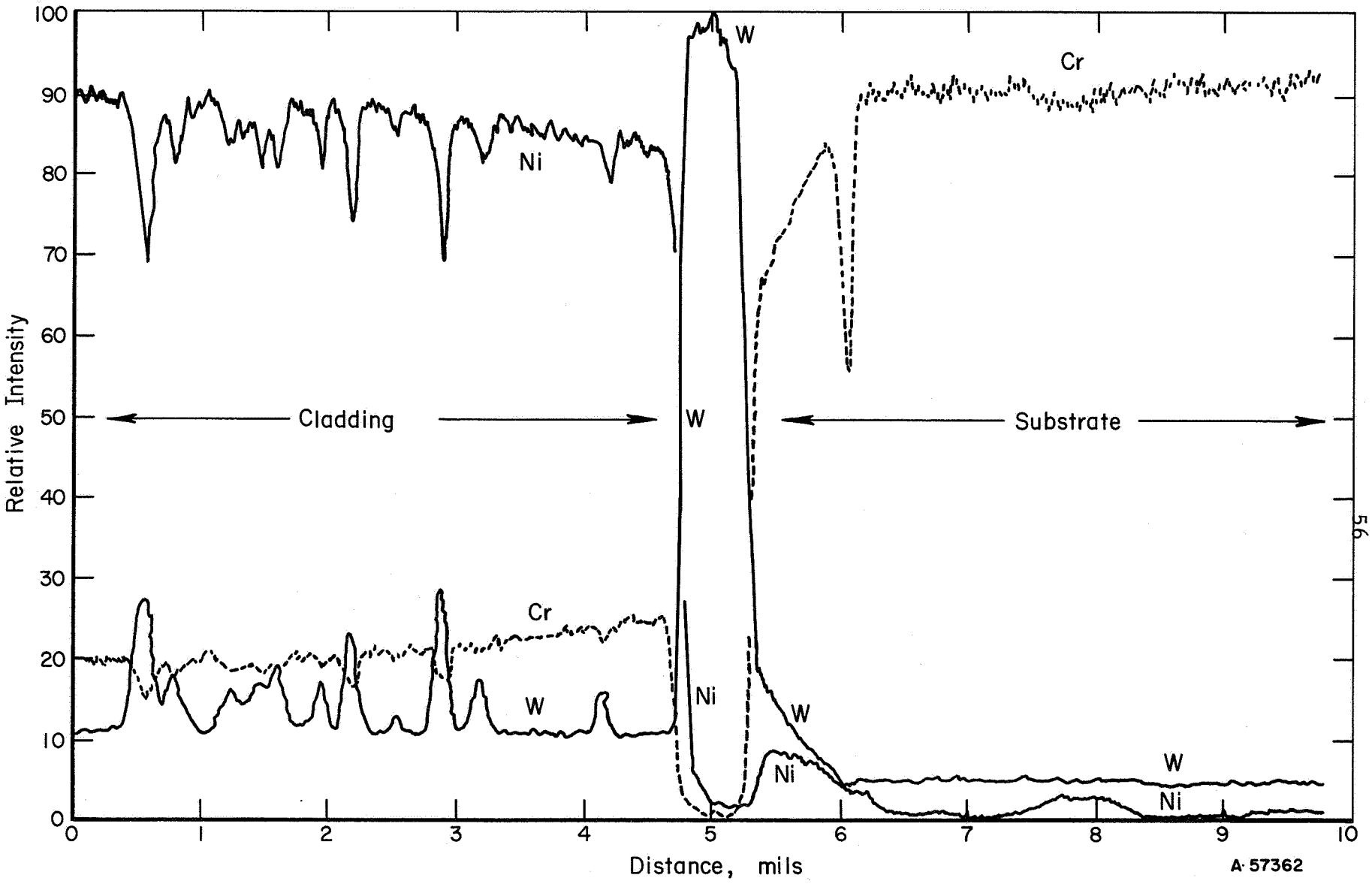

FIGURE 27. MICROPROBE TRAVERSE IN A SOUND REGION NEXT TO A CRACK IN THE TUNGSTEN BARRIER OF SAMPLE I-5, SYSTEM 1a

Sample cyclically oxidized 200 hours at 2100 F.

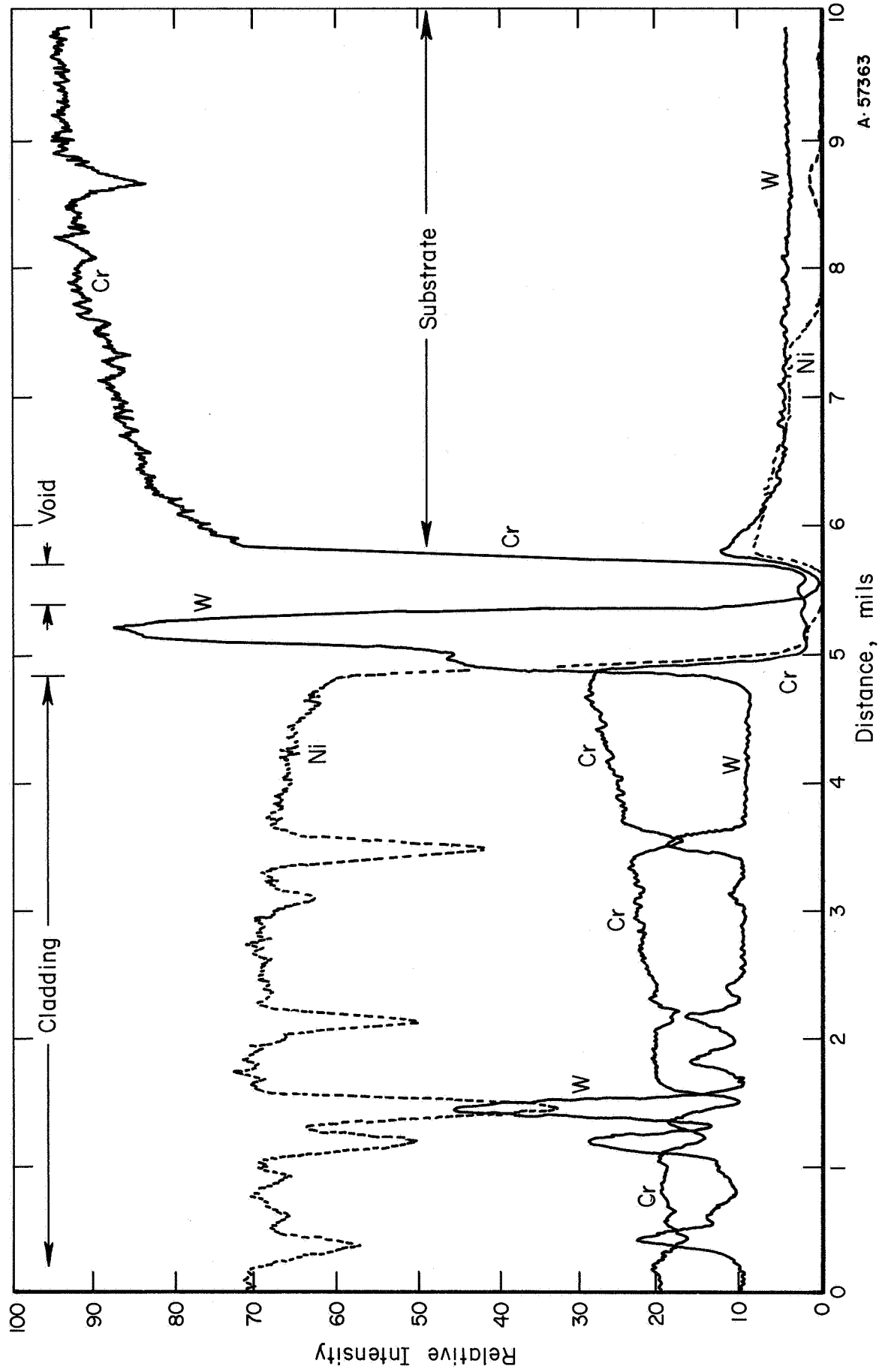

FIGURE 28. MICROPROBE TRAVERSE THROUGH THE DISCONTINUITY IN THE BARRIER LAYER OF SAMPLE I-5, SYSTEM 1a

Sample cyclically oxidized 200 hours at 2100 F.

TABLE 12. KNOOP HARDNESS (100-GRAM LOAD) OF CHROMIUM-5 WEIGHT PERCENT TUNGSTEN ALLOY AFTER CYCLIC OXIDATION (2-HOUR CYCLES) FOR 100 HOURS AT 2100 F[1]

Distance from Barrier:Cr-5W Alloy Interface, mils	System 1a(I-1)		System 2a(II-1)		System 3(III-2)		System 4(IV-1)		System 11(XI-1)		Barrier-free Ni-30Cr: Cr-5W[2]
	Crack Free	Cracked Area	Crack Free	Cracked Area	Crack Free	Cracked Area	Crack Free	Cracked Area	Crack Free	Cracked Area	
0.5	302	-	266	-	225	807	292	700	-	-	-
1	230	329	277	299	210	269	270	486	341	341	855
2	222	311	213	236	225	244	270	266	256	-	894
3	222	236	213	230	244	236	256	241	256	-	940
4	225	230	215	247	244	266	253	241	-	288	1062
5	227	230	206	241	233	230	253	253	232	266	618
10	206	-	213	225	236	-	253	-	266	246	256
20	210	-	220	-	239	-	274	-	221	226	250
Apparent Depth of Contamination, mils	1/2	2	1/2	1	0	1	2	2	1	4	7

(1) Hardness traverses made in two areas, one below a point on the barrier free from cracks and one below a crack in the barrier.

(2) Traverse made on Sample I-1 exposed 100 hours to cyclic oxidation at 2100 F in a region where no barrier was present (along picture frame).

in the barrier. Contamination is often evident about 3 times as deep below a crack in the barrier as when the barrier is crack free. The rapid contamination which occurs when no barrier is present is shown in the last column in this table. Contamination exceeded a depth of 7 mils in this case.

Samples from Systems 1a, 4, and 5 were intentionally defected to determine the ability of a defected cladding layer to protect the remainder of the sample. Thirty-mil-wide saw cuts were made into the cladding to depths of 5, 7, and 10 mils. One defected sample from each system was oxidized for 10 hours at 2100 F. A second sample was oxidized for 10 hours at 2100 F, cooled to room temperature, and then reheated for an additional 40 hours at 2100 F. The appearance of the System 4 sample after 50 hours at 2100 F is shown in Figure 29. The other systems behaved similarly. It is apparent that the balance of the cladding was not seriously damaged by defecting even when the defect penetrated into the chromium alloy. Metallographic examination of the defected samples showed up to 10 mils of oxidation of the barrier layer when the defect penetrated to the barrier. System 1a showed the least damage and System 5 the most. Little nitrogen contamination of the chromium alloy was apparent. Metallographic examination of the region around defects penetrating into the chromium alloy showed a small amount of pitting of the chromium alloy beneath the defect and some slight surface cracking. However, microhardness measurements made baneath the defected area after oxidation showed little change in hardness as a result of oxidation.

Oxidation Resistance at 2300 F

The weight change and protection behavior of samples exposed to cyclic oxidation at 2300 F are presented in Table 13, and photographs of representative samples from each system are shown in Figure 30. Average weight changes for each system are given in Table 14 grouping the samples according to exterior cladding material.

During cyclic oxidation at 2300 F, all specimens developed gross defects in the nickel-base claddings at locations over the juncture between the substrate and the picture frame. This was usually manifested in less than 100 hours, and the severity of these defects varied from system to system. Whereas at 2100 F, the presence of tungsten barrier layers at edges eliminated this type of defecting, this technique was not effective at 2300 F. Usually tests were continued substantially beyond the point where these defects were first noted, as (1) the major cladding areas were still in good condition, and (2) this was considered a feature of specimen design rather than system behavior. Thus, general behavioral observations such as spalling of oxide from unaffected cladding surfaces, oxide color and character, and metallographic evaluation were more useful as tools of evaluation than weight change measurements. The latter were in surprisingly good agreement with general observations considering the gross problem of edge defecting. The following comments are based on overall observations.

Unaluminized Ni-30Cr-clad samples tended to spall heavily. System 3, containing platinum, showed more extensive spalling than System 11. System 11 (platinum-free) developed a much darker appearing oxide. The aluminized Ni-30Cr-clad samples tended to show a large weight gain. As shown in Figure 30, these samples developed a fairly heavy oxide. The System 6 samples failed quite rapidly, as illustrated in Figure 30, apparently by embrittlement of the cladding layer by rhenium diffusion. In System 5 where platinum was present, samples did not show

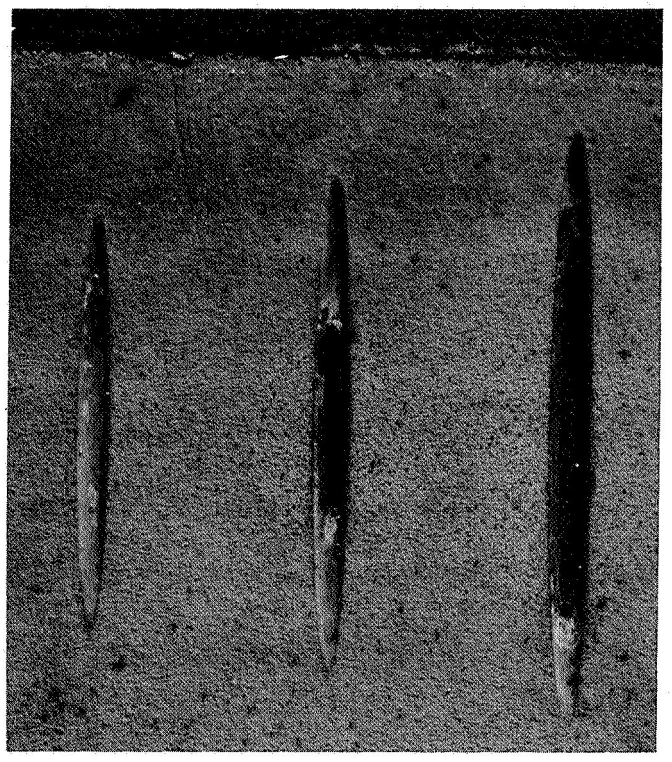

5X 5A862

FIGURE 29. APPEARANCE OF THE SURFACE OF A SAMPLE FROM SYSTEM 4 (IV-11) AFTER 50 HOURS OXIDATION AT 2100 F

TABLE 13. OXIDATION BEHAVIOR DURING CYCLIC OXIDATION AT 2300 F

System	Sample Number	Time to Failure, hr(1)	Weight Gain, mg/cm^2 At 100 hr	Weight Gain, mg/cm^2 At Failure	Comments
1a	I-6	200	1.54	0.99	Corner and edge cracking appeared within about 60 hours.
	I-7	80	-	8.86	Variable spalling. I-6 in best condition.
	I-8	200	6.17	7.24	
1b	I-20	240*	1.44	0.12	Significant oxide spalling after about 150 hours. Corner and edge defects became quite noticeable after about 100 hours in test. I-22 showed early failure at picture frame.
	I-21	160*	2.37	2.70	
	I-22	40	-	7.60	
	I-25	240*	1.70	-4.40	
	I-27	160*	2.16	2.29	
2a	II-5	200	3.61	2.46	Corner and edge damage visible within 100 hours. II-7 shows severe blistering. Spalling late in test.
	II-6	200	2.48	0.17	
	II-7	100	6.78	6.78	
2b	II-22	100	2.61	2.61	Significant oxide spalling after about 150 hours (80 hours for II-22). Blistering developed early in Sample II-25. Corner and edge defects became quite noticeable after 100 hours in test.
	II-25	60*	-	2.45	
	II-26	260*	1.53	-5.00	
	II-27	320*	1.94	-18.70	
	II-28	460*	1.95	-32.90	
2c	No tests				
3	III-5	100	-6.50	-6.50	These samples showed little edge or corner cracking. Spalling began within a few cycles.
	III-6	200	-6.92	-20.10	
	III-7	200	-6.92	-18.00	
4	IV-5	80	-	11.00	Extensive damage to edges and corners of samples occurred fairly early in test. Cladding peeled.
	IV-6	80	-	16.66	
	IV-7	80	-	14.26	
5	V-6	100	9.04	9.04	Samples showed edge and corner failures after about 40 hours. V-8 developed crack in cladding early in test.
	V-7	200	8.30	4.99	
	V-8	10	-	3.00	

TABLE 13. (continued)

System	Sample Number	Time to Failure, hr(1)	Weight Gain, mg/cm^2 At 100 hr	Weight Gain, mg/cm^2 At Failure	Comments
6	VI-5	2	-	0.68	Cladding layer developed extensive cracks; appeared brittle. Some evidence of liquid phase.
	VI-6	6	-	4.9	
	VI-7	6	-	3.3	
7	VII-2	200	-1.03	-0.03	Edge cracking developed early. VII-5 developed surface cracks. VII-2 appeared superior to VII-6.
	VII-5	10	-	2.3	
	VII-6	100	10.84	10.84	
8	VIII-4	140	13.10	21.00	Samples tended to bow and blister. Not too much edge or corner failure.
	VIII-5	100	11.90	11.90	
	VIII-6	200	14.00	15.80	
9	IX-1	2	-	16.1	Extensive cladding bulging.
10	X-3	100	0.44	0.44	Spalled after ~10 hours. Slight corner cracks.
11	XI-2	100	-2.15	-2.15	Spalled immediately. Some corner cracks.
12	XII-5	100	-1.41	-1.41	Spalled after ~ 50 hours. Edge and corner damage.

(1) Samples cycled every 2 hours for first 100 hours and every 20 hours thereafter unless marked with *. *-marked samples cycled every 20 hours throughout the test.

TABLE 14. SUMMARY OF WEIGHT CHANGES DURING CYCLIC OXIDATION AT 2300 F

System	Cladding Layer(1)	Compatibility Layer	Barrier Layer(1)	Weight Gain in 100 hr, mg/cm^2
		Unmodified Ni-30Cr		
11	10 mil Ni-30Cr	-	1.5 mil W	-2.15
3	Ditto	0.5 mil Pt	0.5 mil W	-6.78
		Aluminized Ni-30Cr		
4	5 mil Ni-30Cr:5Al	0.5 mil Pt	0.5 mil W	14.0 in 80 hr
7	Ditto	Ditto	1.0 mil W	-1.03 to 10.84
8	"	1.0 mil Pt	0.5 mil W	13.0
6	"	-	1.0 mil W-25Re	Failed in <10 hr
5	"	0.5 mil Pt	Ditto	8.67
		Aluminized Ni-20Cr-20W		
1a	5 mil Ni-20Cr-20W:5Al	-	0.5 mil W	1.54 to 6.17
2a	Ditto	0.5 mil Pt	Ditto	1.92
1b	"	-	1.5 mil W	2.48 to 6.78
2b	"	0.5 mil Pt	Ditto	2.01
12	"	Ditto	2 mil W-1ThO_2	-1.41
10	"	"	2 mil Mo	0.44
9	"	1 mil V	1.5 mil V	Failed in <10 hr

(1) Alloy compositions and aluminum additions given in weight percent.

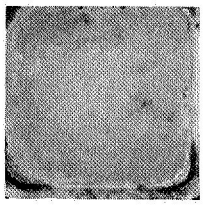

System 1a (I-6)

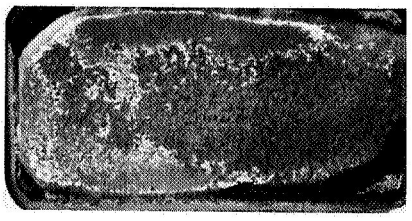

System 1b (I-21)
160-hr test, 20-hr cycles

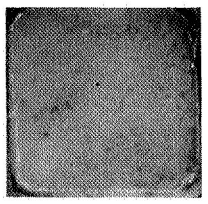

System 2a (II-5)

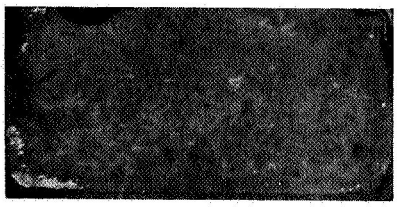

System 2b (II-22)

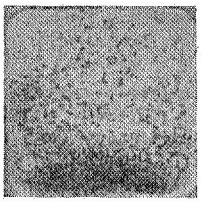

System 3 (III-6)

System 4 (IV-7)

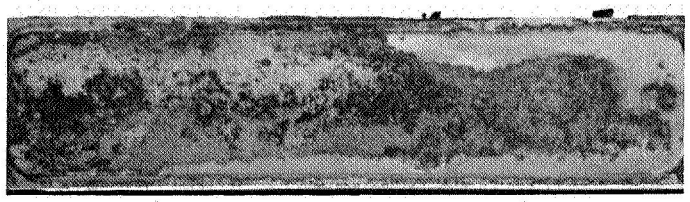

System 5 (V-6)

System 6 (VI-7)
(oxidized 10 hours)

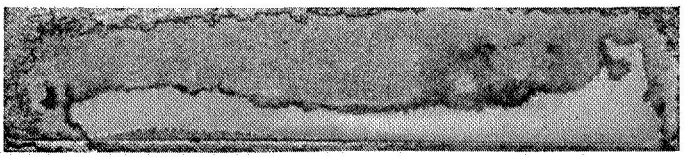

System 7 (VII-6)

FIGURE 30. APPEARANCE OF OXIDATION SAMPLES AFTER 100-HOUR CYCLIC EXPOSURE AT 2300 F WITH 2-HOUR CYCLES (UNLESS NOTED OTHERWISE) [( ) = sample number]

System 8 (VIII-5)

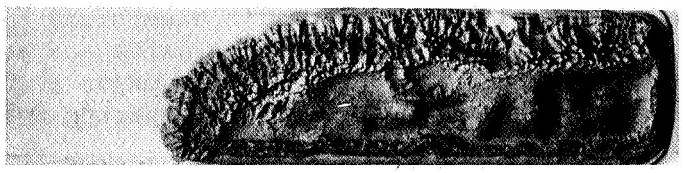

System 9 (IX-1)
(oxidized for 2 hours)

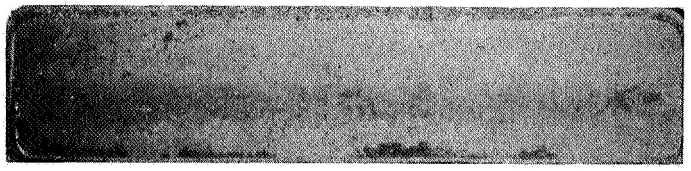

System 10 (X-3)

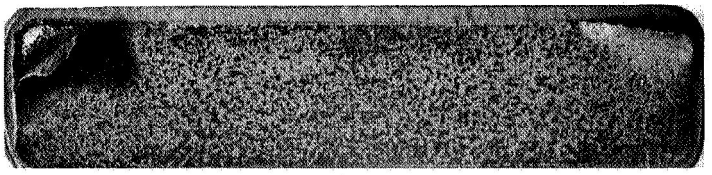

System 11 (XI-2)

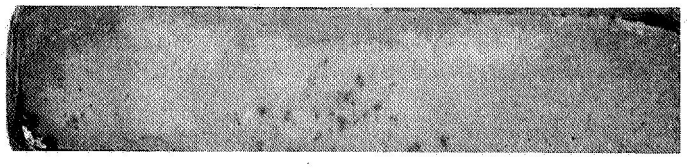

System 12 (XII-5)

FIGURE 30. (continued)

embrittlement of the clad. As suggested in Table 14, these systems showed increasing spalling as the oxidation time increased. The samples clad with aluminized Ni-20Cr-20W showed weight gains that were significantly less than observed in the aluminized Ni-30Cr and the oxides developed appeared thinner and less crusty. Spalling began after a reasonably short time such that within 200 hours the weight gain was normally less than that observed at the end of 100 hours. The onset of spalling was rather variable and may reflect small differences in aluminum content. The presence of platinum in Systems 2a, 2b, 10, and 12 appeared to result in more reproducible weight changes among duplicate samples as compared to the platinum-free systems, 1a and 1b. As shown in Figure 30, platinum did not have a large effect on the appearance of the oxidized samples clad with aluminized Ni-20Cr-20W. Vanadium in System 9 resulted in the formation of a molten oxide and early sample failure. A barrier layer of molybdenum did not result in any major change in surface appearance after oxidation at 2300 F as can be seen by comparing Systems 10 and 12 in Figure 30.

Metallographic examination of the samples after cyclic oxidation at 2300 F showed extensive cracking, pitting, and interdiffusion at the junction between cladding and alloy. Figure 31 shows the structure of a System 1b sample after 240 hours oxidation at 2300 F. Reaction product is visible on both sides of the tungsten barrier which shows extensive cracking. Severe contamination of the chromium-base alloy for some depth below the interface is also present.

Several of the samples were examined to determine the effects of exposure time and cycle frequency on the depth of contamination, crack frequency, and other microstructure changes. These results are presented in Table 15. Both the System 1b and 2b samples showed a progressive loss of barrier with time. The presence of platinum appeared to accelerate the rate of barrier solution. Pitting and contamination also increased with time of exposure. As shown in Figure 32, both Systems 1b and 2b showed about the same rate of contamination, the depth of contamination increasing with time according to the relationship $d \sim t^{1/2}$. The rate of pit growth appears to be more rapid in System 2b than in System 1b, although the time required for pits to form is apparently greater in System 2b than 1b. As was observed after cyclic oxidation at 2100 F, the spacing of cracks in the tungsten barrier layer is at least partially related to the number of cycles. However, contamination was quite uniform and did not appear related to the number of cracks. It is possible that if no cracks were present, contamination would have been somewhat reduced. Interface separation was quite extensive with longer exposures. No significant differences existed between Systems 1b and 2b in this respect. Both Systems 11 and 12 developed fewer cracks in the barrier layer than might have been expected from the results observed for Systems 1b and 2b. The contamination rates were about the same, however. Of particular note is the resistance of the W-1ThO_2 barrier to solution in System 12.

The appearance of the interfacial region of four samples after 100 hours cyclic exposure at 2300 F is shown in Figure 33. Differences in appearance in the contamination region probably reflect differences in type and level of contamination. The System 10 sample showed extensive fragmentation in the molybdenum barrier region. This is attributed to extreme embrittlement of the barrier layer by diffusion. The extensive pitting observed in System 2b is also readily apparent.

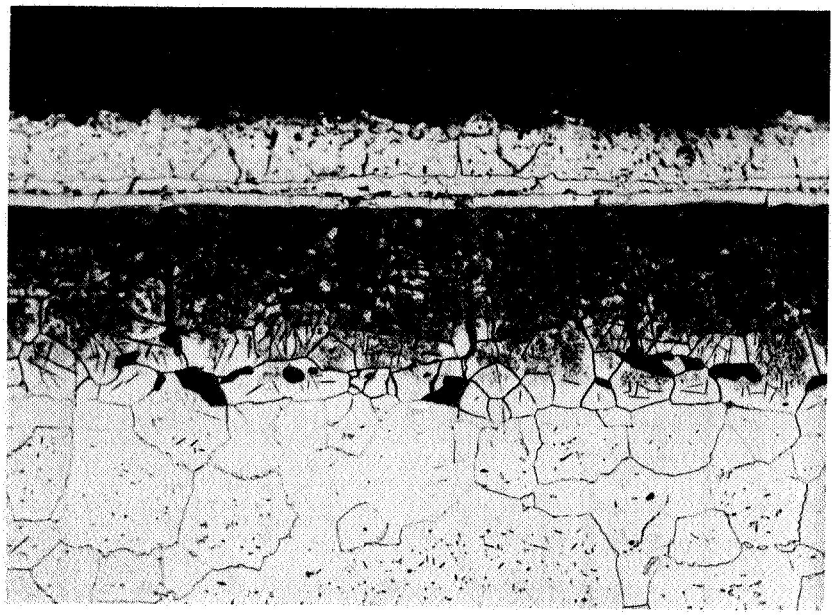

100X 5B230

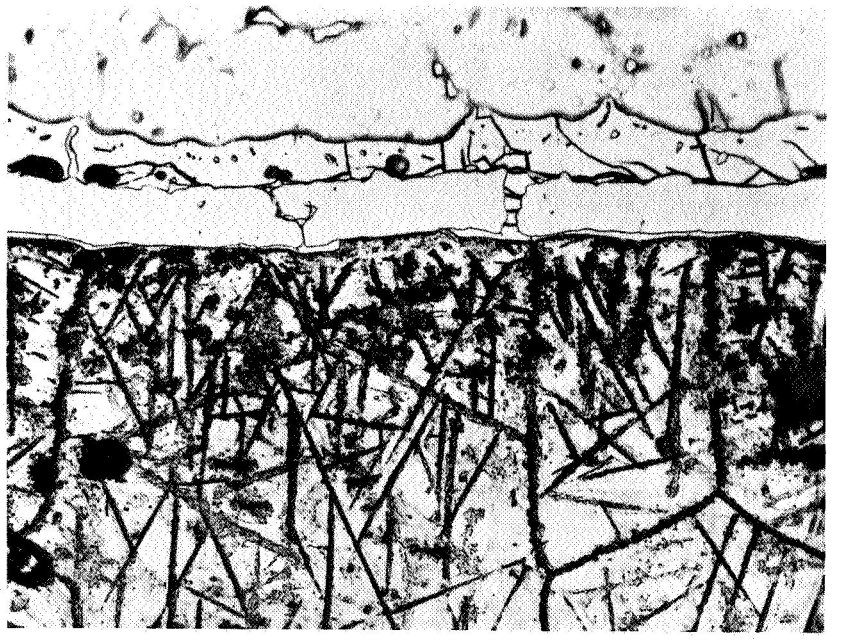

500X 5B231

FIGURE 31. MICROSTRUCTURE OF SYSTEM 1b SAMPLE AFTER CYCLIC OXIDATION FOR 240 HOURS AT 2300 F USING 20-HOUR CYCLES (I-20)

Electrolytic oxalic acid etch.

TABLE 15. RESULTS OF METALLOGRAPHIC SURVEY OF SEVERAL SAMPLES OXIDIZED AT 2300 F

System	Sample Number	Exposure Conditions: Time at 2300 F, hr	Exposure Conditions: No. of Cycles	Thickness, mils, of: Barrier	Thickness, mils, of: Cladding	Chromium Pits, mils: Depth	Chromium Pits, mils: Average Spacing	Depth of Visible Contamination, mils	Interface Separation: Clad:Barrier	Interface Separation: Barrier:Cr
1b	I-22	40	20	1.0	5.6	3.2	5.3	4.0	Some	None
	I-21	160	8	0.7	5.6	7.2	7.7	7.3	Lots	None
	I-20	240	12	0.6	4.8	10.1	3.7	10.0	Lots	None
2b	II-22	100	50	0.9	6.4	3.1	5.4	6.7	Some	None
	II-36	120	6	1.0	6.1	3.3	-	6.4	Some	None
	II-37	200	10	0.9	6.5	6.2	10.7	8.2	None	None
	II-26	260	13	<0.1	5.1	8.5	6.4	13.5	Lots	Lots
	II-28	460	23	0	4.7	16.0	-	15.7	Lots	Lots
11	XI-2	100	50	1.0	9.7	1.5	9.8	6.3	None	Lots
12	XII-5	100	50	2.2	6.0	4.8	9.7	6.2	Some	Lots

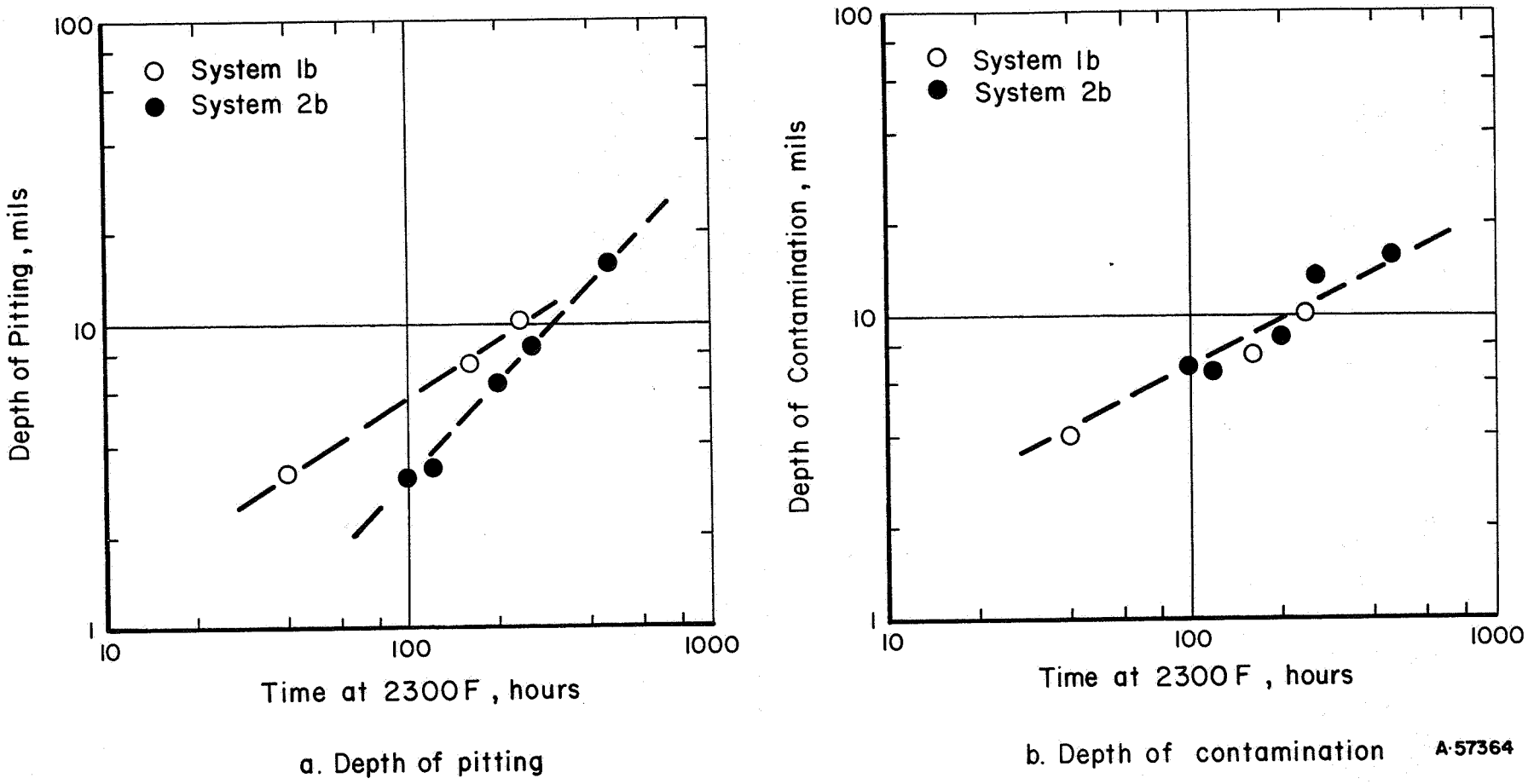

FIGURE 32. DEPENDENCE OF DEPTH OF PITTING AND CONTAMINATION ON TIME OF OXIDATION AT 2300 F

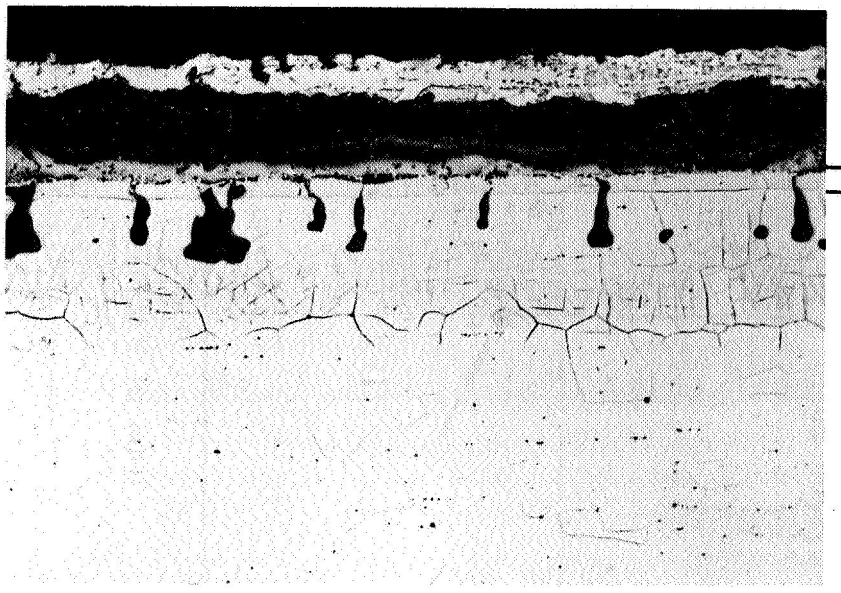

100X System 2b (II-22) 5B219

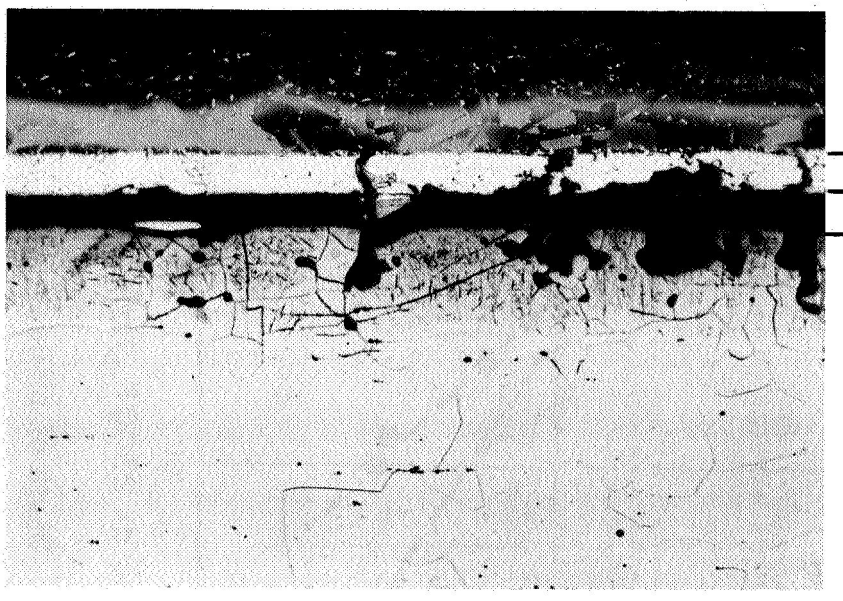

100X System 12 (XII-5) 5B228

FIGURE 33. APPEARANCE OF SAMPLES AFTER CYCLIC OXIDATION AT 2300 F FOR 100 HOURS USING 2-HOUR CYCLES

Electrolytic oxalic acid etch.

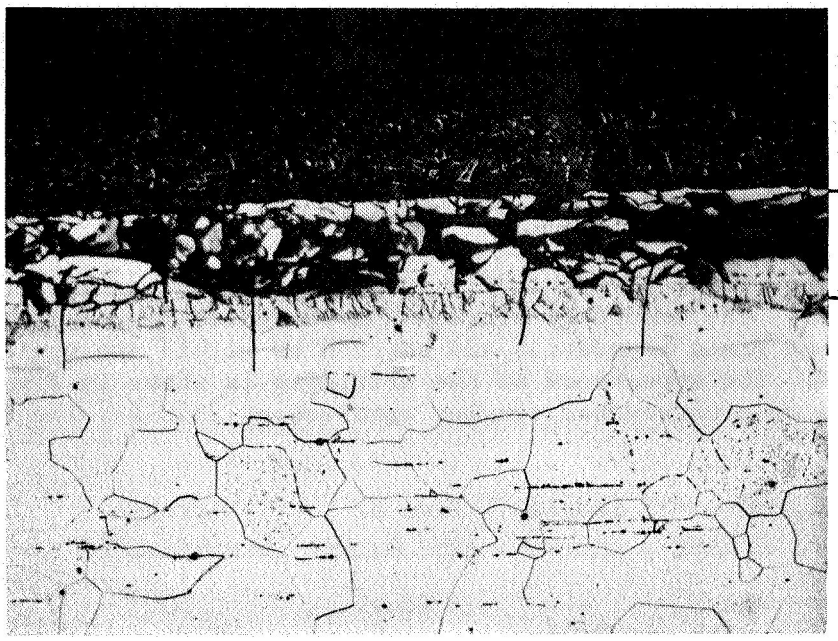

100X System 10 (X-3) 5B220

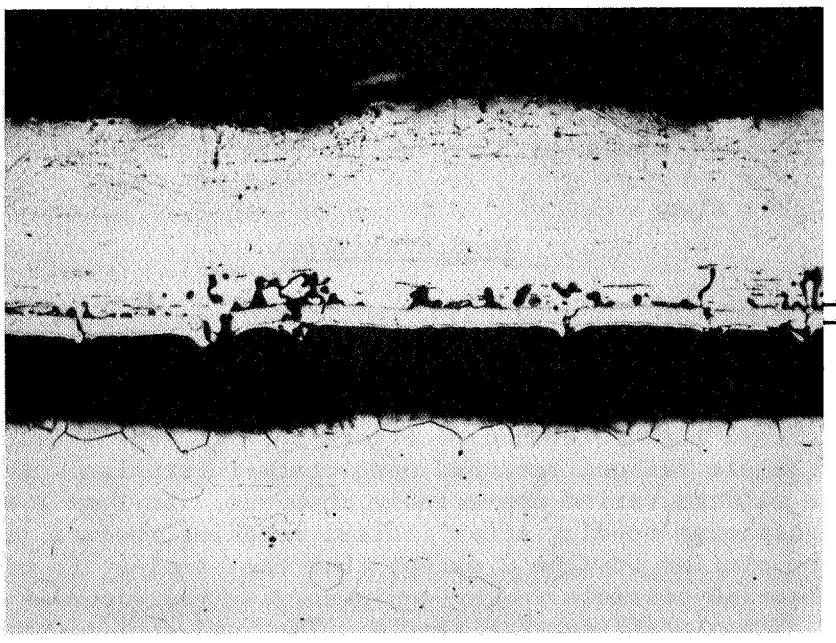

100X System 11 (XI-2) 5B224

FIGURE 33. (continued)

Barrier layer solution at 2300 F apparently was a major factor in the poor behavior of certain systems. The W-25Re barrier used in Systems 5 and 6 was rapidly dissolved as shown in Figure 34. Thinner tungsten barriers were also completely dissolved as shown in Figure 35. It is apparent that the maintenance of an effective barrier layer during cyclic oxidation is a major problem. The present work suggests that a W-1ThO_2 barrier may be necessary to insure that solution does not occur during exposure periods of several hundred hours. Since the platinum compatibility layer appears to accelerate solution of the tungsten, this layer is probably undesirable.

Nitriding was observed in all samples cyclically oxidized at 2300 F for 100 hours or more. The amount of nitriding appeared to be heaviest near the surface, but was present at grain boundaries and as needles within the grains throughout the sample thickness. The appearance of the nitriding is shown in Figure 36. Analysis for nitrogen was made on several samples oxidized at 2300 F. The results are listed below:

System	Sample Number	Time at 2300 F, hr	Nitrogen Content, ppm
Base	-	None	50
1b	I-21	160	1800
10	X-3	100	570
11	XI-2	100	2200

It is obvious that serious contamination is present. At least part of the nitrogen contamination may result from edge or corner defects. However, as shown in Figure 37, it appears that the nitriding from this source is limited to the vicinity of the edge and corner tears. Thus, the present results suggest that the metallic cladding systems are not adequate to prevent nitrogen contamination at 2300 F.

Bend Evaluation

Bend tests were conducted according to MAB specifications as outlined earlier. During bending, load-deflection curves were obtained, typical examples of which are shown in Figure 38. Four general types of behavior were observed which may be described with reference to Figure 38. In Type 1 load-deflection curves, complete sample failure occurred upon crack initiation. The amount of deflection before failure varied appreciably, however. In Type 2 curves, the sample withstood significant bending after initial cracking, before final failure. Type 3 curves were similar to Type 2 except that the samples did not fail within the limiting deflection possible in the equipment.* Type 4 curves represent the bend behavior of a completely ductile sample. The bend angles were calculated from the load-deflection curves assuming no elastic deformation in the sample. The angle for initiation of cracking and for final failure, as well as the type of load-deflection curves, are reported to describe the bend behavior of the materials evaluated.

---

*More recent work has indicated that load-deflection curves similar to the Type 3 curves can result from sticking of the sample against the bend equipment as well as from minor surface cracking. Therefore, the exact interpretation of the load-deflection curves where minor irregularities occur is in doubt.

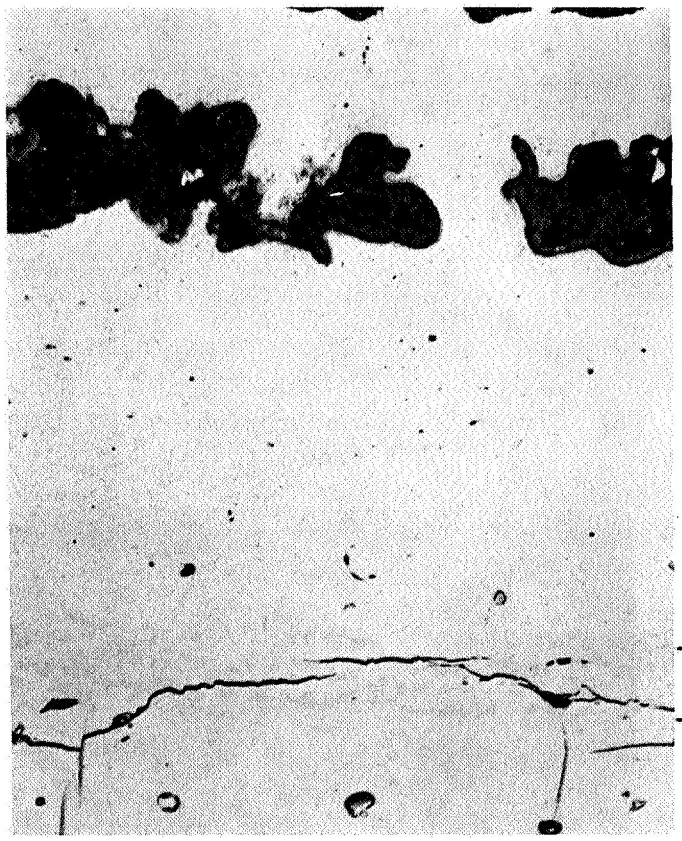

500X As polished 6A051

FIGURE 34. SOLUTION OF W-25 WEIGHT PERCENT Re BARRIER IN A SYSTEM 5 SAMPLE CYCLICALLY OXIDIZED FOR 10 HOURS AT 2300 F

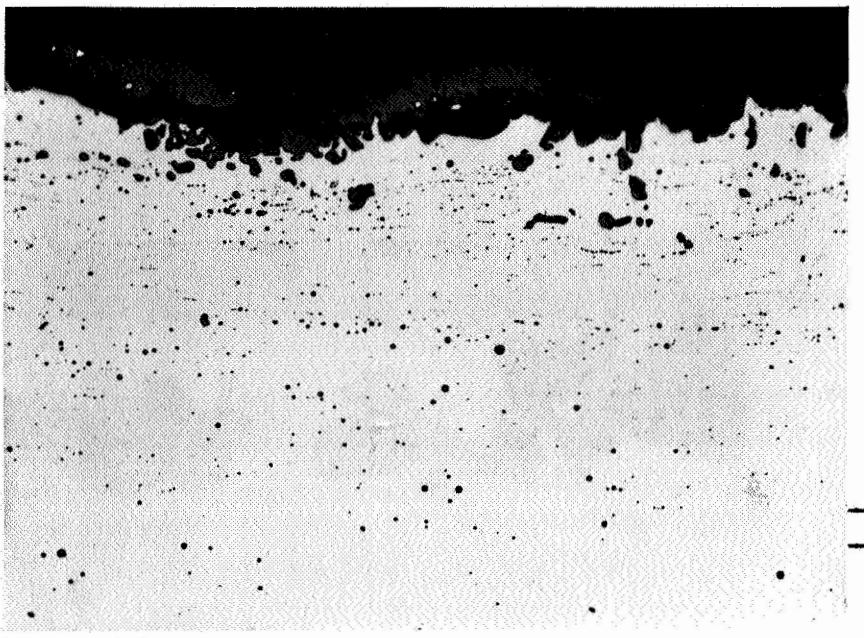

250X (a) System 3--200-hour exposure (III-7) 6A696

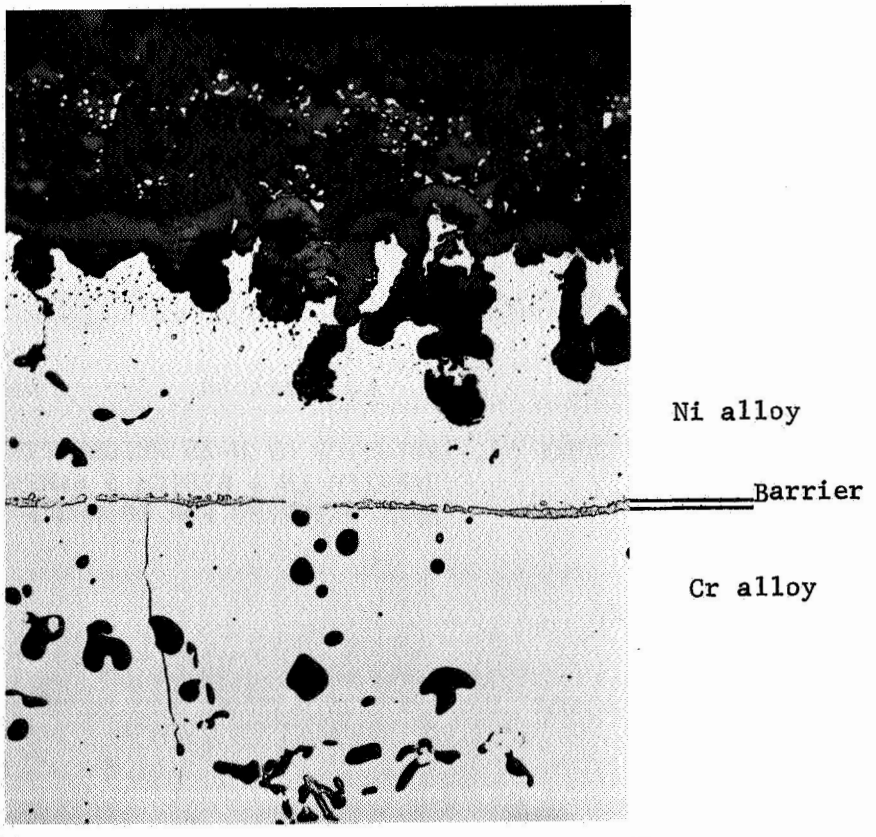

250X 8A781

(b) System 7--100-hour exposure (VII-6)

FIGURE 35. SOLUTION OF 0.5-MIL TUNGSTEN BARRIER DURING CYCLIC OXIDATION AT 2300 F

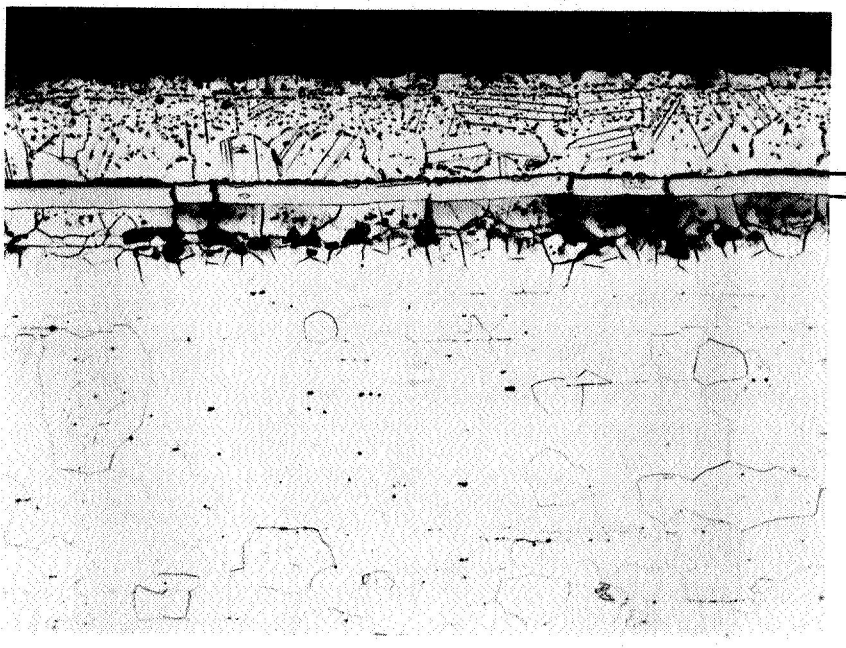

100X 5B216

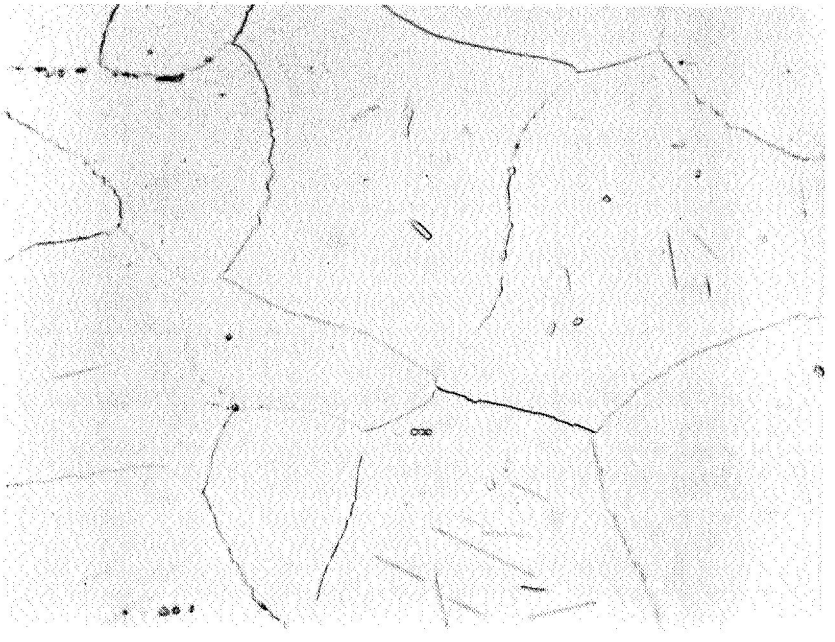

500X (from region well below surface contamination shown above) 5B217

FIGURE 36. NITRIDING OF A SYSTEM 1b SAMPLE CYCLICALLY OXIDIZED 40 HOURS AT 2300 F (I-22)

40X

8B625
8B626

FIGURE 37. NITRIDING IN A SYSTEM 1b SAMPLE CYCLICALLY OXIDIZED 40 HOURS AT 2300 F

Electrolytic oxalic acid etch.

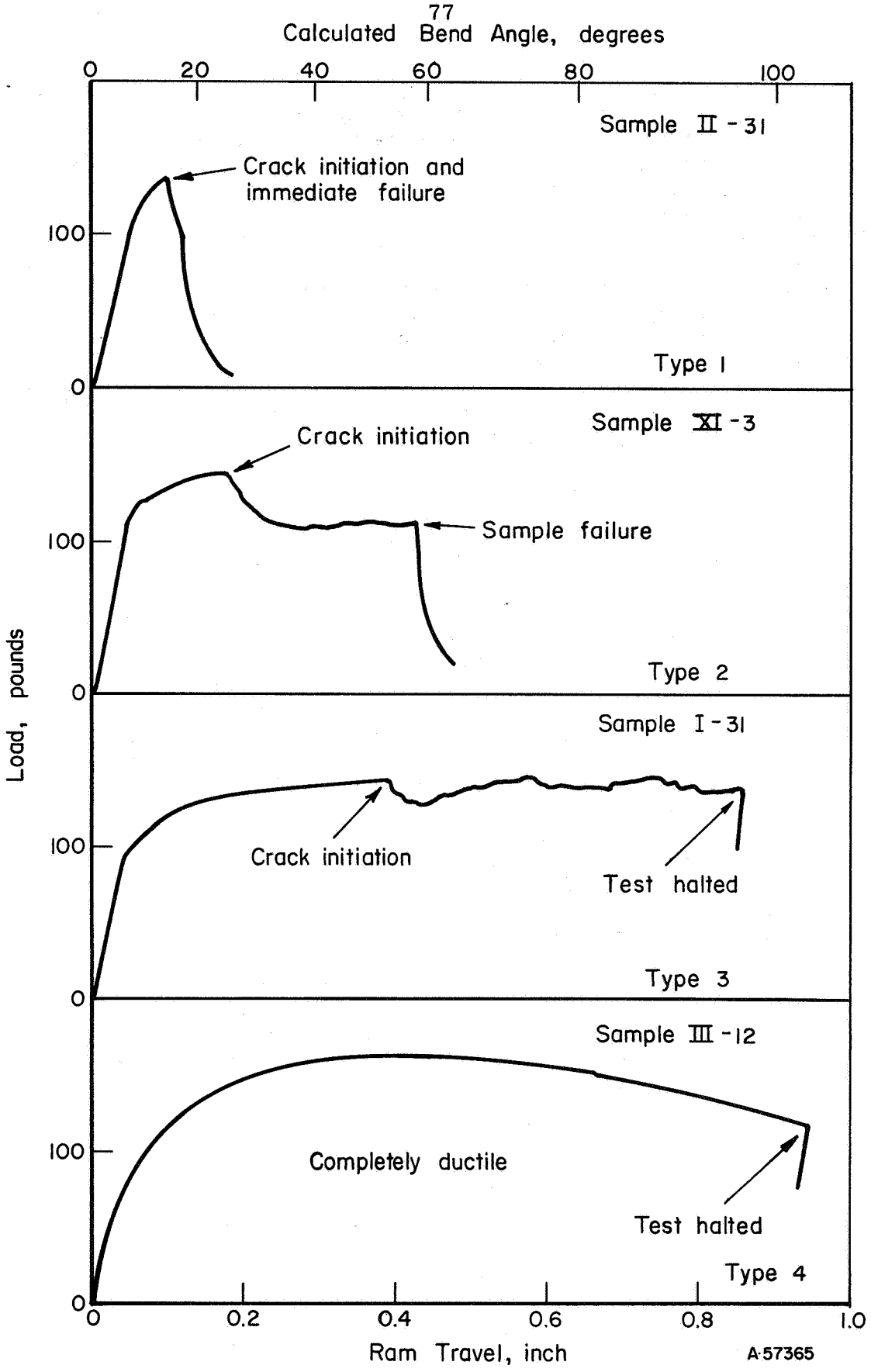

FIGURE 38. TYPICAL LOAD-DEFLECTION CURVES

As a means of checking out the equipment, several unclad chromium samples were tested. These samples showed either Type 1 or Type 4 load-deflection curves. Samples were tested either as received, after recrystallization at 2100 F, or after oxidation for 2, 10, and 25 hours at 2100 F. The results of the bend tests on the unclad chromium-5 tungsten material are shown in Table 16. Both the as-received and recrystallized material showed a transition from ductile to brittle behavior between 500 and 600 F. A value of 440 F was reported by the supplier (see Table 2) which is in reasonable agreement with the present results considering the small number of samples tested and probable differences in specimen preparation. The recrystallized material appeared to have a slightly lower transition temperature than the wrought as-received material which was contrary to expectations. As anticipated, oxidation at 2100 F increased the ductile-brittle transition quite significantly. For times up to about 25 hours, the transition temperature appeared to increase linearly with the square root of oxidation time at 2100 F (DBTT = T_o + $kt^{1/2}$, with T_o = 550 F and k = 150 F/$hr^{1/2}$). The samples showed either Type 1 or Type 4 load-deflection curves, and failure occurred at low bend angles in brittle material.

A number of clad samples were oxidized at 2100 F using 20-hour oxidation cycles in preparation for bend testing. The oxidation behavior of these samples is given in Table 17. As observed previously during examination of oxidation behavior, a significant amount of variability in weight gain results were observed. Bend properties of these samples are given in Table 18. Because of the poor bend properties observed, not all samples which were oxidized were bend tested. The ductile-brittle transition temperature of all systems examined was degraded by cyclic oxidation at 2100 F. This undoubtedly is traceable to the metallic contamination of the chromium-5 tungsten alloy which occurred during cyclic oxidation by diffusion of cladding material through the tungsten diffusion barrier. A further indication that this is the case is the frequency of Type 2 and 3 load-deflection curves shown in Table 18. These curves are believed to be the result of early surface cracking followed by crack arrest in the more ductile matrix. The microstructure of a bend sample showing the Type 3 load-deflection curve is shown in Figures 39 and 40. It can be seen that cracks are originating at the barrier layer:chromium alloy interface, but not progressing too deeply into the chromium alloy. Deformation is evident in the chromium alloy, reflecting its basic ductility.

Since some ductility must be present for observation of Types 2 and 3 load-deflection curves, it is possible to obtain an approximate indication of the relative ductility of the various cladding systems by noting the transition from Type 1 to Type 2, 3, or 4 load-deflection curves. A tabulation of the location of the ductility transition is presented below.

System	Oxidation Time, hr	Ductility Transition Temp., F
1a	100	1000-1200
1b	300	1200-1400
2a	100	1000-1200
2b	300	1400-1600
3	100	800-1000
4	100	1400-1600
5	100	1500-1600
6	100	>1600

TABLE 16. BEND PROPERTIES OF CHROMIUM-5 WEIGHT PERCENT TUNGSTEN ALLOY (Heat 64-100)

Condition	Bend Temp., F	Bend Angle (degrees) at Failure	Type of Load-Deflection Curve(1)
As-received	500	<10	1
	600	>100	4
Recrystallized at 2100 F for 2 hours	500	70	1
	600	>100	4
Oxidized 2 hours at 2100 F	600	<10	1
	800	>100	4
	1000	>100	4
Oxidized 10 hours at 2100 F	1000	<10	1
	1100	>100	4
	1200	>100	4
Oxidized 25 hours at 2100 F	1100	<10	1
	1200	>100	4

(1) Load-deflection curves are illustrated in Figure 38.

TABLE 17. OXIDATION BEHAVIOR OF BEND SAMPLES OXIDIZED AT 2100 F USING 20-HOUR CYCLES

System	Sample Number	Weight Gain, mg/cm^2, in 100 hr	300 hr	600 hr
1a	I-10	0.81		
	-11	0.75		
	-12	0.60		
	-13	0.69		
	-14	0.74		
	-15	0.69		
1b	I-28		1.31	
	-29		0.93	
	-30		0.86	
	-13		0.88	
2a	II-11	0.70		
	-12	1.02		
	-13	0.97		
	-14	0.81		
	-15	0.80		
	-16	0.82		
2b	II-30		1.00	
	-31		1.14	
	-32		0.84	
	-33		1.03	
	-43		1.06	
	-44		1.66(1)	
	-45			1.50
	-46			1.65
	-48			1.35
	-49			1.13
	-50			1.10
2c	Not tested			
3	III-8	1.26		
	-9	1.44		
	-10	1.53		
3 (cont.)	III-11	1.63		
	-12	1.59		
	-13	1.69		
4	IV-13	1.24		
	-14	1.01		
	-15	1.48		
	-16	0.98		
	-17	0.48		
	-18	0.74		
5	V-10	1.47		
	-11	1.46		
	-12	1.50		
	-13	1.10		
	-14	0.95		
	-15	0.88		
6	VI-8	1.24		
	-9	1.42		
	-10	1.50		
	-11	0.98		
	-12	0.83		
	-13	0.97		
7	Not tested			
8	Not tested			
9	Not tested			
10	Not tested			
11	Not tested			
12	Not tested			

(1) Picture frame:cladding separation at ends of sample.

TABLE 18. BEND TEST RESULTS FOR SAMPLES CYCLICALLY OXIDIZED AT 2100 F

System	Sample Number	Oxidation Time, hr	Bend Temp., F	Bend Angle (degrees) at Crack Initiation	Bend Angle (degrees) at Failure	Type of Load-Deflection Curve(3)
1a	I-10	100	700	<10	<10	1
	-14	"	1000	30	30	1
	-13	"	1200	45	75	2
	-12	"	1400	45	45	1
	-11	"	1600	30	30	3
1b	I-28	300	1000	<10	<10	1
	-29	"	1200	15	15	1
	-30	"	1400	30	45	2
	-31	"	1600	50	>100	3
2a	II-11	100	75	<5	<5	1
	-16	"	800	10	10	1
	-15	"	1000	55	55	1
	-14	"	1200	30	>110	3
	-13	"	1400	45	>110	3
	-12	"	1600	50	90	2
2b	II-30	300	1000	<5	<5	1
	-31	"	1200	<5	<5	1
	-32	"	1400	30	30	1
	-33	"	1600	40	>105	3
	-49(1)	600	800	<5	<10	1
3	III-13	100	800	10	10	1
	-12	"	1000	>110	>110	4
	-8	"	1000	<30	(2)	-
	-11	"	1200	30	>105	3
	-10	"	1400	65	65	1
	-9	"	1600	50	>120	3
4	IV-13	100	1200	<5	10	2
	-16	"	1200	<10	<10	1
	-15	"	1400	20	20	1
	-14	"	1600	>105	>105	4
5	V-12	100	1400	<10	<10	1
	-10	"	1500	<10	<10	1
	-11	"	1600	20	85	2
6	VI-9	100	1400	<5	20	2
	-8	"	1600	30	30	1

(1) Sample tested without removing picture frame.

(2) Test halted at 30 degrees.

(3) See Figure 38 for illustration of four types of curves.

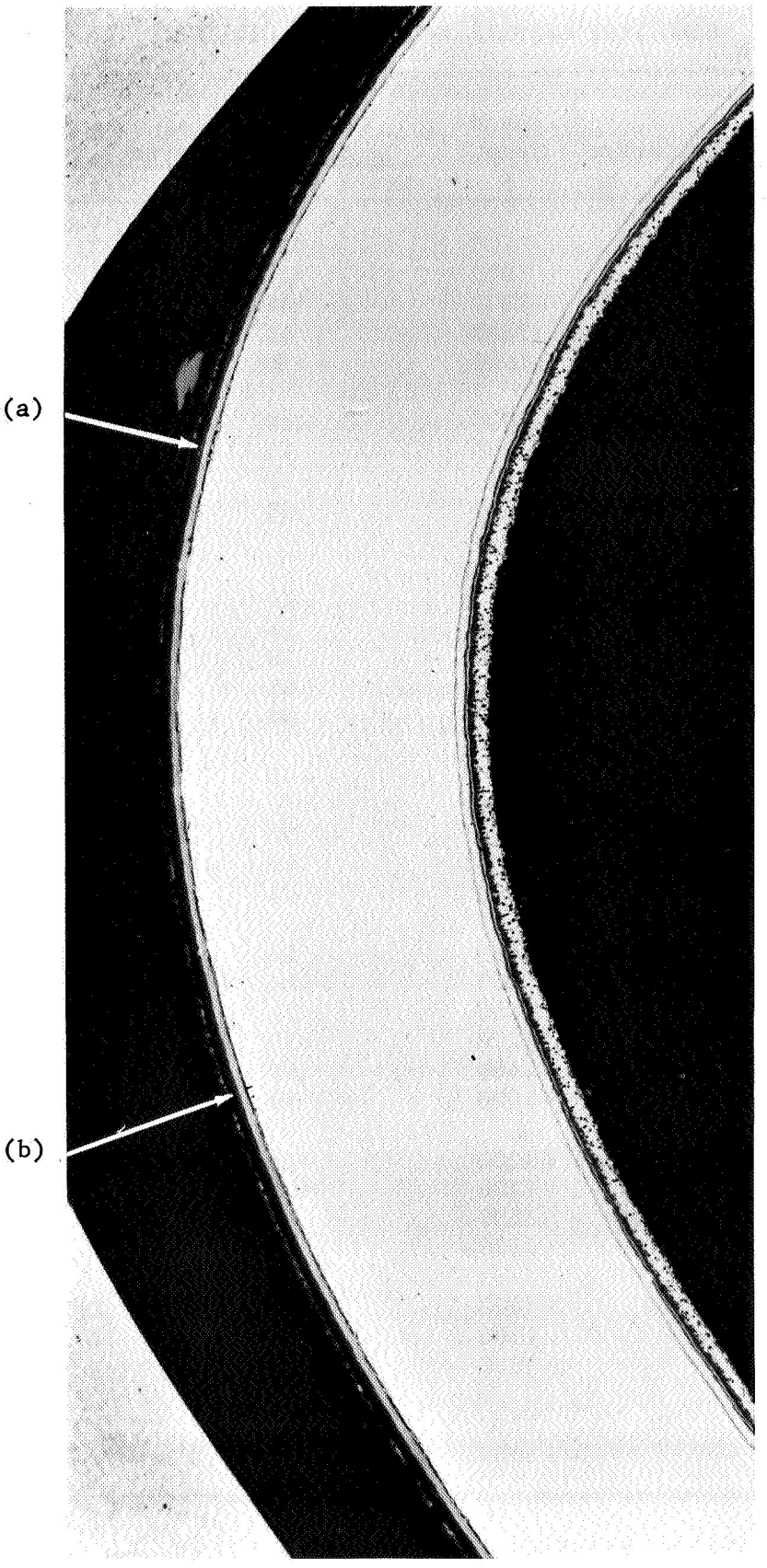

25X 1B556

FIGURE 39. MICROSTRUCTURE OF BEND SAMPLE II-14

System 2a, oxidized 100 hours at 2100 F and bend tested at 1200 F.

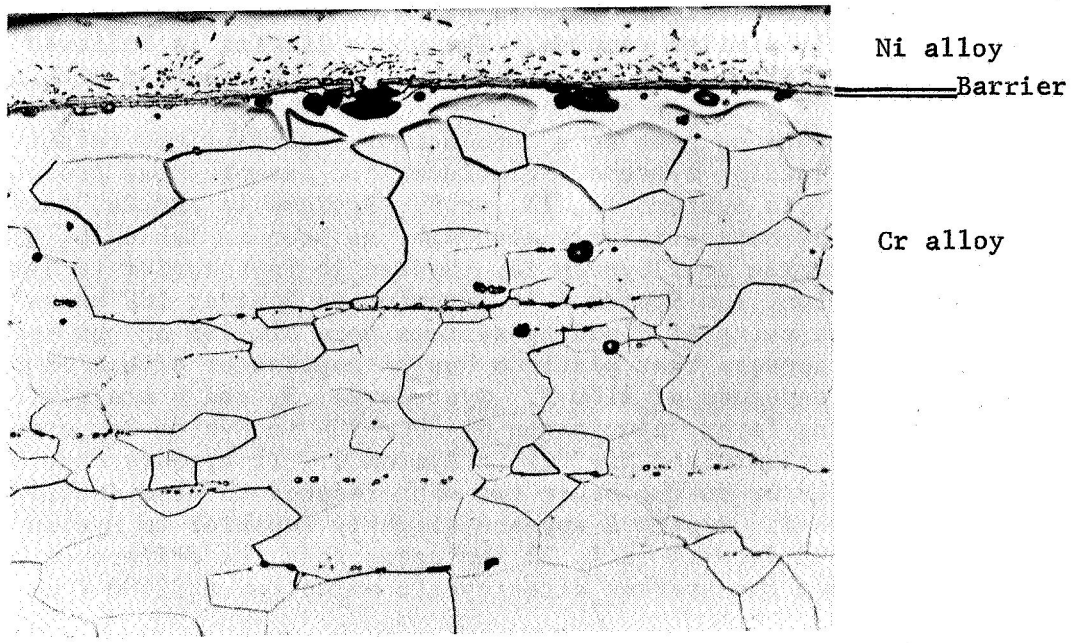

250X (a) Pitted region 1B562

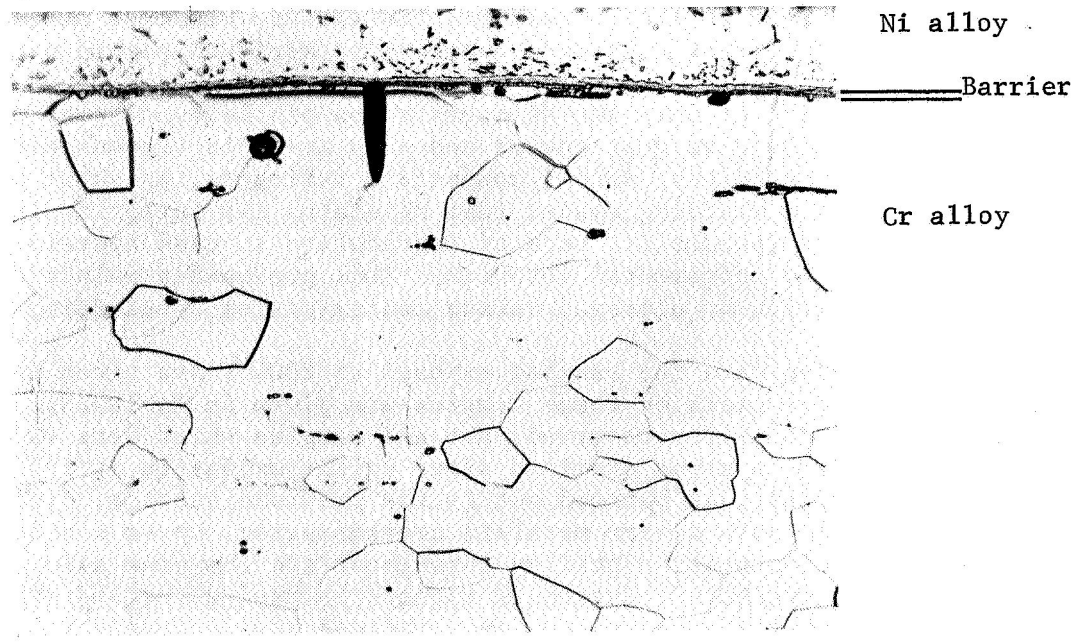

250X (b) Cracked region 1B563

FIGURE 40. STRUCTURE OF TENSION SIDE OF BEND SAMPLE II-14 (see Figure 39)

Examination of Table 18 shows that there is some question about the exact placement of the ductility transition. This is believed to result from slight differences between supposedly similar samples. The above listing is believed to represent a reasonable interpretation of these data but must be examined with caution.

These data suggest some conclusions regarding the relative bend ductility of the various cladding systems. Platinum, for example, was present in Systems 2a, 2b, and 5 but not in Systems 1a, 1b, or 6. Systems 1a and 2a, oxidized for 100 hours, appear to behave similarly although, as seen in Table 18, System 2a is slightly more ductile than System 1a. System 2b is inferior to System 1b after 300 hours' oxidation, and System 6 is inferior to 5 after 100 hours' oxidation. Since these three pairs of cladding systems were similar except for the presence of platinum, it appears that platinum has no consistent effect on bend ductility after oxidation exposure at 2100 F. Systems 2a, 3, and 4 are similar except for the outer cladding layer, aluminized Ni-20Cr-20W in System 2a, unmodified Ni-30Cr in System 3, and aluminized Ni-30Cr in System 4. It appears that System 4 is considerably inferior to the other two with respect to bend ductility after cyclic oxidation at 2100 F. System 3 appears slightly superior to System 2a, but a close examination of the data in Table 18 indicates that the difference between the bend ductility of these two systems after cyclic oxidation at 2100 F is small.

It was considered possible that the poor bend ductility observed in the samples oxidized at 2100 F might be due to cracking introduced into the samples during removal of the Ni-30Cr picture frame assembly and grinding of the sample edges. One sample, II-49, was, therefore, bend tested at 800 F without removal of the picture frame assembly. As shown in Table 18, this sample also failed in a brittle manner. This indicates that brittle failure was most probably the result of damage occuring during oxidation exposure rather than sample preparation.

Comparison of the rate of degradation of the bend transition temperature by oxidation at 2100 F of unprotected and clad Cr-5W is tenuous because of the limited data. Nonetheless, such a comparison indicates, as shown in Figure 41, that even lacking a cladding system that maintains its integrity in cyclic oxidation exposure, the (parabolic) rate of degradation in clad systems appears to be roughly 1/3 that of unprotected chromium. This presumably relates to the difference between contamination by nitrogen versus contamination by cladding metals.

Oxidation data for samples exposed at 2300 F are given in Table 19 and the results of bend tests on these samples are given in Table 20. Again, because of the poor bend ductility observed, not all samples which were oxidized were bend tested. All of the systems examined after cyclic oxidation at 2300 F showed very poor bend properties. As pointed out in the previous section, cyclic oxidation at 2300 F resulted in both severe metallic contamination, up to 6 mils in 100 hours, and general grain boundary nitriding throughout the chromium alloy thickness. Of the four systems evaluated, System 10 appears to have withstood exposure at 2300 F the best. This system appeared to have nitrided less severely than the others based upon metallographic examination and analysis for nitrogen. However, it is believed that this was due primarily to early separation of the cladding from the chromium alloy caused by embrittlement of the barrier region, which probably reduced the extent of metallic contamination of the chromium alloy. The use of System 10 to protect chromium at 2300 F is not considered practical.

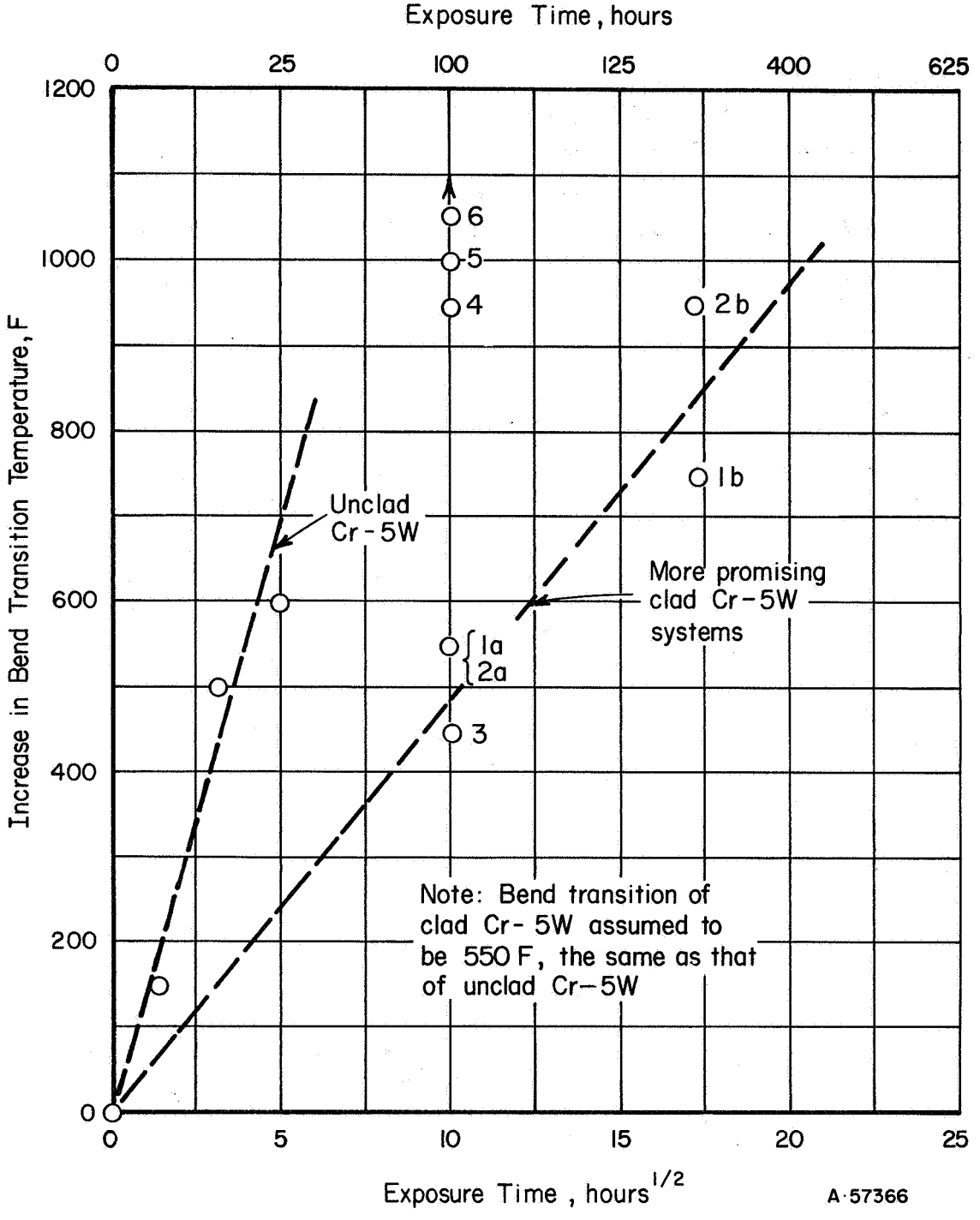

FIGURE 41. CHANGE IN BEND-TRANSITION TEMPERATURE AS A FUNCTION OF TIME OF OXIDATION EXPOSURE AT 2100 F

Numbers beside closed points indicate cladding system.

TABLE 19. OXIDATION BEHAVIOR OF BEND SAMPLES OXIDIZED AT 2300 F USING 20-HOUR CYCLES

System	Sample Number	Oxidation Time, hr	Weight Gain, mg/cm^2	Comments
1a	Not tested			
1b	Ditto			
2a	"			
2b	II-36	120	2.53	
	-39	"	3.10	
	-40	"	2.63	
	-41	"	2.67	Fracture at cladding:picture frame on one end.
	-49	"	2.32	
	-51	"	2.00	
	-29	200	3.11	Extensive fracture along cladding: picture frame junction.
	-34	"	2.59	Ditto
	-35	"	3.84	"
	-37	"	3.72	"
	-38	"	3.86	"
	-42	"	0.94	"
2c	Not tested			
3	Ditto			
4	"			
5	"			
6	"			
7	"			
8	"			
9	"			
10	X-1	80	-0.69	Severe blistering occurred.
	-2	100	0.86	Some blistering.
	-5	"	1.63	Slight blistering.
11	XI-3	"	-0.95	
	-4	"	0.93	
	-5	"	-0.03	
12	XII-1	"	2.00	Fracture at cladding:picture frame on one end.
	-2	"	1.51	
	-3	"	1.35	Ditto

TABLE 20. BEND TEST RESULTS FOR SAMPLES CYCLICALLY OXIDIZED AT 2300 F

System	Sample Number	Oxidation Time, hr	Bend Temp., F	Bend Angle (degrees) at Crack Initiation	Bend Angle (degrees) at Failure	Type of Load-Deflection Curve(1)
2b	II-51	120	1400	<5	<5	1
	-36	"	1600	<5	45	2
	-38	200	1400	<5	<5	1
	-37	"	1600	15	15	1
10	X-2	100	1400	<10	35	2
	-5	"	1600	10	40	2
11	XI-4	"	1200	<5	<5	1
	-3	"	1600	25	60	2
12	XII-1	"	1400	<5	<5	1
	-2	"	1600	20	45	2

(1) See Figure 38 for an illustration of the four types of load-deflection curves.

System 9 was known from the oxidation studies to have very poor oxidation resistance. Therefore, the bend samples from this system were evaluated without any oxidation exposure. The results are summarized below:

Sample Number	Test Temp., F	Bend Angle (degrees) for Crack Initiation	Failure
IX-5	800	<5	<10
-2	1000	25	25
-4	1200	25	25

All samples showed Type 1 load-deflection curves. Vanadium, used as a compatibility layer in this system, is apparently extremely damaging to ductility. Embrittlement resulted from the thermal treatments required for aluminizing and homogenizing the cladding system alone even with no oxidation exposure.

An illustration of the relatively low ductility observed during bend evaluation is given in Figure 42 which shows the type of cracking observed in several oxidized samples tested at 1600 F and one unoxidized sample tested at 1000 F. The two samples tested after 2100 F oxidation exposure show some ductility, System 1b being more ductile than System 2b. Very limited ductility was observed in the samples tested at 2300 F, however.

The poor bend ductility observed in the clad chromium alloy samples after cyclic oxidation at 2100 F is attributed to contamination during exposure. At 2100 F, contamination is largely the result of metallic diffusion between the cladding materials and the chromium alloy. It is believed that contamination is occurring more rapidly through the cracks developed in the tungsten barrier layer. The cracking of the barrier layer is attributed to low cycle thermal fatigue resulting from thermal expansion mismatch between the cladding layer and picture-frame nickel-base alloys, which have high expansion coefficients, and the tungsten barrier layer and chromium alloy sample which have low expansion coefficients. This problem should be reduced by eliminating the reasonably massive nickel alloy picture frame and improving the properties of the barrier layer. A thicker tungsten barrier layer might also be beneficial.

DISCUSSION OF RESULTS AND CONCLUSIONS

None of the cladding systems examined appeared capable of protecting chromium alloys from oxidation or nitrogen embrittlement during cyclic oxidation at 2300 F. Although aluminized Ni-30Cr and Ni-20Cr-20W alloys are sufficiently resistant to oxidation to be useful as 5-mil-thick cladding layers, severe nitrogen contamination of the chromium alloy occurred. Unaluminized Ni-30Cr has useful oxidation resistance as a 10-mil-thick cladding layer but similarly did not protect the substrate from nitrogen contamination. Nitrides were visible throughout the samples. Also, metallic contamination of the oxidized chromium alloy sample extended to a depth of about 7 mils in 100 hours and appeared to be increasing linearly with time to the one-half power. Contamination was apparently occurring by diffusion of some cladding component through the barrier layer. Nickel is suspected to be the diffusing element.

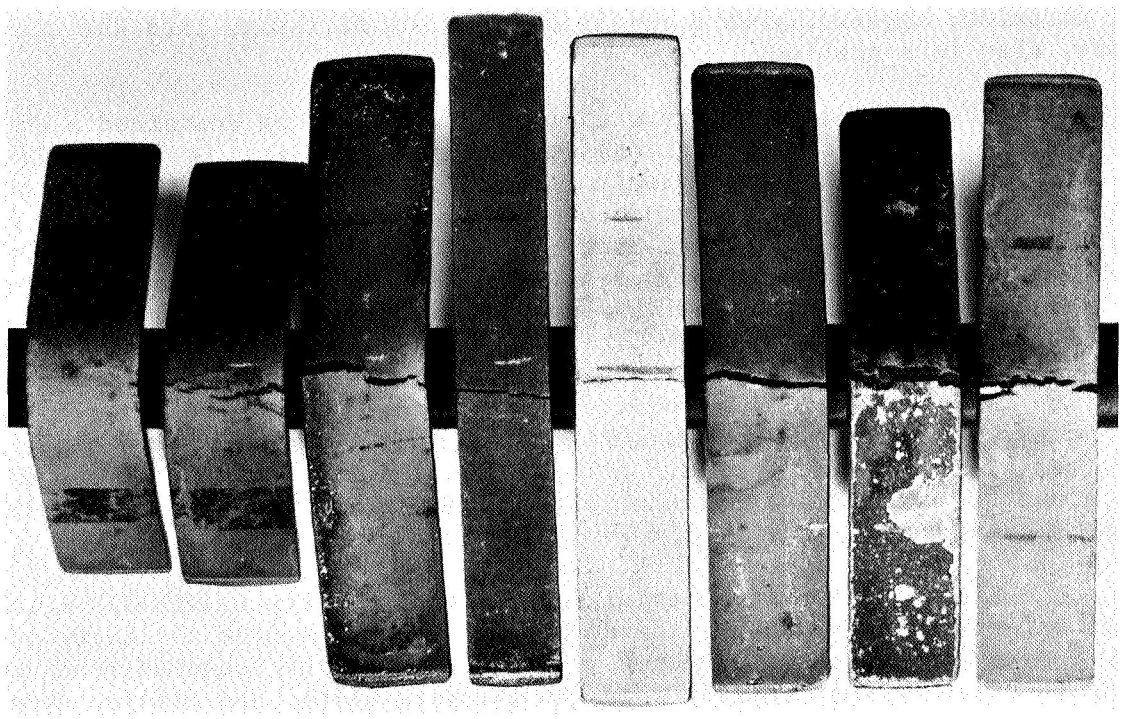

Sample No.	I-31	II-33	II-36	II-37	IX-2	X-5	XI-3	XII-2
System	1b	2b	2b	2b	9	10	11	12
Oxid. Temp., F	2100	2100	2300	2300	-	2300	2300	2300
Oxid. Time, hr	300	300	120	200	-	100	100	100
Bend Test	1600	1600	1600	1600	1000	1600	1600	1600
Failure Type (see Figure 38)	3	3	2	1	1	2	2	2

FIGURE 42. PHOTOGRAPH OF SEVERAL BEND SAMPLES AFTER TESTING

Perhaps more surprising, none of the systems examined was useful under cyclic conditions at 2100 F, although the extent of damage to the base metal was considerably less than that observed at 2300 F. No nitrogen contamination was observed, but metallic contamination extended about 2 mils in 100 hours. Again, a linear rate of contamination with time to the one-half power was observed. In this case, also, diffusion through the barrier layer was apparently the origin of contamination.

It is obvious from these studies that nickel-base alloys can adequately protect chromium-base alloys from oxidation at 2300 F and from both oxidation and nitrogen contamination at 2100 F. However, contamination of chromium-base alloys by nickel is quite rapid at both temperatures and the cladding layer must be kept away from the chromium alloy by a suitable barrier layer. If this is not done, the alloy is embrittled quite rapidly by metallic contamination. Void formation in the chromium, apparently as a result of chromium diffusion into the nickel-base alloy, also is a problem.

The bulk of the systems examined in this study contained a tungsten barrier layer. It was found that tungsten was dissolved into both the nickel-base cladding alloy and into the chromium alloy. At 2100 F, the solution rate was quite slow except in those systems containing a platinum compatibility layer between the cladding and barrier layer. At 2300 F, the solution rate of the barrier layer was such that within 200 hours the 0.5-mil-tungsten barrier was largely consumed when a platinum compatibility layer was present, and significantly reduced in thickness even in the absence of platinum. In addition, the tungsten barrier layer was found to develop cracks during cyclic oxidation testing. Thermal fatigue from the cyclic exposure is suspected. The amount of cracking appeared to be related to the number of cycles, and uncycled samples were generally crack free. Increasing the tungsten barrier layer thickness from 0.5 mil to 1.5 mil thickness did not appear to alter the amount of cracking significantly, and bend properties at 2100 F were unaffected by this change.

Several alternate barrier layer materials were examined. A tungsten-25 rhenium barrier was studied with the hope that the improved ductility of this alloy might reduce the cracking tendency. Unfortunately, the tungsten-rhenium alloy was found to dissolve very rapidly into the cladding alloy, and failure occurred by this mechanism. A thoriated tungsten alloy was examined with the aim or retarding cracking by improving the strength, increasing the recrystallization temperature, and providing an overlapped bamboo, rather than equiaxed, grain structure in the barrier layer. Only a limited number of samples were prepared, and, unfortunately, based on present knowledge, this system also contained platinum. The amount of cracking was less than half that observed in the most similar system with an unalloyed tungsten barrier (System 2b). Contamination rates were reduced at 2100 F by about 50 percent. At 2300 F, although the amount of cracking was less, the depth of contamination was not significantly changed, nor was bend ductility after cyclic oxidation improved. A molybdenum barrier layer was also examined briefly in a cladding system containing both aluminized Ni-20Cr-20W and a platinum compatibility layer. Almost complete fragmentation of the barrier material occurred during both 2100 and 2300 F cyclic oxidation exposure, apparently the result of interdiffusion between nickel and molybdenum.

As already indicated, a platinum compatibility layer between the cladding alloy and tungsten barrier layer was not beneficial, and greatly increased the solution rate of the tungsten barrier layer. A vanadium compatibility layer was examined, but also was found to be unattractive. Vanadium diffused through the cladding

layer and resulted in greatly accelerated oxidation of the cladding. Neither material appears worthy of further consideration.

Despite the failure to protect chromium-base alloys from oxidation and embrittlement during cyclic temperature exposure to oxidizing conditions, the present work has apparently defined the principal problem area. This is the maintenance of an intact barrier layer between the cladding alloy and the chromium alloy to prevent interdiffusion and embrittlement of the chromium alloy. However, other factors may also be contributing to the embrittlement observed in the material exposed to cyclic oxidation at 2100 or 2300 F. These include thermal instability of the Cr-5W alloy, embrittlement from the small amount of tungsten dissolved in the chromium alloy during exposure, and damage to the material accompanying bend sample preparation after cyclic exposure.

The present work has shown that the gas-pressure bonding method can be used to provide multi-layer metallic claddings on chromium-base alloys. All of the systems examined could be bonded successfully. In order to firmly establish the basis for substrate embrittlement and to attempt to define the extent to which each of the possible causes was effective, further work was performed. These studies are described in the Specialized Studies section which follows.

SPECIALIZED STUDIES

As indicated in the preceding section, several possible mechanisms for system embrittlement were uncovered in this investigation. The extent of each of these appeared to be resolvable with relatively small amounts of additional study. Thus, such studies were suggested by NASA and were performed as part of an expansion of the original program. They are described below.

Improved Methods of Sample Preparation

The chromium alloy samples prepared in the initial program were surface ground to provide a smooth surface and were enclosed in a nickel-30 weight percent chromium alloy yoke which had to be removed by cutting and grinding before bend tests could be performed. As a result of the marked brittleness of the chromium-tungsten alloy near room temperature, both of the operations could have produced microcracks in the specimen surface. These microcracks, if present, would be expected to be quite harmful to bend ductility. It was decided to prepare a limited number of System 1b samples by an alternate technique to determine if grinding or cutting cracks were contributing to poor bend ductility. Thus, chromium-tungsten alloy samples were prepared by electropolishing and the electropolished samples were subsequently clad using a wrap-around technique. The wrap-around procedure eliminated the yoke structure and permitted bend testing of the samples after oxidation exposure without any further cutting or grinding of the sample edges.

The samples used in these studies were prepared from chromium alloy Lot 67-100. The analysis and bend properties of this material are given in Table 2. This material had a somewhat lower bend transition temperature in the longitudinal direction than material from Lot 64-100 which was used in preparing all previous System 1b samples but a higher transition temperature in the transverse direction.

Preliminary investigation showed that a very good surface could be produced by removing approximately 3 mils per side by electropolishing. The composition of the electropolishing bath and its operating conditions are given in Table 21. Surface roughness was significantly reduced by the electropolishing operation as shown below:

Sample Condition	Direction of Measurement	Surface Roughness, microinches
As-received	Longitudinal	60-75
	Transverse	80-100
Electropolished	Longitudinal	18-35
	Transverse	22-50

No mechanical surface preparation of the as-received material was required before electropolishing.

To insure that the electropolishing treatment was not in some way harmful to bend properties, several chromium-tungsten alloy bend samples were electropolished and tested to determine their ductile-brittle bend transition temperature. The edges of the 3/4 x 3-1/2-inch bend samples were rounded by hand polishing on 400-grit paper prior to electropolishing. The results of these tests are presented in Table 22. Since the transition temperature was less than 300 F in these tests, as compared to a value of 300 F reported by the material supplier (Table 2), it appears that electropolishing is not harmful to the transition temperature and may actually be somewhat beneficial, a situation typical of the Group VIA bcc metals.

The wrap-around technique used to prepare clad samples is shown in Figure 43. The chromium alloy samples were very carefully hand ground to provide a generous end radius and to round the edges prior to electropolishing. After electropolishing, the samples were inspected using dye-penetrant methods to insure that the chromium alloy was crack free. Only completely crack-free samples were used. The tungsten barrier layer was cut slightly larger than the sample and tack-welded in place. The nickel-chromium-tungsten cladding alloy was cut at least 1/8-inch larger than the barrier layer. The cladding assembly was then enclosed in a steel envelope, using molybdenum foil for protection against iron contamination, and gas-pressure bonded. Gas-pressure bonding was accomplished at 2150 F using a 10,000 psi pressure applied for 2 hours. Aluminizing and homogenizing techniques were identical to those used in the initial work. Aluminum weight gain data are given in the Appendix, Table A-1.

Samples of System 1b were oxidized for 100 hours at 2100 F using 20-hour oxidation cycles before bend tests were performed. The average weight gain of the five samples which were oxidized was 0.83 mg/cm^2, in good agreement with the weight gain observed in previously exposed System 1b samples (see Table 9).

Bend test data for samples clad with System 1b (1.5 mil tungsten, 5 mils Ni-20Cr-20W alloy aluminized to provide about 5 weight percent aluminum) using the wrap-around technique are given in Table 23. As shown in Table 23, the transition temperature was between 1300 and 1400 F. The System 1b samples prepared in the previous studies and exposed to cyclic oxidation for 300 hours at 2100 F showed a transition temperature between 1200 and 1400 F (see Table 18). Partial ductility was measured at 1400 F in the tests reported in Table 18, whereas the new samples showed complete ductility at 1400 F. This difference can probably be attributed to the difference in oxidation time, 300 hours versus 100 hours. It was not necessary to

TABLE 21. ELECTROPOLISHING BATH USED TO PREPARE CHROMIUM ALLOY SAMPLES

Bath Composition	
Constituent	Amount by Weight
Sulphuric Acid	60 percent
Ortho-Phosphoric Acid	20 percent
Citric Acid	10 percent
Water	10 percent
Bath Operating Conditions	
Current Density	2 amps/in^2
Temperature Range	140-160 F
Rate of Chromium Alloy Removal	0.1 mil/min.
Cathode Material	Stainless Steel

TABLE 22. BEND PROPERTIES OF ELECTROPOLISHED CHROMIUM-5 WEIGHT PERCENT TUNGSTEN ALLOY FROM LOT 67-100 (Bend axis in rolling direction)(1)

Bend Temp., F	Bend Angle (degrees) at Failure	Type of Load-Deflection Curve(2)
750	>100	4
660	>105	4
500	>105	4
435	>110	4
300	>100	4

(1) DBTT of as-received material was 300 F with bend axis in rolling direction; 600 F with bend axis transverse.

(2) See Figure 38 for an illustration of the four types of load-deflection curves. Although the load-deflection curves resembled Type 3 curves to some degree, dye-penetrant inspection of the surface after testing showed no cracks to be present. Therefore, Type 4 ratings were assigned.

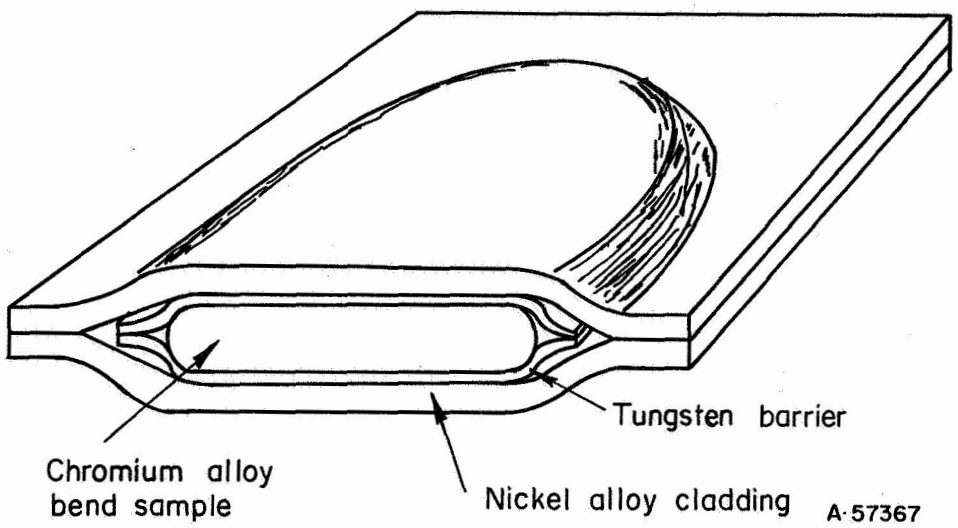

a. Drawing of the Wrap-Around Sample Construction; Entire Assembly Enclosed in Evacuated Steel Envelope for Gas-Pressure Bonding

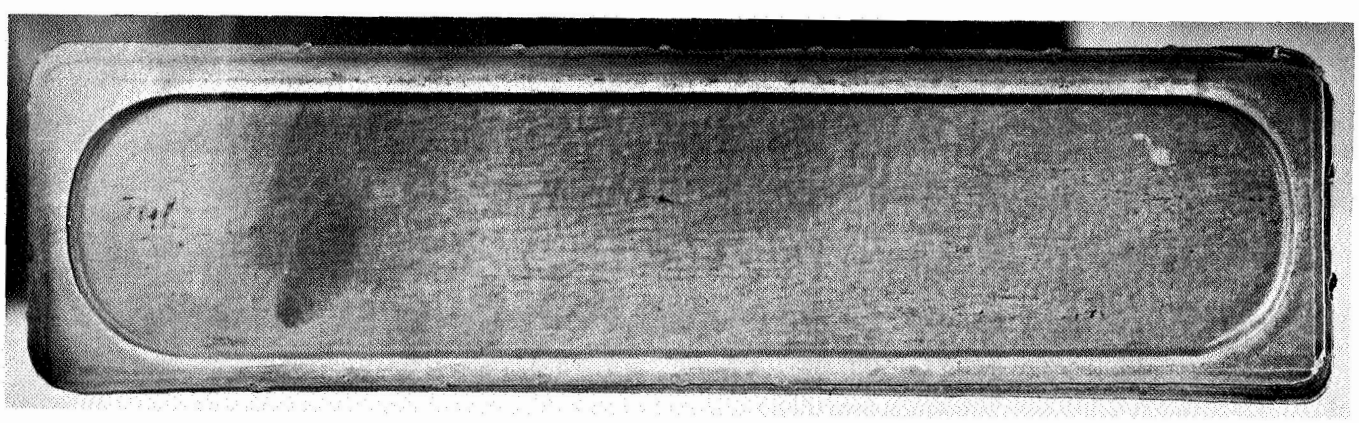

2X 8B825

b. Photograph of Sample After Gas-Pressure Bonding and Removal of Steel Envelope

FIGURE 43. ILLUSTRATION ON THE WRAP-AROUND CLADDING TECHNIQUE

TABLE 23. BEND PROPERTIES OF SYSTEM 1b-CLAD SAMPLES (PREPARED BY THE WRAP-AROUND TECHNIQUE) AFTER CYCLIC OXIDATION FOR 100 HOURS AT 2100 F

Sample Number	Bend Temp., F	Bend Angle (degrees) at Crack Initiation	Bend Angle (degrees) at Failure	Type of Load-Deflection Curve(1)
1b-6	1200	<15	<15	1
1b-1(2)	1200	-	-	-
1b-4	1300	20	20	1
1b-5	1400	>110	>110	4

(1) See Figure 38 for an illustration of the four types of load-deflection curves.

(2) Specimen was broken during preparation for testing.

remove any edge material before bend testing. Thus, the possibility of introducing microcracks into the chromium alloy was eliminated. Therefore, the poor bend ductility of oxidized System 1b observed in the initial investigation was not related to microcracks developed in the chromium alloy during either initial surface preparation of the chromium alloy or the edge grinding of bend test samples after oxidation exposure.

The microstructure of a System 1b sample prepared by the wrap-around technique is shown in Figure 44. Excellent bonding was achieved. Some recrystallization was observed in the tungsten barrier layer at the tungsten:nickel alloy interface. No other evidence of diffusion between cladding components was seen. The microstructure after 100 hours' cyclic oxidation at 2100 F is shown in Figure 45. Comparison with Figure 23 shows considerable similarity in appearance of the cladding layer. Although a few cracks were visible in the barrier layer, there was no surface cracking apparent in the chromium alloy when the cladding and barrier layer were stripped off the sample.

The new samples showed a noticeable difference in tungsten barrier layer appearance from one side to the other. One side (Side 2 in Figure 45) appeared to show extensive recrystallization, whereas the other side (Side 1) did not. Occasional patches of what appeared to be recrystallized grains were apparent on the side that retained the predominantly fibered grain structure. Microhardness readings were made on both sides at the locations shown in Figure 45 with the following results:

Location	Knoop Hardness Number, 25-gm load	
	Side 2 (Recrystallized W)	Side 1 (Wrought)
Aluminized Ni Alloy Cladding (range)	280-540	240-420
W Barrier (4 typical readings)	560,570,560,542	552,552,552,552
Cr-5W Substrate		
0.2 mil from W	315	357
0.6 Ditto	475	285
1.0 "	310	330
1.4 "	335	392
1.8 "	335	300
2.2 "	335	288
2.6 "	330	-
3.0 "	335	-
5.0 "	300	292
7.0 "	300	-
9.0 "	292	-

These data, although not conclusive, suggest the possibility of mild contamination hardening to a depth between 3 and 5 mils (7 and 12 microns) in the substrate beneath the recrystallized tungsten. Hardening is negligible by comparison underneath the wrought tungsten layer. Recrystallization of the tungsten layer was not accompanied by a gross decrease in hardness. Retention of a fibered grain structure appears to increase the effectiveness of tungsten diffusion barriera in System 1b.

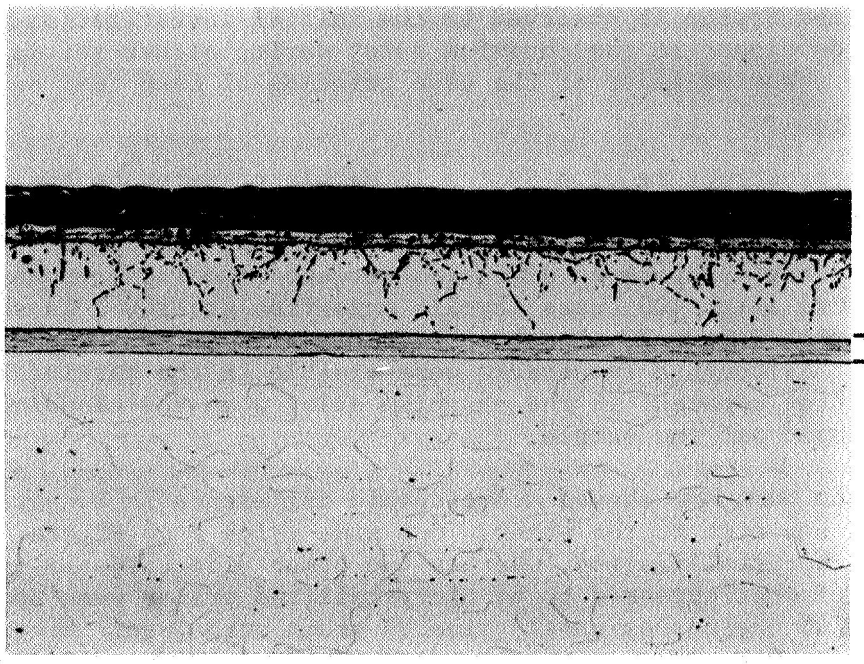

100X 60554

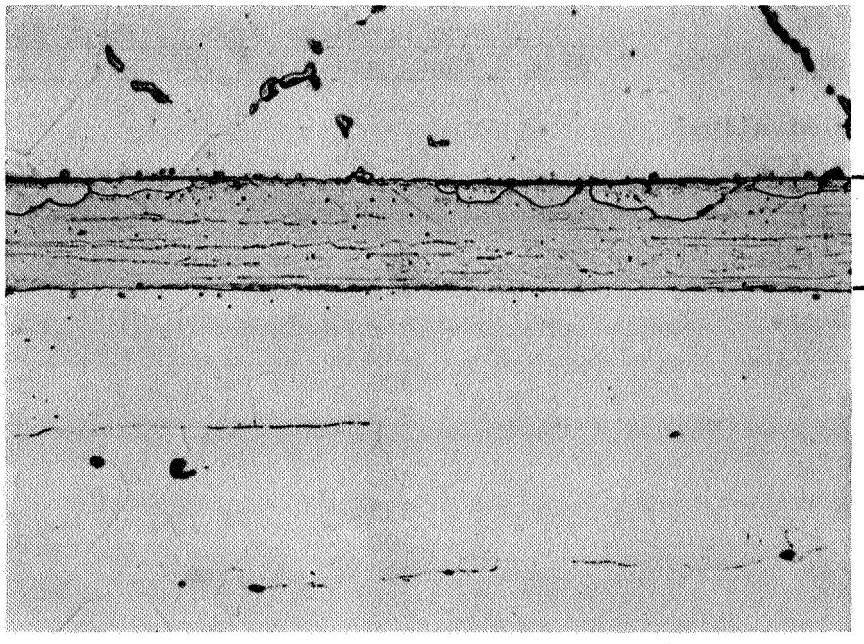

500X 60553

FIGURE 44. MICROSTRUCTURE OF SYSTEM 1b SAMPLE PREPARED BY THE WRAP-AROUND TECHNIQUE (Sample 1b-3)

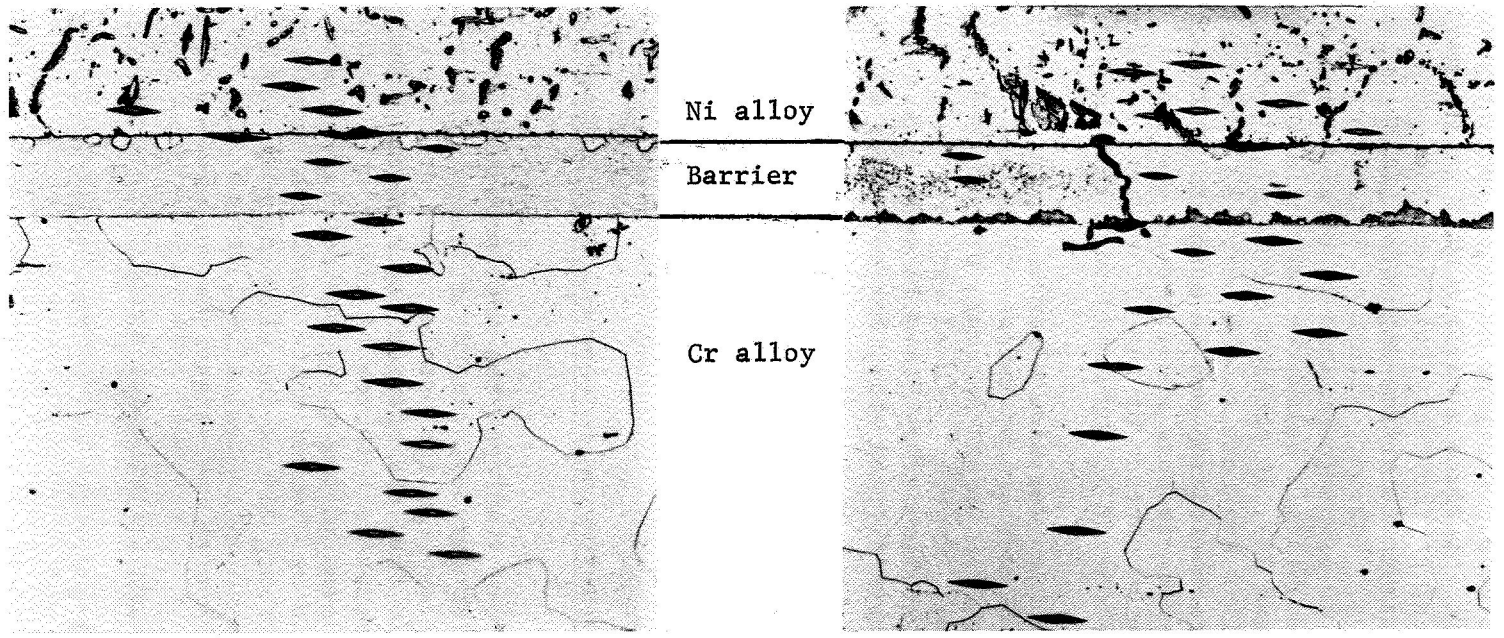

FIGURE 45. APPEARANCE OF SYSTEM 1b SAMPLE PREPARED BY WRAP-AROUND TECHNIQUE AND CYCLICALLY OXIDIZED FOR 100 HOURS AT 2100 F (Sample 1b-2)

The variatinns in nickel, tungsten, and chromium contents on the two sides of this sample were determined by microprobe analysis. The composition changes through the barrier layer are shown in Figure 46. Both barrier layers showed a high chromium content, 4 weight percent, which is about the solubility limit of chromium in tungsten at 2100 F. A higher chromium content was observed near the nickel alloy:barrier layer interface, a maximum of 5 weight percent on the wrought side and 8.3 weight percent on the recrystallized side. The chromium gradient near the nickel alloy:barrier layer interface suggests that chromium was being picked up from the nickel-base alloy. However, alternate interpretations are possible. In these additional studies no significant loss in chromium was detected in the chromium alloy in the area immediately below the barrier:alloy interface. In earlier studies (see Figures 27 and 28), an obvious decrease in chromium content was observed in the chromium alloy adjacent to the barrier. The failure to observe a similar effect with the refabrication may be a result of the thicker barrier and shorter oxidation time. Both factors would reduce the amount of material transferred. The small increase in chromium content of the nickel-base alloy near the barrier as observed in the present study is in agreement with the results of the earlier studies.

Nickel contamination was also observed in the barrier layer near the cladding:barrier interface. Higher concentrations of nickel were observed at the interfaces in the wrought side, 5.0 weight percent, as compared to 1.9 weight percent in the recrystallized side. However, nickel was detected throughout the barrier layer and well into the chromium alloy (~4 mils deep, substantiating hardness traverse results) on the recrystallized side, but only near the nickel alloy:barrier layer interface on the wrought side. Nickel contents as high as 1.5 weight percent were measured in grain boundaries of the chromium alloy beneath the recrystallized barrier layer. The analysis also indicated a tungsten content of about 6 to 6.5 weight percent, higher than the nominal 4.90 weight percent anticipated. However, no variation in tungsten content was detected from the interface to the maximum depth examined, about 4 mils beneath the barrier layer:chromium alloy interface.

Interdiffusion Between Cladding Components

Based on the above findings, the most probable cause of poor bend ductility in the oxidized samples was believed to be diffusion of a contaminating element into the chromium-base alloy from the barrier layer or the cladding alloy. Alternately, it was considered possible that the barrier layer might be embrittled by contamination, and that it could serve as a source of cracks which would subsequently progress into the chromium alloy, even if the alloy was not itself embrittled. The validity of these assumptions could be checked quite readily by removing the cladding and barrier layers, or by removing all of the cladding plus enough of the chromium alloy to exceed the expected depth of contamination, before bend testing. Several samples were available from the initial investigations which could be used in these studies.

Three systems were selected for study. These were:

System 1b: 1-1/2 mil W:5 mil Ni-20Cr-20W:5 percent Al

System 2b: 1-1/2 mil W:1/2 mil Pt:5 mil Ni-20Cr-20W:5 percent Al

System 11: 1-1/2 mil W:10 mil Ni-30Cr.

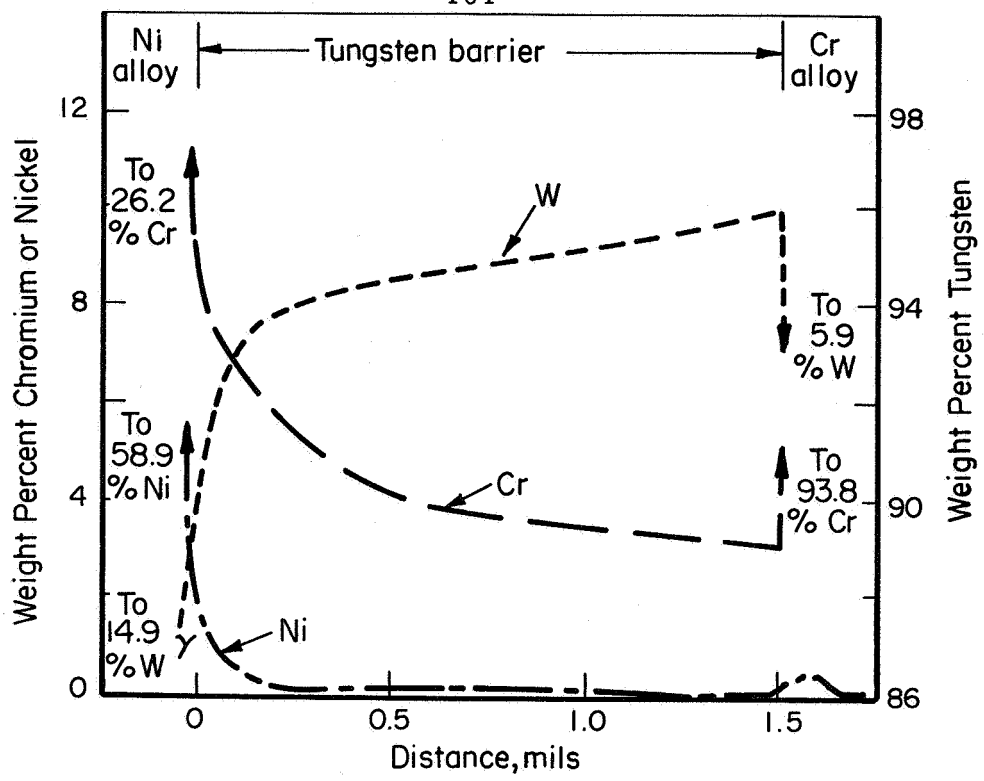

a. Side That Appeared Recrystallized

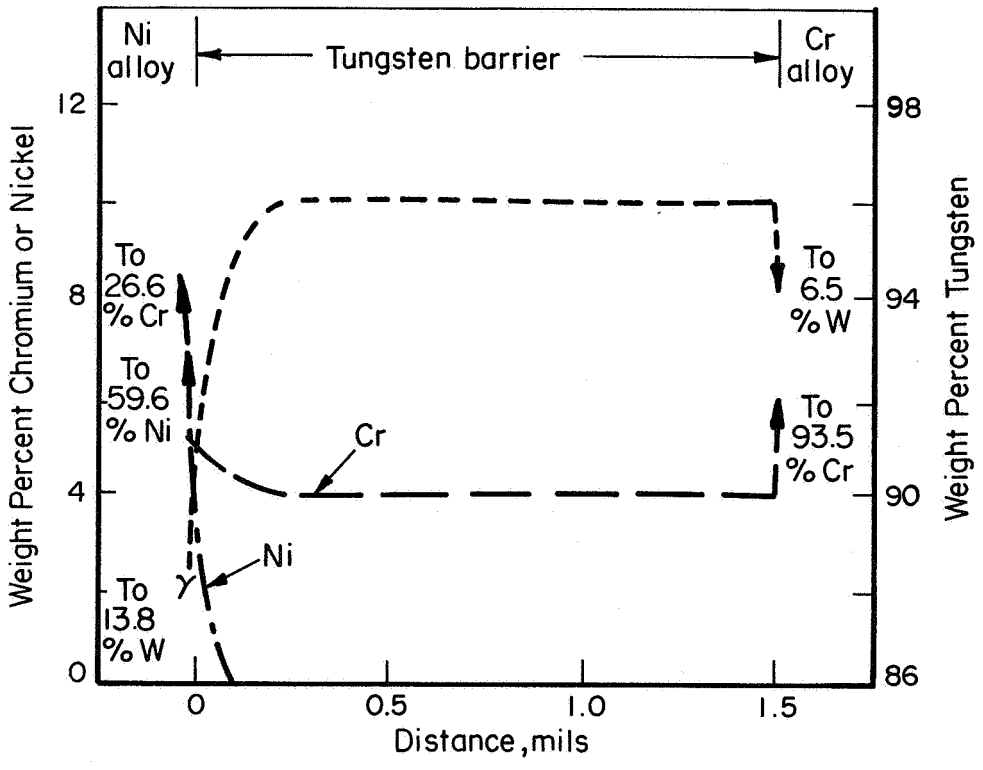

b. Side That Appeared Wrought A-57368

FIGURE 46. VARIATION OF COMPOSITION IN TUNGSTEN BARRIER OF SYSTEM 1b SAMPLE AFTER CYCLIC OXIDATION AT 2100 F (SAMPLE 1b-2)

These systems contained the major elements which were considered potentially responsible for brittleness after oxidation; nickel, aluminum, and platinum. Samples which had been oxidized in earlier studies, but not bend tested, or half lengths of bend samples which failed in a brittle manner, were selected for study. The cladding, barrier layer, and portions of the chromium alloy were removed by a combination of electrolytic and chemical dissolution. Samples studied are indicated in the Appendix, Table A-2.

The appearance of representative samples of these three systems after removal of all of the cladding layer plus about one mil of the chromium alloy is shown in Figures 47 through 49. The Systems 1b and 2b samples had been exposed to cyclic oxidation for 600 hours at 2100 F before cladding removal while the System 11 sample had been exposed to cyclic oxidation for 100 hours at 2300 F. A considerable amount of surface cracking was obvious in all three samples. In addition, the System 1b sample appeared to show preferential (grain boundary?) attack suggesting some degree of alloy segregation. The crack pattern in Systems 1b and 2b samples is typical of that observed in material failing by heat checking, or thermal fatigue, and presumably developed during cyclic oxidation exposure. The amount of cracking in the System 11 sample was considerably less than that in the other two systems. Although the number of cycles was less, the maximum temperature was 2300 F. It is surprising, therefore, that such a large difference in crack pattern developed. Absence of the aluminizing and homogenizing treatments in System 11 may, in part, account for this difference. The cracks shown in Figures 47 through 49 have apparently been chemically enlarged, and, except for this increased size, they are quite similar to those shown in the photomicrographs reproduced in Figures 24, 25, and 33. Electropolishing these samples to remove an additional 5 to 7 mils of chromium alloy resulted in elimination of the crack pattern on the surface.

Examination of declad samples showed that a considerable number of edge cracks were introduced by the cutting operation used to remove the nickel-chromium alloy yoke from the bend samples. This is shown by comparing the two samples shown in Figure 50. The first was sectioned in the normal manner to remove the yoke, while the second sample was hand ground to remove most of the yoke and chemically etched to remove that portion adjacent to the sample. At a later time, the samples were declad. Although some enlargement of edge cracks occurred during cladding removal, it is obvious that severe edge cracking was developed by the sectioning operation. Surprisingly, both the bend tests of material with the yoke intact (Sample II-49, System 2b) and the reexamination of System 1b samples prepared by the wrap-around technique indicated that this rather severe edge cracking had relatively little effect on bend ductility.

Bend tests were performed on System 1b samples which had been cyclically oxidized at 2100 or 2300 F and then treated to remove all of the cladding plus approximately 1, 8, or 15 mils of chromium alloy. No cracks were present after removal of 8 or 15 mils of chromium alloy. The results of the bend tests are presented in Table 24. In samples oxidized at 2100 F, the ductile-brittle transition temperature was apparently quite close to 300 F after removal of all of the cladding layer plus 8 or more mils of chromium-base alloy. This is about 800 F below the bend transition temperature of approximately 1400 F measured on the samples as clad (see Table 18). When only the cladding material and 1 mil of alloy was removed, the transition temperature was decreased less than 200 F, if at all. Removal of the cladding plus 7 mils of alloy from the sample exposed at 2300 F resulted in a bend transition temperature between 800 and 1200 F as compared to a value of greater than 1600 F measured for the clad sample (see Table 20).

20X 1C903

FIGURE 47. SURFACE APPEARANCE OF SYSTEM 1b SAMPLE AFTER CYCLIC OXIDATION AT 2100 F AND DECLADDING (Sample I-24, 600 hr at 2100 F, 20-hr cycles)

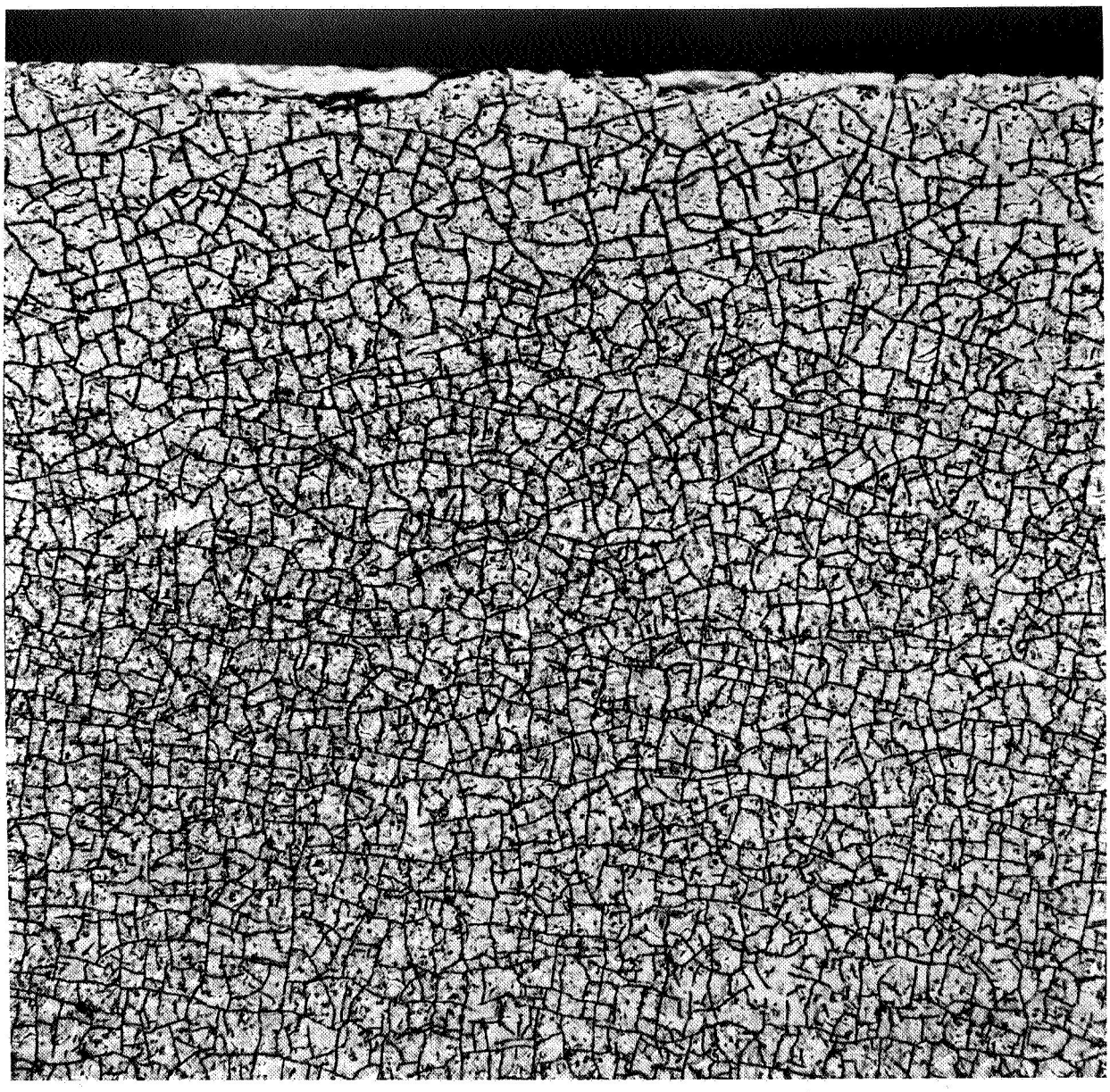

20X 1C909

FIGURE 48. SURFACE APPEARANCE OF SYSTEM 2b SAMPLE AFTER CYCLIC OXIDATION AND DECLADDING (Sample II-50, 600 hr at 2100 F, 20-hr cycles)

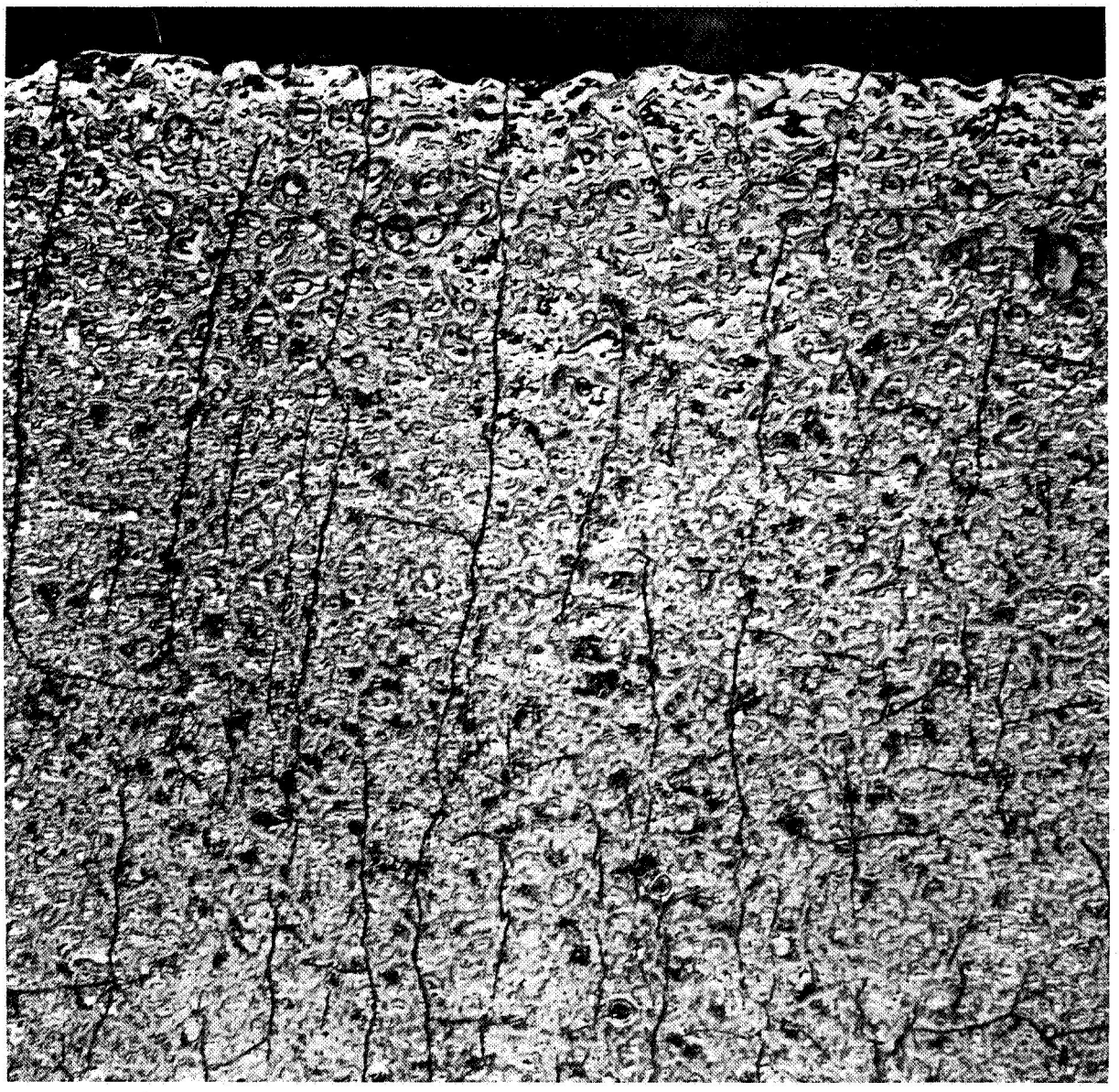

20X 1C911

FIGURE 49. SURFACE APPEARANCE OF SYSTEM 11 SAMPLE AFTER CYCLIC OXIDATION AT 2300 F AND DECLADDING (Sample XI-5, 100 hr at 2300 F, 20-hr cycles)

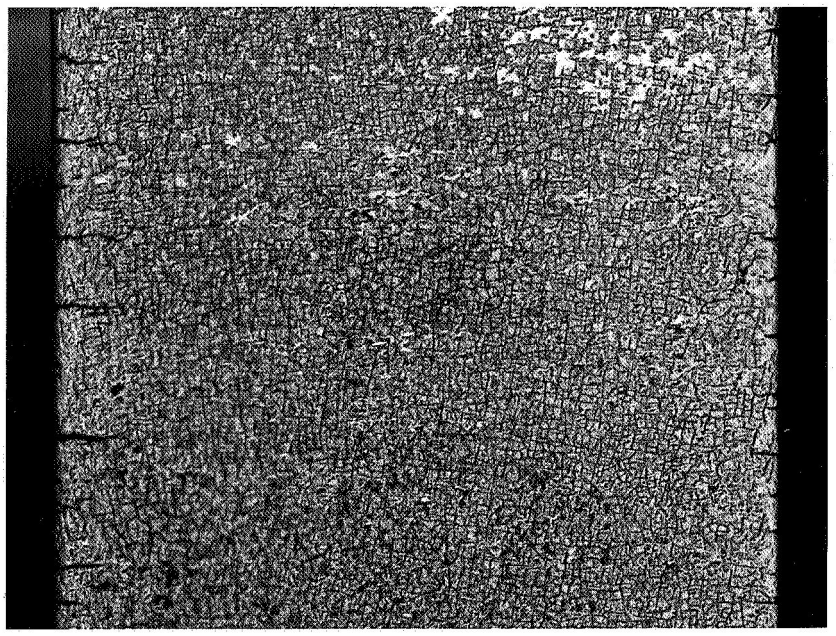

5X 1C906

(a) Edge cracks in sample cut from yoke (Sample II-44)

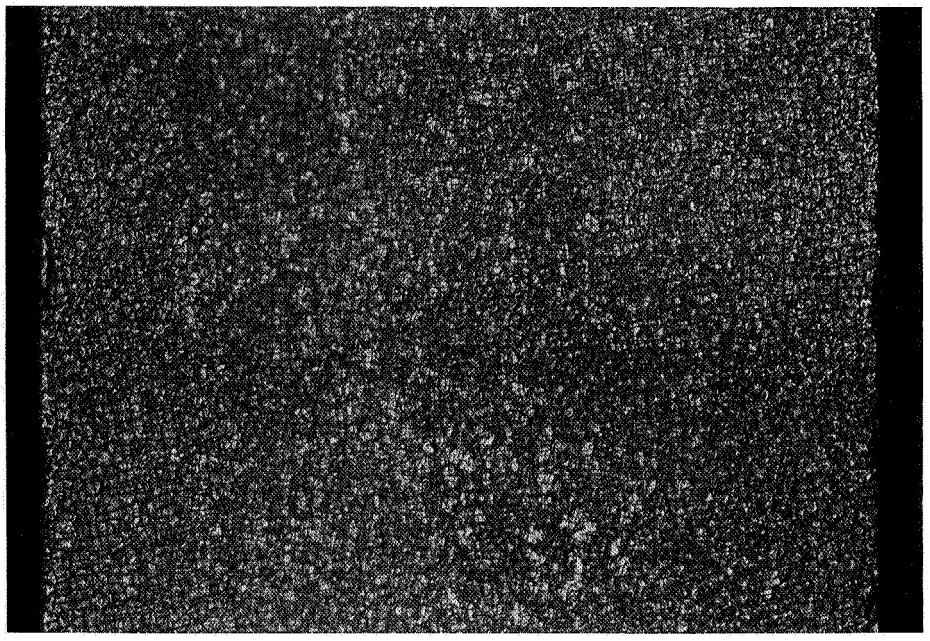

5X 1C908

(b) Absence of edge cracks in sample ground and etched from yoke (Sample II-50)

FIGURE 50. EFFECT OF METHOD OF YOKE REMOVAL ON EDGE CRACKING

TABLE 24. BEND PROPERTIES OF SYSTEM 1b SAMPLES AFTER CYCLIC OXIDATION, DECLADDING, AND REMOVAL OF VARYING AMOUNTS OF CHROMIUM ALLOY

Sample Number	Amount of Cr Alloy Removed, mils	Bend Temp., F	Bend Angle (degrees) at Crack Initiation	Bend Angle (degrees) at Failure	Type of Load-Deflection Curve[1]
		Oxidized 600 hr at 2100 F, 20-hr cycles			
II-44	1	1200	<10	<10	1
-50	9	1000	>90	>90	4
-48	8	520	>110	>110	4
-48[2]	8	300	>30	>30	4
-45	14	810	>105	>105	4
-46	15	315	<5	<5	1
		Oxidized 120 hr at 2300 F, 20-hr cycles			
II-39	1	1410	<5	<5	1
-47	7	1200	>80	>80	4
-47[2]	7	800	<10	<10	1

(1) See Figure 38 for an illustration of the four types of load-deflection curves.

(2) One-half of previously fractured sample retested.

X-ray fluorescence measurements were made on the surface of three samples after various amounts of metal removal and compared with the surface analysis of the alloy base. The results are shown in Table 25. A large increase in Ni and Pt content was found immediately below the cladding surface of samples oxidized at 2100 F. Removal of 15 mils of chromium alloy was adequate to eliminate this difference. Removal of 7 mils from the sample oxidized at 2300 F was not adequate to remove all of the Ni or Pt contamination. It is obvious from these data that contamination from Ni and Pt occurs quite rapidly. No apparent contamination from W or Al was measured. The X-ray fluorescence measurements were not sensitive enough to measure small differences in tungsten content of the type which would result from diffusion of chromium into the cladding layers, and no analysis for changes in chromium content at the surface was made.

These studies showed that removal of the contaminated region adjacent to the cladding would greatly improve bend ductility. Since poor bend ductility was observed after cyclic oxidation in both platinum-containing and platinum-free samples (see Tables 18 and 20), it is likely that nickel diffusion into the chromium-tungsten alloy is a more significant factor than platinum diffusion. As will be shown later in the studies of thermal stability of the chromium-tungsten alloy, chromium diffusion into the cladding alloy may also be a factor in the poor bend ductility.

As a further aid in defining the source of contamination of clad chromium-tungsten alloy samples during oxidation exposure, three new cladding systems were prepared. These systems are identified below:

System	Barrier Layer	Cladding Layer	Aluminized
13	1.5 mil W	None	No
14	None	5 mil Ni-30 weight percent Cr	No
15	0.5 mil W	5 mil Ni-30 weight percent Cr	Yes (5 weight percent)

Aluminizing data for System 15 samples and the disposition of the various samples from all three systems are included in Appendix Tables A-1 and A-2. All samples were prepared using an electropolished chromium alloy substrate and the wrap-around technique shown in Figure 43. Gas-pressure bonding was accomplished at 2150 F using a 10,000 psi pressure applied for 2 hours. Systems 13 and 15 samples were prepared using Lot 67-100 chromium alloy while System 14 samples were prepared using Lot 64-100 chromium alloy.

System 13 samples were exposed at 2100 F in a high-purity argon atmosphere (99.999 percent min.). Samples were encapsulated in clear quartz tubes and cycled to 2100 F using five cycles of either 2 hours or 20 hours to give a total time of 10 or 100 hours at temperature. It was anticipated that if thermal fatigue of the tungsten and/or interdiffusion of tungsten at the chromium alloy surface were the primary causes of failure, these samples would be embrittled, but that they would be ductile if nickel or chromium diffusinn was responsible. To provide a basis for comparison, some samples were tested as clad.

The System 14 samples (no tungsten barrier under Ni-30Cr) were cyclically exposed in air at 2100 F using five 20-hour cycles. System 15 (tungsten barrier under aluminized Ni-30Cr) samples were exposed for 100 hours at 2100 F using both

TABLE 25. RELATIVE CONTENTS OF INTERDIFFUSING ELEMENTS AT SEVERAL DEPTHS IN DECLAD SYSTEM 1b SAMPLES

Sample Number	Amount of Cr Alloy Removed, mils	Cyclic Oxidation Exposure, 20-hr cycles	Relative Content(1) of Ni	Pt	Al	W
64-100 unclad base	-	None	A	B	C	D
II-44	1	600 hr at 2100 F	60A	100B	C	D
-45	14	Ditto	A	B	C	D
-47	7	120 hr at 2300 F	5A	2B	C	D

(1) These data are comparative analyses, the three bend samples being compared to the base. Thus, the as-received base contains A percent nickel (a very small trace quantity) since all other constituents besides Cr, W, Y, S, and the interstitials are less than 1000 ppm, and Sample II-44 contains sixty times as much nickel as the base. Absolute quantities are not known.

cyclic and continuous exposures. System 14 was expected to be severely embrittled since interdiffusion would occur unchecked in the absence of a tungsten barrier. System 15 was expected to be embrittled by cyclic exposure but not by continuous exposure if diffusion occurred primarily through cracks in the barrier, and equally in both exposures if cracking of the barrier was not the major factor.

Surfaces of the exposed (argon) System 13 samples showed no visual evidence of the exposure. The tungsten foil edges protruding around the sample were brittle, and some chipping occurred during handling after exposure. Weight change data were thus meaningless on those samples. No cracks were present in the tungsten foil.

The average weight gain of Systems 14 and 15 samples during oxidation exposure at 2100 F was as follows:

System 14	100-hr cyclic exposure	2.29 mg/cm^2
System 15	100-hr cyclic exposure	0.77 mg/cm^2
System 15	100-hr continuous exposure	0.45 mg/cm^2

The weight gain for System 14 samples was somewhat higher, and for System 15 samples somewhat lower than expected from earlier work on similar systems (see Table 9). The differences were relatively small, however, and probably are not significant. Weight gain data and appearance of samples after exposure indicated complete protection of the substrates from oxidation.

Bend test results for these three systems after exposure at 2100 F are shown in Table 26. It is apparent from the data that the tungsten cladding process used in System 13 samples increased the transition temperature somewhat since electropolished chromium alloy from Lot 67-100 had a transition temperature of <300 F. A part of this difference may be the result of recrystallization of the chromium alloy during gas-pressure bonding. Thermal cycling for either 10 or 100 hours at 2100 F did not appear to alter the ductility transition temperature significantly. Tungsten contamination from the barrier layer is apparently not a major contributor to the poor bend ductility observed in clad samples after oxidation. System 14 was severely embrittled by cyclic exposure at 2100 F, as was anticipated, the transition temperature being raised to near 1400 F. System 15 samples were also severely embrittled by exposure to cyclic oxidation at 2100 F. In this case, the transition temperature was near 1500 F. Since previous work has suggested that aluminum does not contribute significantly to loss of bend properties (see page 84), it is concluded that a 1/2-mil tungsten barrier layer has little effect on interdiffusion and may actually be somewhat detrimental. Rather surprisingly, continuous oxidation for 100 hours resulted in almost the same bend properties as cyclic oxidation. This result suggests that interdiffusion is not primarily related to thermal cracking of the barrier. One sample of each system was declad before exposure at 2100 F and examined for the presence of cracks in the substrate. None were found. A similar examination after exposure at 2100 F showed cracks to be present in Systems 14 and 15 samples, but not in System 13 samples. The amount of surface cracking in oxidized System 15 samples appeared greater after cyclic exposure than after noncyclic exposure. The crack pattern observed in a System 15 sample after cyclic oxidation exposure is shown in Figure 51. Comparison with the crack patterns shown in Figures 47 through 49 indicates a lesser degree of cracking in this sample. This may be related either to the fewer number of cycles or to the difference in sample cladding technique (yoke versus wrap-around). As indicated earlier, System 1b samples (1.5 mil barrier versus 0.5 mil W barrier in System 15) prepared by the wrap-around technique and cycled five times at 2100 F using 20-hour cycles showed no surface cracks on decladding.

TABLE 26. BEND PROPERTIES OF THREE CLADDING SYSTEMS AFTER EXPOSURE AT 2100 F

System	Sample Number	Bend Temp., F	Bend Angle (degrees) at Crack Initiation	Bend Angle (degrees) at Failure	Type of Load-Deflection Curve(1)
		No Exposure, tested as clad			
13	13-16	600	<10	<10	1
	-15	700	<5	<5	1
	-14	800	>90	>90	4
	-13	1200	>90	>90	4
		Exposed 10 hr at 2100 F in Argon, 2-hr cycles			
13	13-3	600	<5	<5	1
	-4	700	20	20	1
	-2	800	>90	>90	4
	-1	1200	>105	>105	4
		Exposed 100 hr at 2100 F in Argon, 20-hr cycles			
13	13-9	600	30	30	1
	-10	700	20	20	1
	-8	800	>100	>100	4
	-7	1200	>100	>100	4
		Exposed 100 hr at 2100 F in Air, 20-hr cycles			
14	14-2	1200	15	15	1
	-3	1400	50	50	1
	-4	1500	>100	>100	4
	-1	1600	>100	>100	4
15	15-10	1200	20	20	1
	-11	1400	30	30	1
	-9	1500	35	35	1
	-8	1600	>100	>100	4
		Continuous Exposure for 100 hr at 2100 F in Air			
15	15-1	1200	25	25	1
	-3	1400	35	35	1
	-4	1500	50	50	1
	-5	1600	>100	>100	4

(1) See Figure 38 for an illustration of the four types of load-deflection curves.

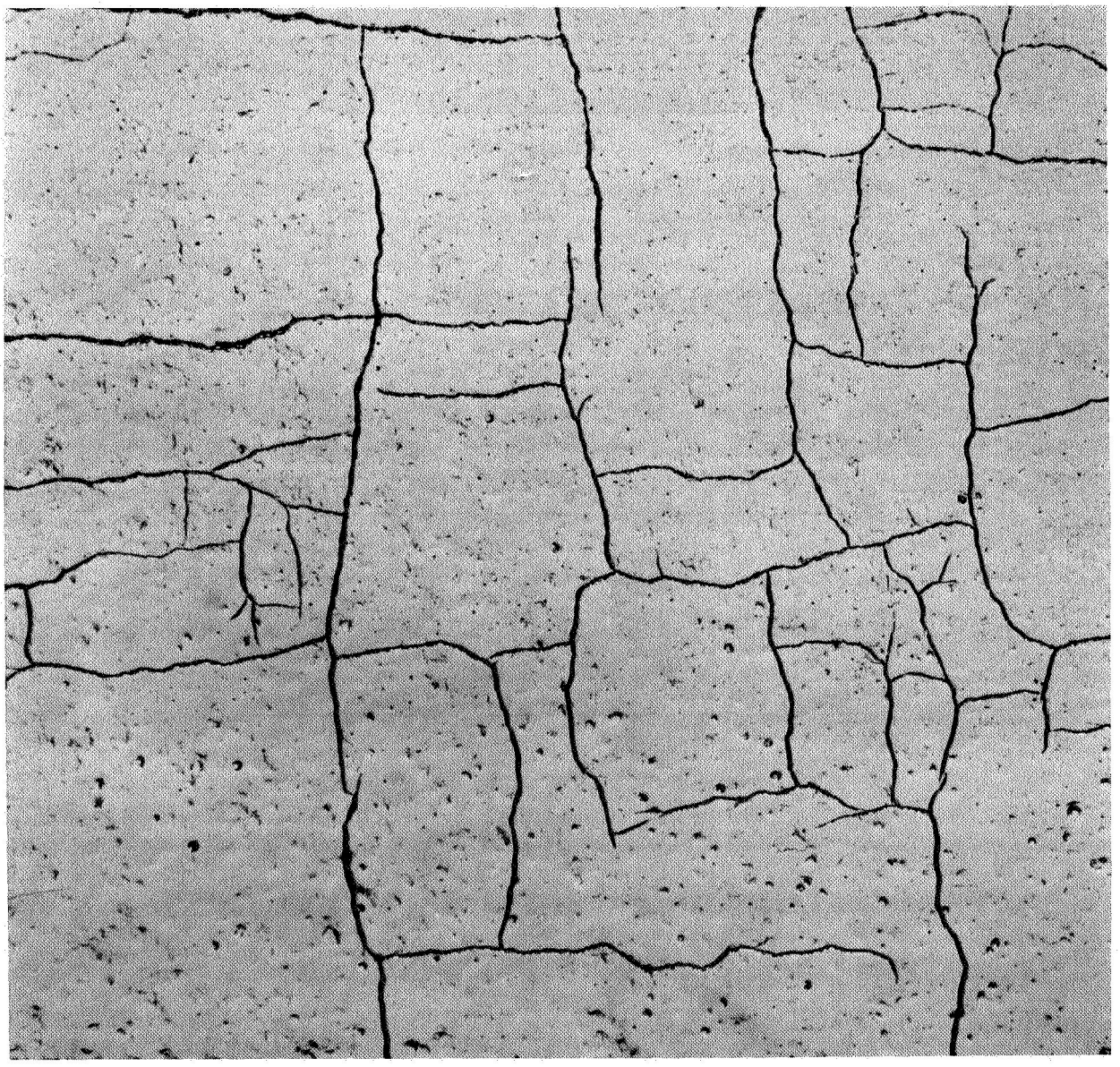

20X 6C750

FIGURE 51. SURFACE APPEARANCE OF SYSTEM 15 SAMPLE AFTER CYCLIC OXIDATION AT 2100 F AND DECLADDING (Sample 15-7, 100 hr at 2100 F, 20-hr cycles)

The microstructure of System 13 both as-clad and after cyclic exposure for 100 hours at 2100 F is shown in Figure 52. No cracking was apparent in the tungsten layer. Some grain growth appeared to have occurred in the chromium alloy during cyclic exposure. A small band of recrystallized tungsten may also have developed near the tungsten:chromium alloy interface.

System 14 samples showed evidence of contamination in the as-clad samples, as shown in Figure 53. Contamination was evident visually to a depth of about 0.7 mil. An unusual large blocky phase was also present at the interface. After cyclic oxidation at 2100 F, the depth of heavy contamination was increased to about 1.1 mil as shown in Figure 54. The blocky phase was seen at a considerably greater depth in this case, no longer coexisting with the dark precipitate contamination. Grain boundary cracking appeared to have occurred in the heavily contaminated region. Microhardness readings were made on this system after cyclic oxidation with the results shown in Table 27. Appreciable hardness increase was apparent to a depth of almost 4 mils. Earlier measurements, made on samples contained in a yoke of Ni-30 weight percent chromium, indicated as much as 7 mils contamination as shown in Table 12. The blocky phase was considerably harder than the material adjacent to it. Knoop hardness readings using a 25-gram load gave the following results:

Blocky phase	1100 to 1480 KHN
Adjacent Cr alloy matrix	615 KHN

System 15 also showed some evidence of contamination in the clad condition as shown in Figure 55. The contaminated regions tended to be associated with recrystallized-appearing areas in the barrier layer. After continuous oxidation for 100 hours at 2100 F, considerably more contamination was present, as shown in Figure 56. Again, contamination appeared related to recrystallization in the barrier layer. Cracking of the barrier layer was not extensive, but cracks were frequently observed in the chromium alloy in contaminated regions. Two sides of one sample are illustrated in Figure 56 to point out a variation in tungsten observed in all of the samples prepared using the wrap-around technique. It is readily seen that the barrier layer is quite different on one side as compared to the other. Major differences in thickness are evident. A check of the as-received tungsten foil showed tungsten thickness variation as follows:

0.5 mil stock	0.4 to 0.7 mil
1.5 mil stock	1.7 to 2.3 mils

In addition, it appeared that the thinner material recrystallized more readily, or perhaps contaminated more rapidly, than the thicker material. (Bacause this two-sidedness was even more pronounced in System 1b, factors other than barrier layer thickness are obviously important.) Since tungsten material was randomly selected in preparing clad samples, these differences in behavior resulted in some difficulty in analyzing the test results.

The appearance of the System 15 sample exposed to cyclic oxidation is shown in Figure 57. This sample showed major amounts of pitting in the nickel cladding alloy and in the chromium alloy. In general, it appeared in much worse shape than the samples exposed to static oxidation.

The extensive degradation of the barrier layer in System 15, and the relatively small changes in tungsten appearance in System 13, indicate that aluminized nickel-chromium alloy is reacting with the barrier layer and resulting in its rapid

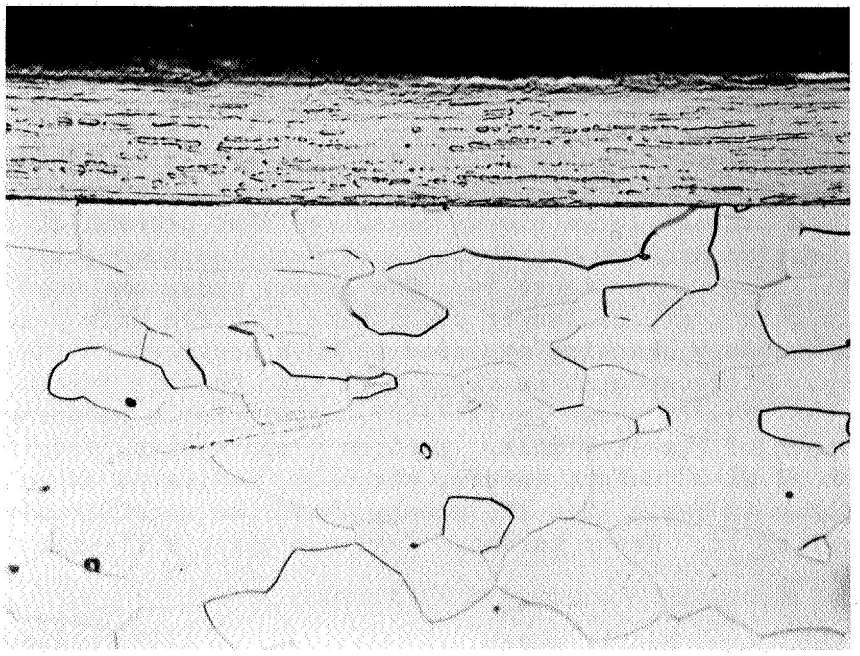

500X (a) As clad 60552

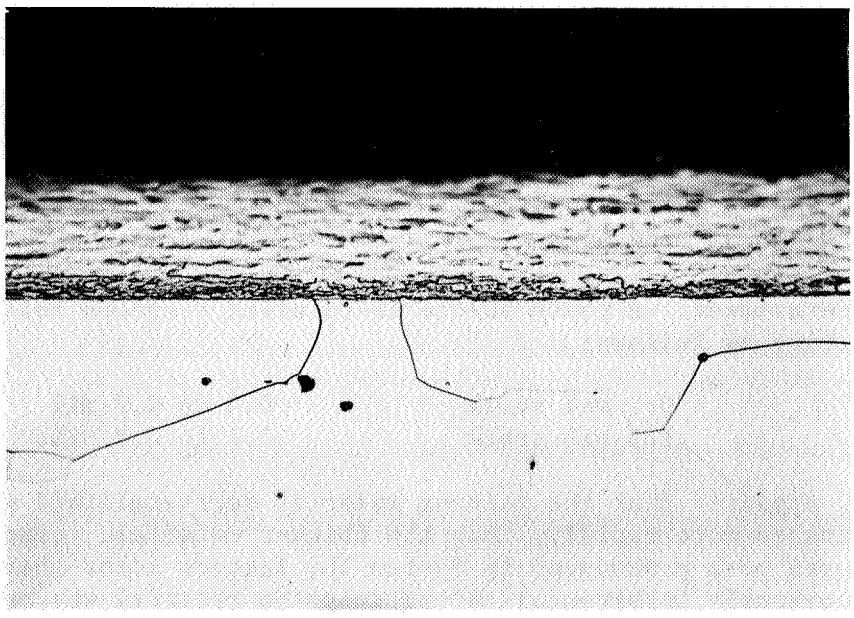

500X 60561

(b) Cyclically exposed in argon for 100 hr at 2100 F

FIGURE 52. MICROSTRUCTURE OF SYSTEM 13 SAMPLES

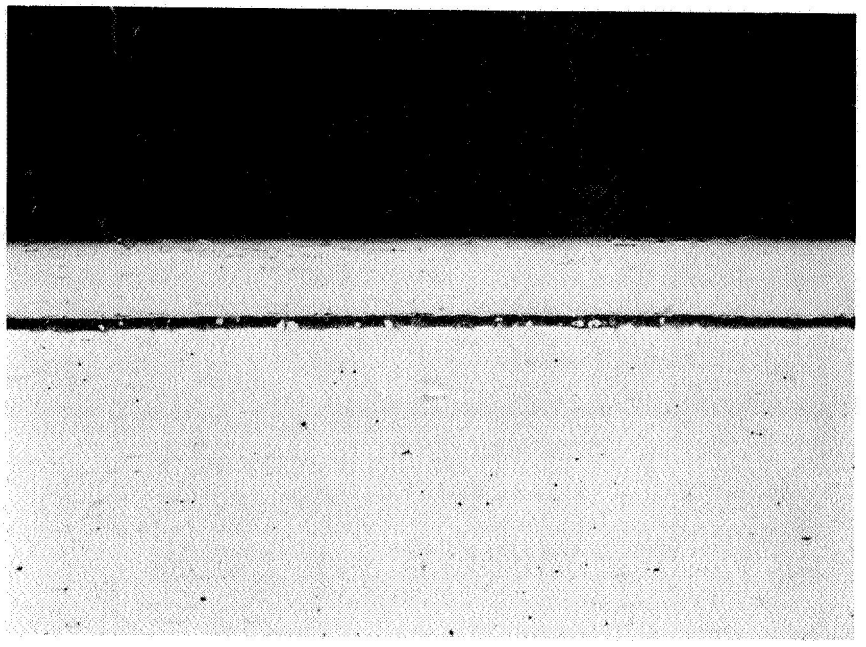

100X 60558

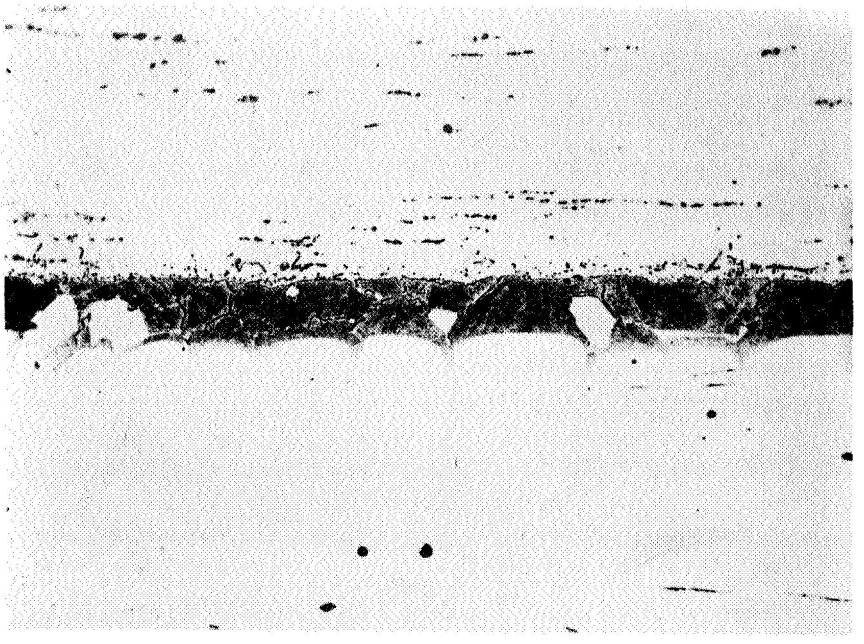

500X 60557

FIGURE 53. MICROSTRUCTURE OF SYSTEM 14, AS CLAD (Sample 14-7

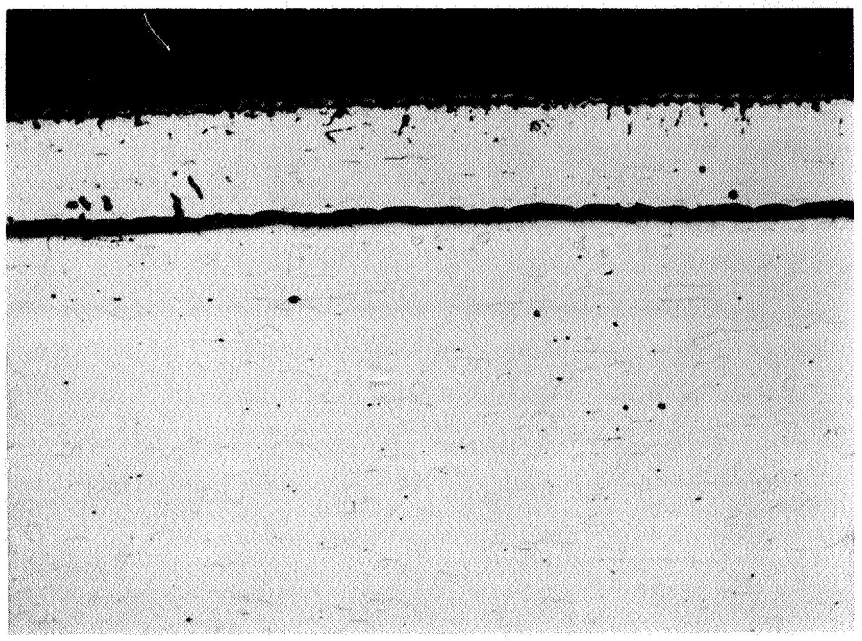

100X 60570

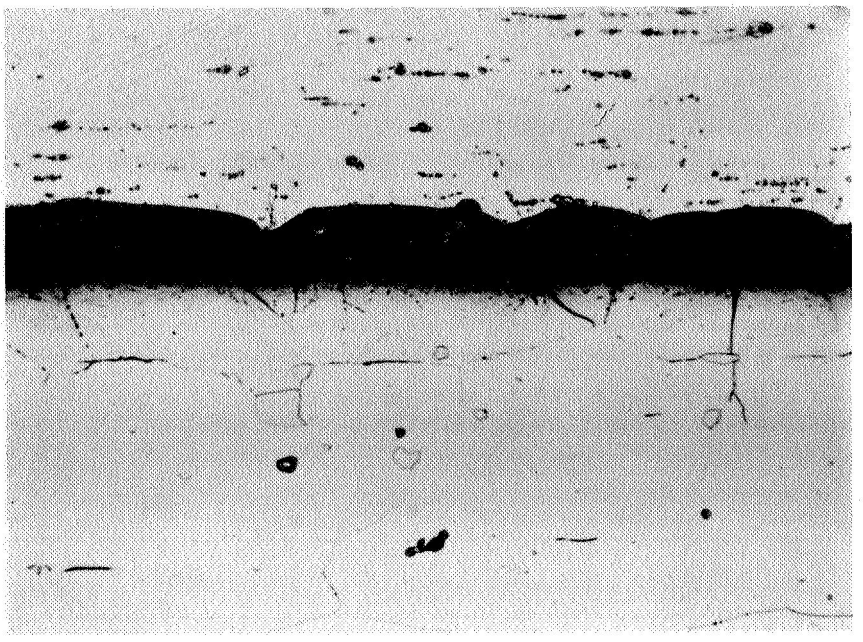

500X 60571

FIGURE 54. MICROSTRUCTURE OF SYSTEM 14 SAMPLE AFTER 100-HR CYCLIC OXIDATION AT 2100 F (Sample 14-6)

TABLE 27. KNOOP HARDNESS OF SYSTEM 14 SAMPLE AFTER 100-HOUR CYCLIC OXIDATION AT 2100 F (25-gm LOAD)

Distance from Cladding:Cr Alloy Interface, mils	Knoop Hardness Number	Microstructural Region
-3.0	310	Ni-30 weight percent Cr cladding
-2.2	244	Ditto
-1.4	195	"
-0.6	260	"
-0.2	342	"
0.2	780	Heavy precipitate zone
0.6	780	Ditto
1.0	1010	Clear zone with different etch response and few hard particles
1.4	570	Ditto
1.8	540	"
2.2	680	"
3.0	634	"
3.8	360	"
4.2	290	Unaffected Cr alloy
5.4	295	Ditto
7.0	280	"

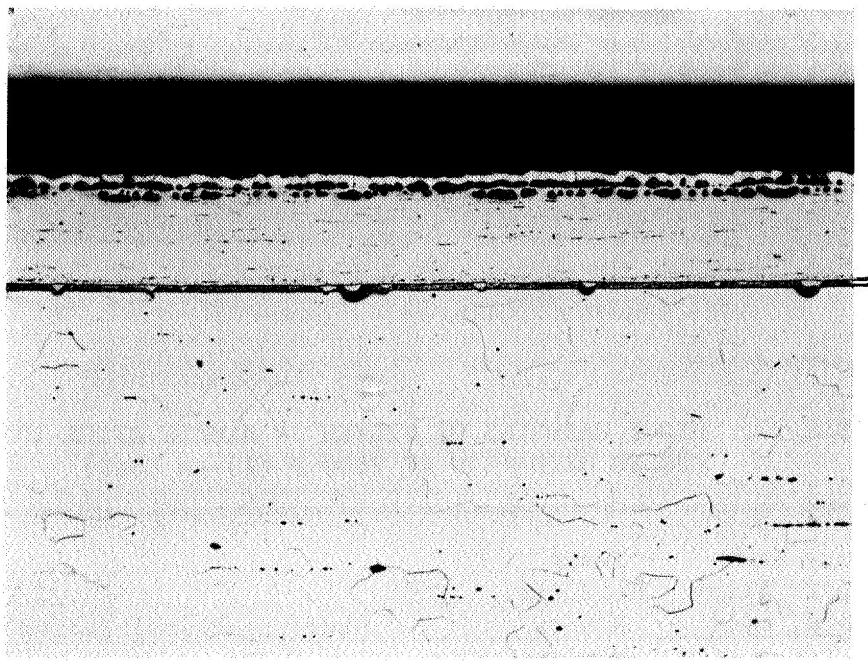

100X 60555

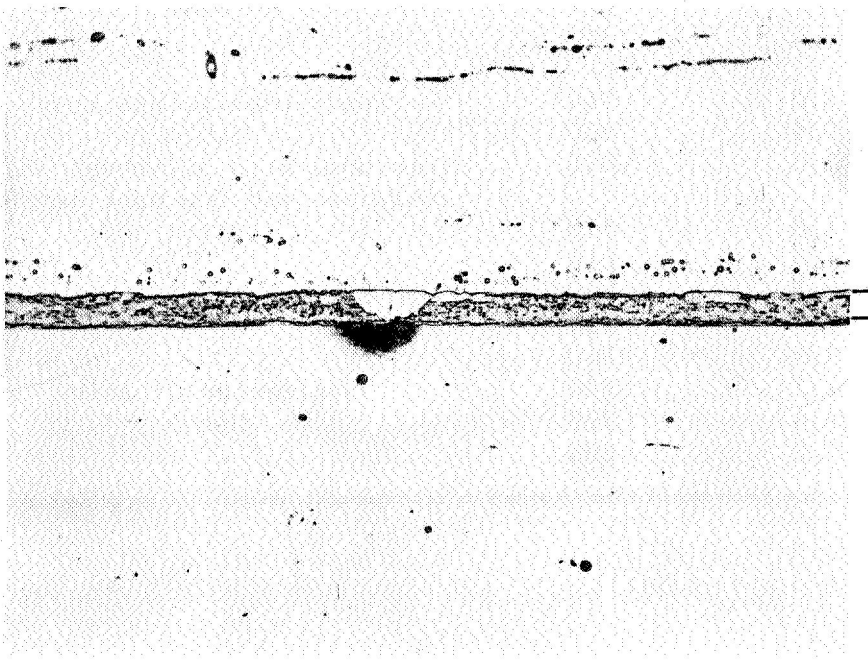

500X 60556

FIGURE 55. MICROSTRUCTURE OF SYSTEM 15 SAMPLE, AS CLAD (Sample 15-2)

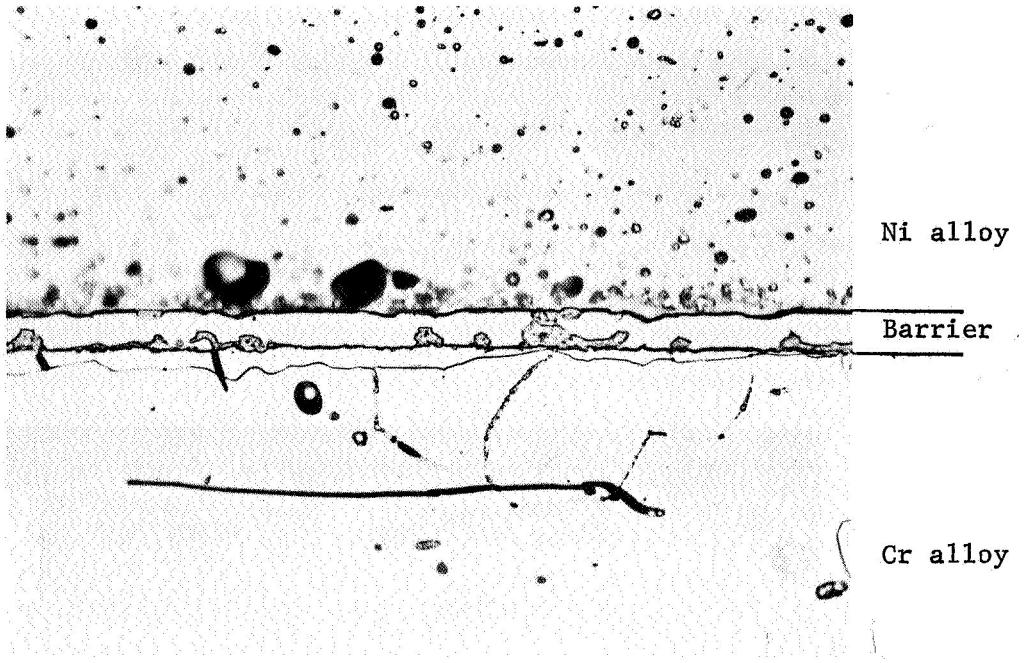

500X 60559

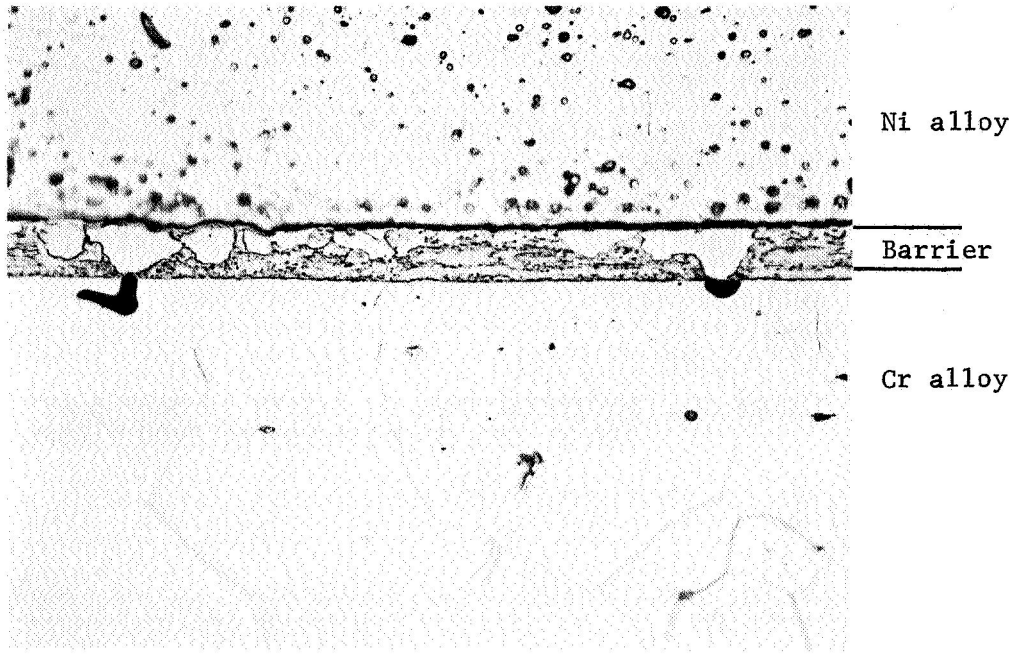

500X 60560

FIGURE 56. MICROSTRUCTURE OF SYSTEM 15 SAMPLE AFTER 100-HOUR CONTINUOUS OXIDATION AT 2100 F

Two sides of sample shown (Sample 15-6).

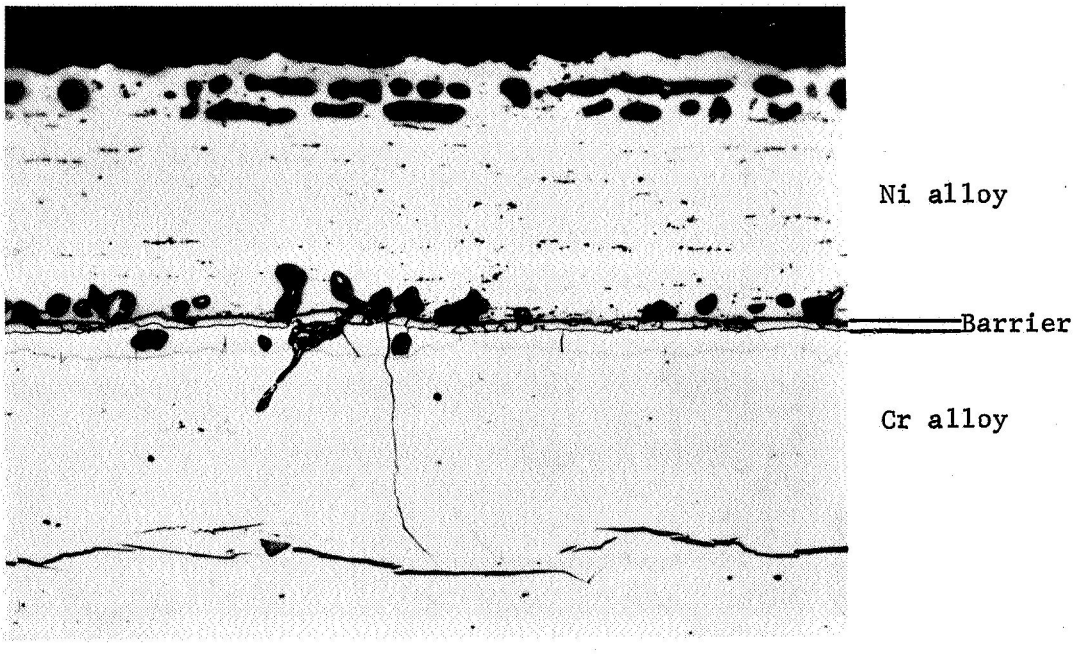

FIGURE 57. MICROSTRUCTURE OF SYSTEM 15 SAMPLE AFTER 100-HR CYCLIC OXIDATION AT 2100 F (Sample 15-7)

destruction. As can be seen by comparing the results presented earlier for samples clad with aluminized Ni-Cr-W alloy, this tungsten-containing cladding material seems somewhat more compatible with tungsten but still attacks it fairly rapidly. Improvements in cladding systems should concentrate on protecting the barrier layer from attack by the nickel-base cladding alloy.

Thermal Stability of Chromium-5 Weight Percent Tungsten

It was considered that the chromium-base alloy might itself be subject to instability, and that the contamination observed metallographically in clad samples after oxidation might not be the only cause of poor bend ductility. To check this possibility, electropolished bend samples from Lot 67-100 were encapsulated in an atmosphere of high-purity argon (99.999 percent) and thermally cycled between room temperature and 2100 or 2300 F to simulate the thermal cycles used during oxidation testing. Samples were cycled either for 10 hours using 2-hour cycles or for 100 hours using 20-hour cycles. The bend properties after thermal cycling are shown in Table 28. The ductile-brittle transition temperature is seen to vary with thermal exposure as follows:

None (see Table 22)	<300 F
10 hr at 2100 F	600-750 F
100 hr at 2100 F	1000-1100 F
10 hr at 2300 F	1000-1100 F
100 hr at 2300 F	1000-1100 F

None of the samples showed any obvious surface discoloration. Some discoloration of the quartz tube was observed, however. Surprisingly, the loss of ductility accompanying thermal cycling appeared to reach a limiting value of about 1000-1100 F instead of increasing with exposure time or temperature.

Several thermally cycled samples were bend tested after removal of 3 to 10 mils of material from the surfaces by electropolishing. As shown in Table 29, some improvement in ductility occurred in samples cycled 10 hours at 2100 or 2300 F, but even removal of 10 mils of material was not adequate to substantially decrease the ductility transition temperature in samples cycled for 100 hours at 2100 or 2300 F. It should be noted that the chromium alloy recrystallized during thermal exposure in argon, while the base ductility measurements were made on material in the wrought condition.

Microstructures of samples cycled for 10 hours at 2100 and 2300 F are shown in Figure 58. The only microstructural feature of note is the finer grain size near the surface. There is no evidence of void formation, contamination, or surface cracking. Microhardness traverses made on these samples were unable to detect any difference in hardness between the surface and the center. The average Knoop hardness (10-gm load) after thermal cycling for 10 hours at either 2100 or 2300 F was 280. The hardness of the as-received alloy (wrought structure) was 415.

As shown below, analysis of three samples for nitrogen showed no increase in nitrogen content as a result of thermal cycling in argon:

TABLE 28. BEND PROPERTIES OF THERMALLY CYCLED CHROMIUM-5 WEIGHT PERCENT TUNGSTEN ALLOY (1)

Bend Temp., F	Bend Angle (degrees) at Failure (2)	Type of Load-Deflection Curve (3)
	Exposed 10 hr at 2100 F, 2-hr cycles	
500	<5	1
600	<5	1
750	>100	4
1000	>100	4
	Exposed 100 hr at 2100 F, 20-hr cycles	
750	<5	1
1000	<5	1
1100	>85	4
1200	>105	4
	Exposed 10 hr at 2300 F, 2-hr cycles	
440	<5	1
1000	<5	1
1100	>70	4
1200	>100	4
1440	>105	4
	Exposed 100 hr at 2300 F, 20-hr cycles	
1000	<5	1
1100	>100	4
1200	>110	4

(1) Electropolished specimens were cycled within argon-filled capsules.

(2) Crack initiation immediately preceded failure in all cases.

(3) See Figure 38 for an illustration of four types of load-deflection curves.

TABLE 29. BEND PROPERTIES OF THERMALLY CYCLED CHROMIUM ALLOY SAMPLES AFTER REMOVAL OF SURFACE MATERIAL(1)

Thermal Exposure	Amount of Material Removed, mils/side	Bend Temp., F	Bend Angle (degrees) at Failure(2)	Type of Load-Deflection Curve(3)
10 hr at 2100 F	3	500	50	1
100 hr at 2100 F	4	800	<5	1
Ditto	10	500	<5	1
10 hr at 2300 F	4	1000	>100	4
100 hr at 2300 F	3	800	<5	1
Ditto	10	500	<5	1

(1) Electropolished specimens were cycled within argon-filled capsules.

(2) Cracking immediately preceded failure.

(3) See Figure 38 for an illustration of the four types of load-deflection curves.

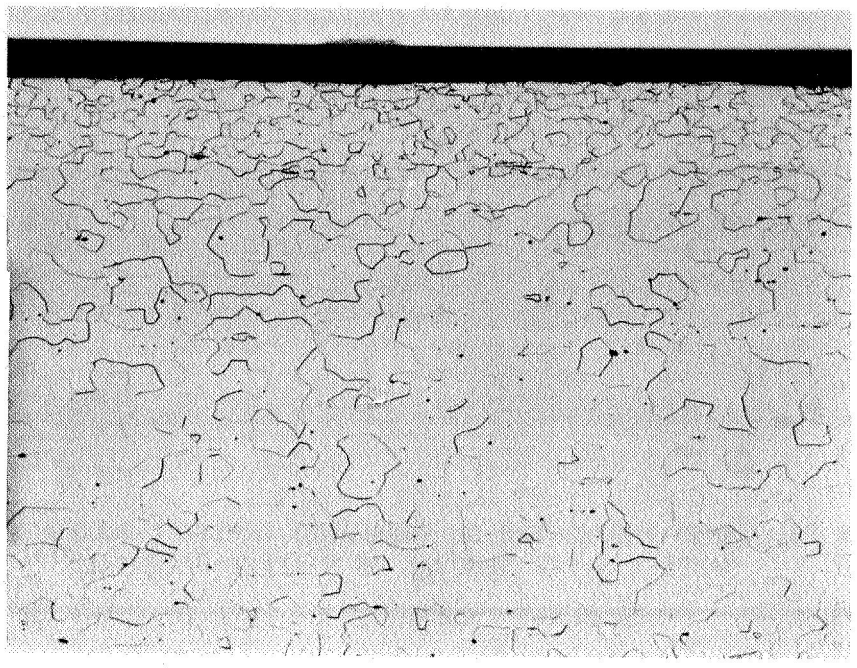

100X (a) 10 hr at 2100 F 1C785

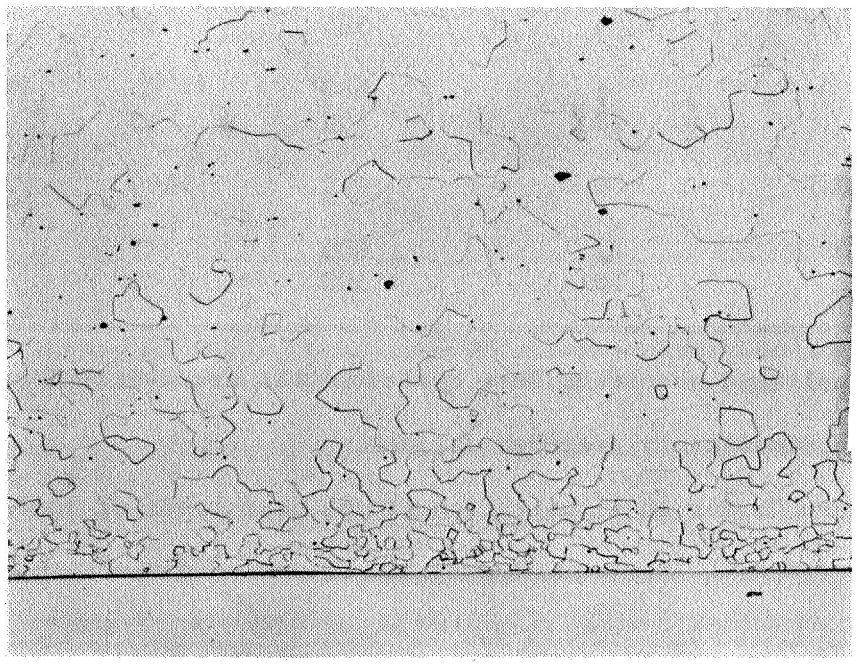

100X (b) 10 hr at 2300 F 1C784

FIGURE 58. MICROSTRUCTURE OF CHROMIUM-TUNGSTEN ALLOY AFTER THERMAL EXPOSURE IN ARGON (2-hr cycles)

	Nitrogen Content, ppm
As electropolished	50
Cycled 10 hr at 2100 F	50
Cycled 10 hr at 2300 F	50

X-ray fluorescence analysis was used to determine whether there was any contamination from silicon or loss in chromium during argon exposure. These results are shown below:

	Relative Content at 10 Micron Depth	
	Silicon	Chromium
As electropolished	A	B
Cycled 10 hr at 2300 F	15A	0.75 B

Since the silicon content was low to start with, the increase shown is not believed to account for the observed increase in transition temperature. It is reported that silicon has a relatively small effect on the transition temperature[17]. A 25-percent loss in chromium, on the other hand, would increase the effective surface tungsten content to about 7 percent, and tungsten is reported to rapidly increase the transition temperature of chromium[17]. The apparent limiting value of change in transition temperature may represent a restriction in chromium diffusion rate as the tungsten content near the surface is increased.

The instability of the chromium-5 weight percent tungsten alloy seems at least partially related to tungsten enrichment of the surface due to the loss of chromium. This suggests that chromium diffusion through the barrier layer in clad samples may be a factor in their poor bend ductility.

New Coating System

In conjunction with the studies just described, a brief examination of two alternate coating systems, vapor deposited silicon and iron-chromium-aluminum alloy clad, was also made. 3-1/2 x 3/4-inch samples of Lot 64-100 were siliconized and six 3-1/2 x 3/4-inch samples of Lot 64-100 were clad with iron-chromium-aluminum alloy. These systems are numbered 16 and 17, respectively.

Six samples were siliconized in a stainless steel retort containing a mixture of 99 weight percent silicon powder (-200 mesh) and 1 weight percent sodium fluoride. The retort was evacuated and then filled with argon to a pressure of 800 mm mercury. The pressure was maintained at 800 mm during the siliconizing treatment which consisted of heating the assembly to 1800 F, holding 1 hour and 40 minutes at temperature, and cooling in air. Weight gain during siliconizing varied from 17 to 23 mg/cm^2 with an average value for the six samples of 19 mg/cm^2.

The twelve samples clad with the iron-base alloy were prepared by gas-pressure bonding. A 5-mil sheet of Fe-22Cr-5Al was bonded to these samples without a barrier layer. A molybdenum sheet was used between the iron-base alloy and the steel envelope during gas-pressure bonding to prevent contamination from carbon.

The siliconized samples, System 16, were bend tested as-coated to determine the effect of siliconizing on bend ductility. Bend angles varied with test temperature as follows:

Temp., F	Bend Angle (degrees) at Failure
1200	<20
1300	>90 (Type 2 curve, crack formation at 20 degrees)
1400	>100

The transition temperature was quite close to 1300 F. In view of the poor bend ductility as siliconized, no samples were exposed to cyclic oxidation.

Six of the iron-base, alloy-clad System 17 samples were exposed to cyclic oxidation at 2100 F using 20-hour cycles. After the first cycle, it was apparent that severe oxidation was occurring. Oxidation tests of the as-received foil used in cladding the System 17 samples showed that the oxidation rate of the clad samples was significantly greater than that of the foil. Contamination of the iron-base alloy by molybdenum was considered the most probable cause of the poor oxidation resistance. X-ray fluorescense analysis showed clad samples to contain 400 times more molybdenum in the cladding than was originally present in the foil. Removal of 2 mils of cladding reduced this only to 100 times the base value. It was concluded that the cladding was seriously contaminated with molybdenum during gas-pressure bonding and further work on these samples was stopped.

PREPARATION OF EROSION BARS

Nine Cr-5W erosion test bars approximately 4 x 1 x 1/4 inch with a wedge-shaped cross-section on one edge were clad with a 1-1/2-mil tungsten-barrier foil and 5-mil Ni-20Cr-20W outer cladding and were aluminized (System 1b). These bars were supplied to NASA for dynamic testing in a high-temperature environment.

Preliminary tests with various bonding fixtures indicated that totally compressed coverage of foils over the nose area (leading edge) would be a problem. It was found that cladding foils gathered at the sample nose forming a gross wrinkle and a void between the clad and substrate. Such voids might cause premature failure of the cladding system during test and were, therefore, undesirable.

A successful technique was subsequently devised which employed a two-stage operation during bonding. The first stage involved the selective movement of the substrate nose into the fixture so that the cladding foils were smoothed over the nose. During the second stage of the process, the container collapsed to achieve the intimate contact of components required for metallurgical bonding.

The bonding fixture used and selected components of a prototype test bar are illustrated in Figure 59. Missing from the picture are the tungsten foil interlayer at one specimen end, the tungsten foils used to cover the specimen trailing edge, and the container base cover. The carbon steel container had heavy side walls and a "V-shaped" internal slot in its base. The straight side walls of the container were 1/4-inch thick, the sloped walls were 3/16-inch thick, the end walls were 1/8-inch thick, and the cover was 35-mils thick. A 20-mil carbon-steel wrapper was employed to effect an "ironing out" of the foils. For assembly, the foil-encased substrate was placed into the wrapper. The wrapper nose was positioned so

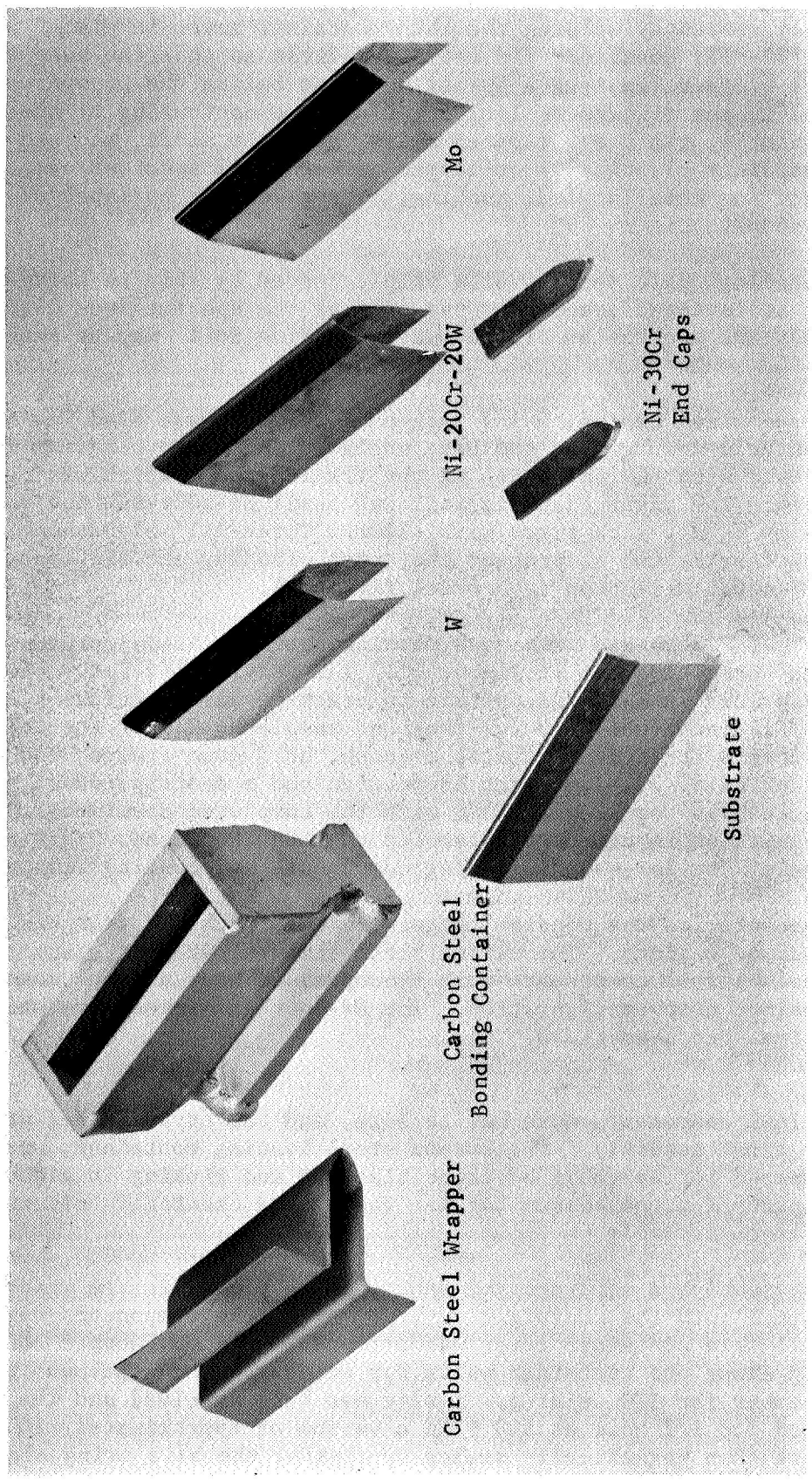

39711

FIGURE 59. BONDING FIXTURE AND SELECTED COMPONENTS USED TO FABRICATE A PROTOTYPE EROSION BAR

that it was 50 mils from seating in the bonding container "V-base". The specimen was hermetically sealed by welding the thin container cover in place. During bonding, the thin (35-mil) container lid collapsed first so that the substrate was driven into its wrapper (causing a 50-mil movement before the wrapper-specimen assembly seated in the fixture V-slot) to effect the contouring of the cladding foils. Subsequently, the heavy tapered sides, straight sides, and end plates of the bonding container plastically collapsed to bring all specimen components into intimate contact for metallurgical bonding. The selective collapse of a bonded container is shown in Figure 60.

A metallographic section of a sample bonded by this technique is shown in Figure 61. It is significant that the nose of the specimen was clad without void formation. The protrusion of the outer cladding foil may be smoothed by honing.

For the final design, 3-1/4 inches of the bar were clad leaving the last 3/4 inch at the hold-down groove and base unclad. The inner cladding foil was 1-1/2-mil tungsten with the exception of the trailing edge which was clad with 1/2-mil tungsten. The outer cladding foil was 5-mil Ni-20Cr-20W and the sample end was capped by a 1/16-inch plate of Ni-30Cr. Three-mil molybdenum foil was utilized during fabrication to protect the outer cladding and bare substrate from contamination (carbon diffusion from steel fixtures).

Ten Cr-5W substrate bars were machined at Battelle's Columbus Laboratories according to the drawing shown in Figure 62. The heavier 1/4-inch-thick Cr-5W stock proved to be appreciably more susceptible to cracking during grinding than the thinner material (1/16-inch) utilized for the bend samples. Six of the ten bars had fine grinding cracks at various locations (nose, hold-down groove, and ends). These samples were studied by dye-penetrant inspection and a description of the defects and their location was supplied to NASA with the completed specimens. There was a considerable variation in dimensions between the ten specimens. This necessitated the fabrication of "tailor-made" cladding components and bonding fixtures.

Components for the bonding containers were machined from carbon steel stock and joined by welding. The carbon steel fixture, wrapper, tungsten, Ni-20Cr-20W, and molybdenum foil components were hydropressed over a steel mandrel to achieve the desired nose configuration. The Ni-30Cr endplates were machined to match the specimen cross-sections.

The foil components were cut to size, and the carbon steel wrapper was positioned for trial assembly. The carbon steel bonding container, wrapper, and cover were prepared for assembly by vapor blasting and rinsing in alcohol. The specimen components and molybdenum barrier foils were chemically cleaned and rinsed in alcohol prior to assembly.

For assembly, a foil-encased specimen was placed in the wrapper which was in turn placed into the container cavity. After the components were seated in the fixture, the thin container cover was clamped in place. Copper cooling blocks were positioned along the container walls for welding. The specimens were placed in an argon chamber for TIG welding. A slit was left unwelded and the samples were vacuum outgassed for 1/2 hour at 500 F in a vacuum of approximately 10^{-5} torr. The samples were then hermetically sealed by closing the slit using electron-beam welding methods. The specimens were leak tested after closure.

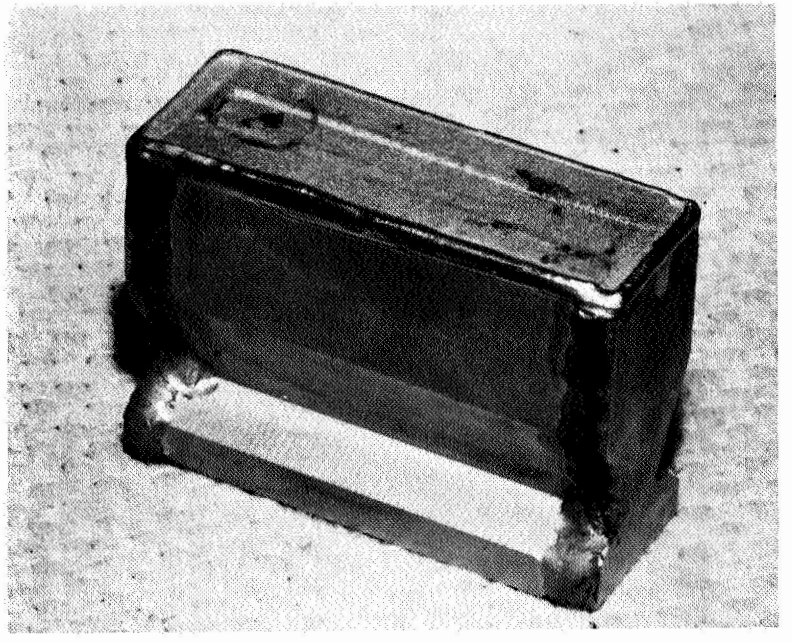

39880

FIGURE 60. BONDING CONTAINER SHOWING SELECTIVE COLLAPSE OF THIN COVER

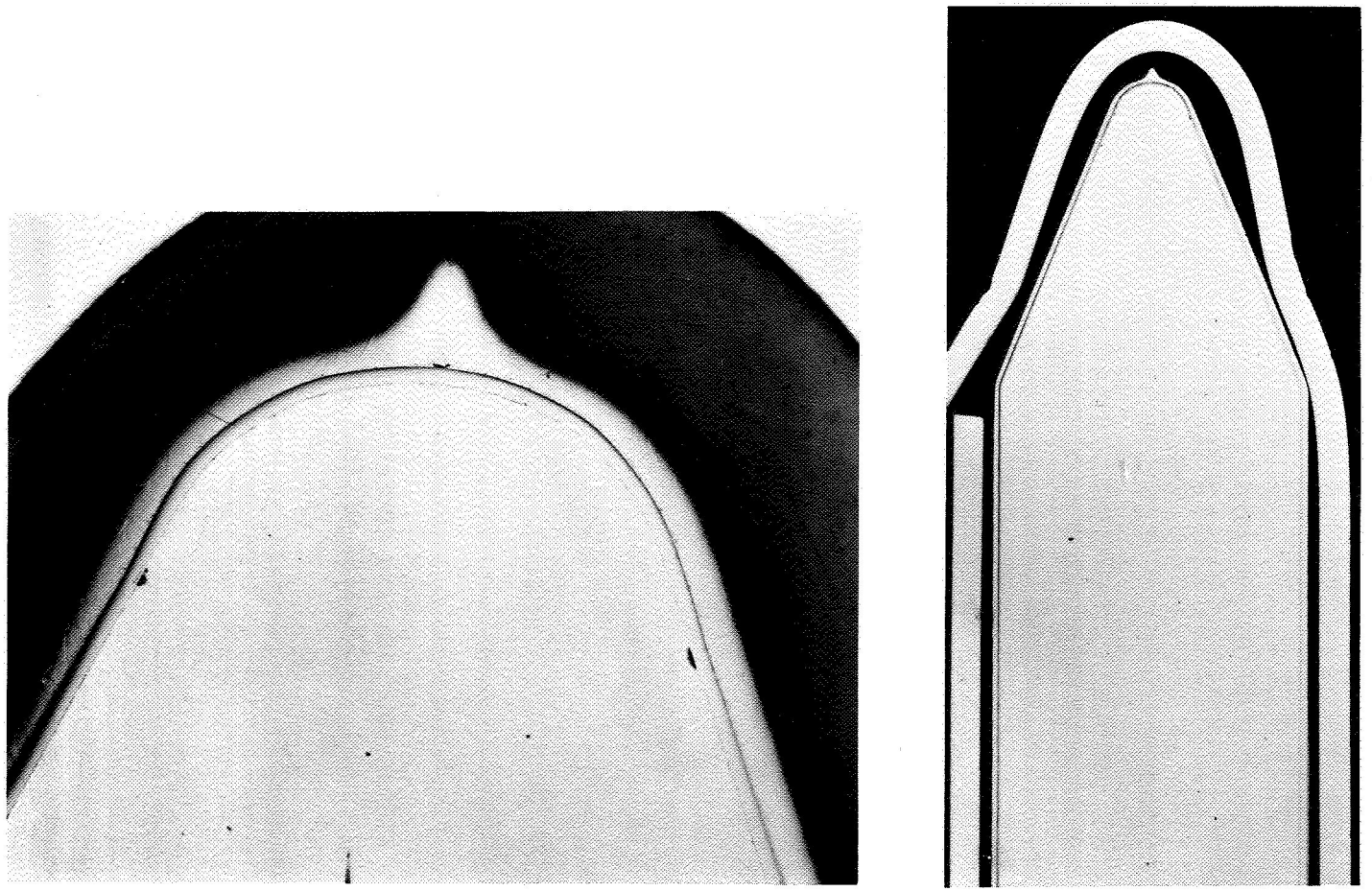

50X Unetched 2C995 6.5X Unetched 2C862

FIGURE 61. METALLOGRAPHIC SECTION SHOWING GOOD COVERAGE AND BONDING OF 1-1/2 MIL W AND 5 MIL Ni-20 WEIGHT PERCENT Cr-20 WEIGHT PERCENT W CLADDING FOILS

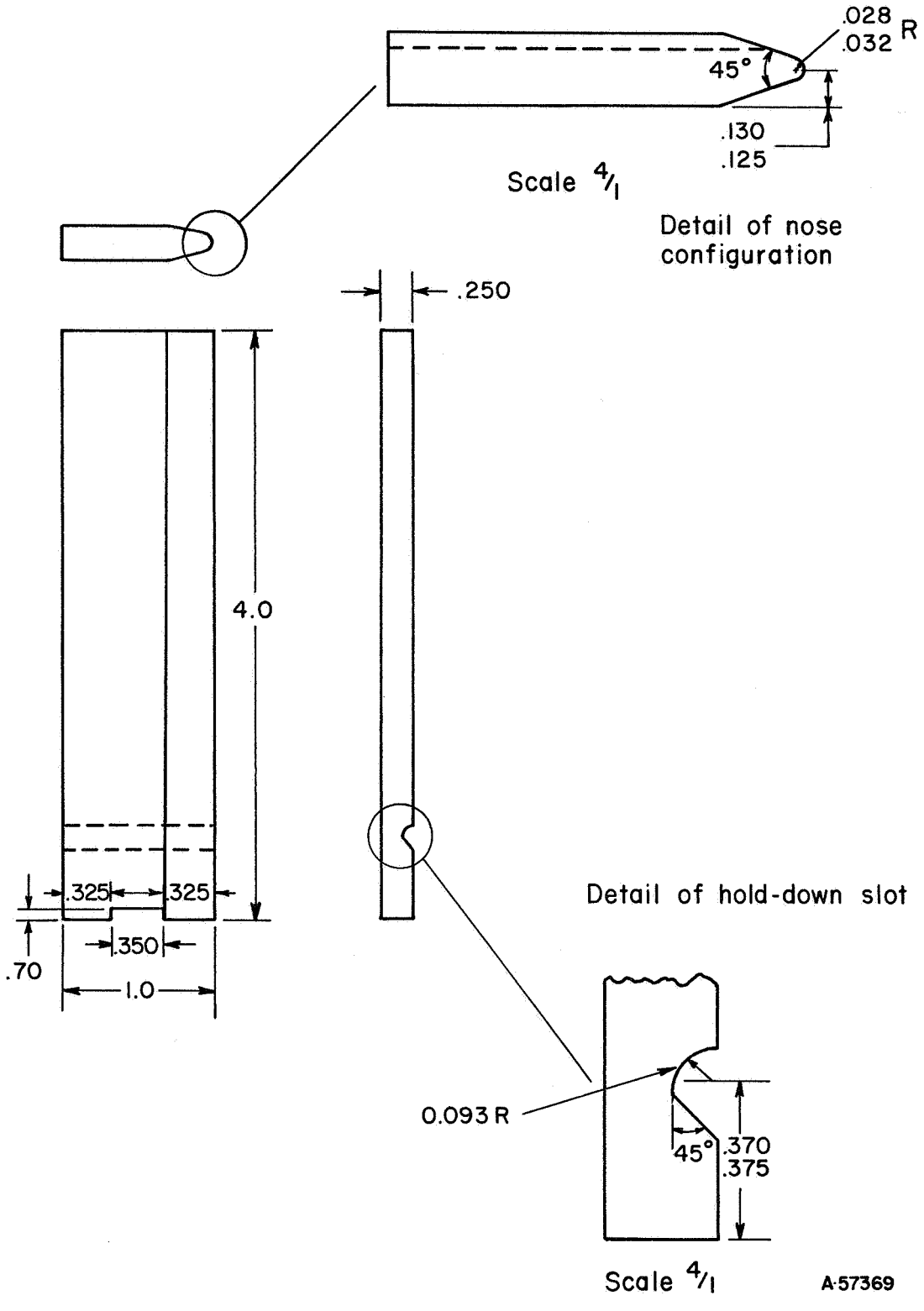

FIGURE 62. EROSION BAR TEST SAMPLE

To accomplish final fabrication of the bars, a special gas-pressure bonding cycle was employed. The specimens were maintained at a nominal pressure of 300 psi while they were heated to 1600 F. The pressure was raised to 10,000 psi to achieve the proper sample movement and container collapse. The cycle was completed by raising the temperature to 2200 F and holding for 2 hours. After bonding, the steel and molybdenum were leached from the nickel-base cladding and unprotected substrate in a nitric acid bath. One of the ten samples, Number 7, was not bonded due to a leak in the steel container and was not processed further. A second sample, Number 1, was very poorly bonded, but was included in the subsequent aluminizing run.

Nine samples were aluminized by heating to 1750 F and holding for 12 hours, using essentially the same procedures applied in processing sheet samples in earlier phases of this program. Homogenization was accomplished by heating in argon for 4 hours at 2100 F followed by 16 hours at 2200 F. The average weight gain of the nine wedge bar samples was 3.6 mg/cm^2 with a range of values of 3.2 to 4.5 mg/cm^2. (See Appendix Table A-1 for the weight gain during aluminizing.) This is somewhat less than the desired aluminum level and is equivalent to an aluminum content of only about 3.0 weight percent. However, because of the shape of the wedge bars and the fact that not all of the bar was clad with nickel, there is some question regarding the weight gain calculation.

During aluminizing, Sample Number 1 showed considerable separation of the cladding along the trailing edge of the wedge bar and lost the nickel alloy end cap. On homogenization, several other samples tended to show some decladding along the trailing edge of the wedge bar. Only Sample Number 5 appeared completely free from this defect. Of the remaining samples, Numbers 2 and 10 appeared in the best condition. The occurrence of this defect was unexpected, and indicates that only marginal bonding occurred between the cladding components on the sides and trailing edges of the wedge bars. Despite these defects, all eight wedge bars were given to NASA for evaluation.

RECOMMENDATIONS

Metallic cladding appears capable of protecting chromium-5 percent tungsten alloy from oxidation at 2100 or 2300 F. However, poor bend properties are observed after exposure. The present work shows that the loss of bend ductility is the result of interdiffusion of alloying elements between the cladding alloy and the chromium alloy. Both chromium and nickel appear to pass through the tungsten barrier layer used to separate the cladding alloy from the chromium alloy, with relative ease. The development of a useful cladding system will require that an improved barrier layer be developed. Two approaches for further studies are suggested:

(1) The tungsten barrier layer could be alloyed so as to reduce the diffusion rates of nickel and chromium. Alloying additions and special thermal-mechanical processing which raise the recrystallization temperature of tungsten or promote the development of a fine grain size should be considered since there is some evidence that a continuous grain boundary through the barrier layer is especially conducive to diffusion. Also, additions which reduce chromium or nickel solubility in tungsten should prove helpful, as should additions which would react with these elements to form stable compounds.

(2) Alternate barrier layers could be considered. These might include multiple metallic layers in which each component retards penetration of one of the diffusing materials. An unalloyed chromium layer between the barrier layer and the chromium-base alloy might prove useful as a means of diluting any interdiffusing elements. Also, it might be possible to use completely impermeable nonmetallic barriers. This latter approach is perhaps less attractive since no nonmetallic barrier materials which would be obviously superior to tungsten are known.

Studies designed to develop improved barrier materials could be most economically carried out using a fundamental approach. Bonded three-layer strips of cladding alloy:barrier layer:chromium alloy could be prepared and sectioned to provide a number of samples for thermal exposure in argon. Metallographic examination and microprobe analysis of variously exposed samples could be used to determine the interdiffusion behavior. These procedures would provide a method of screening a large number of potentially-useful barrier systems rapidly, thus permitting the examination of processing and thickness variables as well as compositional variables. The present work has provided several indications that the tungsten barrier is capable of preventing interdiffusion in certain instances, which would suggest that such a study would be successful.

Since loss of bend ductility is apparently at least partly the result of an increase in ductile-brittle transition of the chromium-base alloy caused by an increased tungsten content at the surface which accompanies a loss of chromium, the present cladding system might prove useful on unalloyed chromium or on selected chromium alloys.

* * * * * * *

The data upon which this report is based are contained in Battelle Memorial Institute Laboratory Record Books No. 22996, 23883, 22578, 23458, and 24778.

DNW/RHE/CAM/JJE/ESB:sam
2-23-68

REFERENCES

(1) Girard, E. H., Clarke, J. F., and Breit, H., "Study of Ductile Coatings for the Oxidation Protection of Columbium and Molybdenum Alloys", Metals and Controls, Inc., Division of Texas Instruments, Final Report, Contract NOw 65-0340-f (May, 1966).

(2) Dickson, D. T., Wimber, R. T., and Stetson, A. R., "Very High Temperature Coatings for Tantalum Alloys", Solar, Division of International Harvester Company, Summary Technical Report AFML-TR-66-317, Contract AF 33(615)-2852 (October, 1966).

(3) Criscione, J. M., Rexer, J., and Fenish, R. G., "High Temperature Protective Coatings for Refractory Metals", Union Carbide Corporation, Yearly Summary Report, Contract NASw-1030 (received May, 1966--report not dated).

(4) Wukusick, C. S., and Collins, J. E., Properties of Fe-Cr-Al Type Alloys Containing Additions of Yttrium", Report No. TM 63-7-3, presented at ASTM Subcommittee on Resistance Heating Materials, Atlantic City, New Jersey (1963).

(5) Ignatov, D. V., and Shamgunova, R. D., "Mechanisms of the Oxidation of Nickel and Chromium Alloys", Moscow, 1960, NASA Technical Translation F-59 (March, 1961).

(6) Houck, J. A., Williams, D. N., and Jaffee, R. I., "Workable Ni-W-Cr Alloys", ASM Transactions Quarterly, Vol. 55, No. 3 p 728 (1962).

(7) Monson, L. A., and Pollock, W. I., "Development of Coatings for Protection of Dispersion Strengthened Ni from Oxidation", E. I. DuPont de Nemours & Company, Inc., First Quarterly Progress Report, Contract AF 33(615)-1704 (July 1-October 1, 1964).

(8) Taylor, A., and Floyd, R. W., "The Constitution of Nickel-Rich Alloys of the Ni-Cr-Al System", Journal of the Institute of Metals, Vol. 81, p 451 (1952-3).

(9) Kornilov, I. I., and Mints, R. S., "Study of the System Ni-Cr-NiAl", Russian Journal of Inorganic Chemistry, Vol. 3, No. 3, p 699 (1958).

(10) Alisova, S. P., Budberg, P. B., and Shakova, K. I., "Equilibrium Diagram of the Al-Cr-Ni-W Quarternary System at 1100 C", Russian Journal of Inorganic Chemistry, Vol. 6, No. 11, p 1318 (1961).

(11) Kornilov, I. I., and Budberg, P. B., "On the Phase Diagram on the Ternary System Ni-Cr-W", Russian Journal of Inorganic Chemistry, Vol. 2, No. 4, p 860 (1957).

(12) Kalinovich, D. F., Korenskiy, I. I., and Smolin, M. D., "Diffusion of the Components of a Nickel-Chromium Alloy in a Wide Composition Range", Fiz. Metal. Metalloved, Vol. 16, No. 4, p 619 (1963).

(13) Passmore, E. M., Boyd, J. E., and Lement, B. S., "Selection of Diffusion Barriers for Use in Protective Coating Systems for Tungsten and Molybdenum", paper presented at the AIME Conference on Applied Aspects of Refractory Metals, Los Angeles, California (December 9-10, 1963).

(14) Goetz, L. J., Hughes, J. R., and Moore, W. F., "The Pilot Production and Evaluation of Chromium Alloy Sheet and Plate", General Electric Company, Final Report NASA CR-72184, Contract Nos. NAS 3-7901 and NAS 3-7919 (March 15, 1967).

(15) "Evaluation Test Methods for Refractory Metal Sheet Material", Report MAB-192-M, Materials Advisory Board, National Academy of Science, Washington, D.C.

(16) Waring, J. L., "Phase Equilibria in the System Aluminum Oxide-Tungsten Oxide", Journal of the American Ceramic Society, Vol. 48, No. 9, p 493 (1965).

(17) Abrahamson, E. P., and Grant, N. J., "Brittle to Ductile Transition of Binary Chromium-Base Alloys", Trans. ASM, Vol. 50, p 705 (1958).

APPENDIX

TABLE A-1. WEIGHT GAIN DURING ALUMINIZING TREATMENTS
(Samples aluminized 12 hours at 1750 F unless otherwise noted)

System	Sample Number	Weight Gain, mg/cm^2 (1)
1a	I-1	5.1
	-2	3.2
	-3	3.3
	-4	3.4
	-5	3.4
	-6	5.2 (2)
	-7	6.6 (2)
	-8	5.9 (2)
	-9	Not determined (2)
	-10	4.5
	-11	4.4
	-12	4.2
	-13	4.1
	-14	4.1
	-15	4.2
1b	I-16	4.1
	-17	4.1
	-18	4.1
	-19	4.1
	-20	4.2
	-21	4.3
	-22	4.1
	-23	4.1
	-24	4.1
	-25	4.2
	-26	4.0
	-27	4.4
	-28	4.7
	-29	4.0
	-30	3.8
	-31	3.8
1b	1b-1	3.9
	-2	3.6
	-3	Not determined
	-4	4.0
	-5	3.7
	-6	4.1
1b	Wedge-1	3.2
	-2	3.3
	-3	3.4
	-4	3.8
	-5	4.4
	-6	3.6
	-8	3.7
	-9	4.0
	-10	4.5
2a	II-1	5.2
	-2	3.1
	-3	3.2
	-4	3.2
	-5	4.9 (2)
	-6	4.9 (2)
	-7	4.8 (2)
	-8	4.2
	-11	4.4
	-12	4.5
	-13	4.7
	-14	4.2
	-15	4.2
	-16	4.2
2b	II-17	3.8
	-18	4.1
	-19	4.1
	-20	4.1
	-21	4.2
	-23	4.0
	-24	4.1
	-25	4.2
	-26	4.5
	-27	4.2
	-28	4.4
	-29	4.1
	-30	3.7
	-31	3.6
	-32	3.7
	-33	3.8
	-34	4.1
	-35	4.8
	-36	4.1
	-37	3.9
	-38	3.9
	-39	4.0
	-40	4.3
	-41	4.8
	-42	4.9
	-43	3.7
	-44	3.7
	-45	3.7
	-46	3.9
	-47	4.4
	-48	3.9
	-49	3.8
	-50	3.9
	-51	4.7

TABLE A-1. (continued)

System	Sample Number	Weight Gain, mg/cm^2(1)
2c	II-9	4.9(2)
	-10	6.7(2)
4	IV-1	5.1
	-2	5.0
	-3	5.0
	-4	5.0
	-5	6.7(2)
	-6	6.9(2)
	-7	7.1(2)
	-8	5.2(2)
	-9	4.3
	-10	4.0
	-11	4.4
	-12	Not determined(2)
	-13	4.5
	-14	4.8
	-15	4.6
	-16	4.3
	-17	4.1
	-18	4.0
5	V-1	3.6
	-2	4.2
	-3	4.2
	-4	3.9
	-5	4.3
	-6	5.6(2)
	-7	5.4(2)
	-8	6.1(2)
	-9	3.9
	-10	4.8
	-11	4.9
	-12	5.0
	-13	4.2
	-14	4.1
	-15	4.1
6	VI-1	3.8
	-2	3.8
	-3	4.1
	-4	5.5(2)
	-5	5.2(2)
	-6	5.8(2)
	-7	5.2(2)
	-8	5.0
	-9	4.8
	-10	5.2
	-11	4.1
	-12	4.2
	-13	4.3
7	VII-1	4.4
	-2	4.5
	-3	4.4
	-4	4.5
	-5	5.6(2)
	-6	5.8(2)
	-7	Not determined(2)
8	VIII-1	4.5
	-2	4.6
	-3	4.4
	-4	5.3
	-5	6.1(2)
	-6	6.3(2)
	-7	6.7(2)
9	IX-1	4.1
	-2	4.4
	-3	4.1
	-4	4.1
	-5	4.2
10	X-1	4.5
	-2	4.4
	-3	3.8
	-4	3.7
	-5	3.9
12	XII-1	4.4
	-2	4.7
	-3	4.2
	-4	4.0
	-5	4.1
15	15-1	3.7
	-2	Not determined
	-3	3.7
	-4	3.8
	-5	3.9
	-6	4.0
	-7	4.0
	-8	4.1
	-9	4.1
	-10	4.2
	-11	4.3
	-12	4.3

Footnotes on following page.

Footnotes for Table A-1

(1) The weight gain data may be converted to weight percent aluminum as follows:

$$\text{Ni30Cr:weight percent Al} = \left(\frac{\text{weight gain}}{\text{weight gain} + 105.5}\right) 100$$

$$\text{Ni-20Cr-20W:weight percent Al} = \left(\frac{\text{weight gain}}{\text{weight gain} + 120.7}\right) 100$$

(2) These samples aluminized for 18 hours at 1750 F instead of 12 hours.

Note: All samples homogenized after aluminizing by annealing in argon for 4 hours at 2100 F followed by 16 hours at 2200 F.

TABLE A-2. SUMMARY OF SAMPLES PREPARED FOR STUDY

System	Sample Number	Sample Size	Oxidation Exposure Temp., F	Oxidation Exposure Time, hr Cycle	Oxidation Exposure Time, hr Total	Examined for
1a	I-1	1 x 1	2100:2:100			Metallography
	-2	"	Defected 2100:10:10			"
	-3	"	Defected 2100:10/40:50			"
	-4	"	2100:2/20:200			(Not tested)(2)
	-5	"	Ditto			Metallography
	-6	"	2300:2/20:200			"
	-7	3/4 x 3-1/2	2300:2:80			"
	-8	"	2300:2/20:200			(Not tested)
	-9	"	None			Metallography
	-10	"	2100:20:100			Bend test--700
	-11	"	Ditto			Bend test--1600
	-12	"	"			Bend test--1400
	-13	"	"			Bend test--1200
	-14	"	"			Bend test--1000
	-15	"	"			(Not tested)(2)
1b	I-16	1 x 2	2100:2:100			Metallography
	-17	"	HLH			"
	-18	"	HL			"
	-19	"	2100:20:600			"
	-20	"	2300:20:240			"
	-21	"	2300:20:160			"
	-22	"	2300:2:40			"
	-23	"	2100:20:60			"
	-24	"	Ditto			(Not tested)(2)
	-25	"	2300:20:240			(Not tested)
	-26	"	2100:20:600			(Not tested)(2)
	-27	"	2300:20:160			Metallography
	-28	3/4 x 3-1/2	2100:20:300			Bend test--1000
	-29	"	Ditto			Bend test--1200(2)
	-30	"	"			Bend test--1400
	-31	"	"			Bend test--1600 (Metallography)
1b	1b-1	"	2100:20:100			Bend test--1200
	-2	"	Ditto			Metallography
	-3	"	None			"
	-4	"	2100:20:100			Bend test--1300
	-5	"	Ditto			Bend test--1400
	-6	"	"			Bend test--1200
2a	II-1	1 x 1	2100:2:100			Metallography
	-2	"	2100:2/20:20			"
	-3	"	Ditto			(Not tested)(2)
	-4	"	None			Ditto
	-5	"	2300:2/20:200			"
	-6	"	Ditto			Metallography
	-7	"	2300:2:100			"

TABLE A-2. (continued)

System	Sample Number	Sample Size	Oxidation Exposure Temp., F	Oxidation Exposure Time, hr Cycle	Oxidation Exposure Time, hr Total	Examined for
2a (cont.)	II-8	3/4 x 3-1/2	None			Metallography (as aluminized & as homogenized)
	-11	"	2100:20:100			Bend test--75
	-12	"	Ditto			Bend test--1600
	-13	"	"			Bend test--1400
	-14	"	"			Bend test--1200
	-15	"	"			Bend test--1000
	-16	"	"			Bend test--800
2b	II-17	1 x 2	2100:2:100			Metallography
	-18	"	2100:20:600			(Not tested)
	-19	"	Ditto			Ditto
	-20	"	"			Metallography
	-21	"	HLH			"
	-22	"	2300:2:100			"
	-23	"	HL			"
	-24	"	2100:20:600			(Not tested)
	-25	"	2300:20:60			Ditto
	-26	"	2300:20:260			Metallography
	-27	"	2300:20:320			(Not tested)
	-28	"	2300:20:460			Metallography
	-29	3/4 x 3-1/2	2300:20:200			(Not tested)
	-30	"	2100:20:300			Bend test--1000
	-31	"	Ditto			Bend test--1200
	-32	"	"			Bend test--1400
	-33	"	"			Bend test--1600 (Metallography)
	-34	"	2300:20:200			(Not tested)
	-35	"	Ditto			(Not tested)(2)
	-36	"	2300:20:120			Bend test--1600 (Metallography)
	-37	"	2300:20:200			Bend test--1600 (Metallography)
	-38	"	Ditto			Bend test--1400
	-39	"	2300:20:120			(Not tested)(2)
	-40	"	Ditto			Ditto
	-41	"	"			"
	-42	"	2300:20:200			(Not tested)
	-43	"	2100:20:300			(Not tested)(2)
	-44	"	Ditto			Ditto
	-45	"	2100:20:600			"
	-46	"	Ditto			"
	-47	"	2300:20:120			"
	-48	"	2100:20:600			"
	-49	"	Ditto			Bend test--800 (in yoke)
	-50	"	"			(Not tested)(2)
	-51	"	2300:20:120			Bend test--1400

TABLE A-2. (continued)

System	Sample Number	Sample Size	Oxidation Exposure Temp., F	Time, hr Cycle	Total	Examined for
2c	II-9	1 x 1	2100:2/20:200			Metallography
	-10	"	2100:2:200			"
3	III-1	"	2100:2/20:200			"
	-2	"	2100:2:100			"
	-3	"	2100:2/20:200			(Not tested)
	-4	"	None			Ditto
	-5	"	2300:2:100			Metallography
	-6	"	2300:2/20:200			(Not tested)
	-7	"	Ditto			Metallography
	-8	3/4 x 3-1/2	2100:20:100			Bend test--1000
	-9	"	Ditto			Bend test--1600
	-10	"	"			Bend test--1400
	-11	"	"			Bend test--1200
	-12	"	"			Bend test-1000
	-13	"	"			Bend test-800
4	IV-1	1 x 1	2100:2:100			Metallography
	-2	"	2100:2/20:200			(Not tested)
	-3	"	Ditto			Metallography
	-4	"	None			"
	-5	"	2300:2:80			"
	-6	"	Ditto			(Not tested)
	-7	"	"			Ditto
	-8	3/4 x 3-1/2	None			"
	-9	"	Defected 2100:10:10			Metallography
	-10	"	None			(Not tested)
	-11	"	Defected 2100:10/40:50			Metallography
	-12	"	None			"
	-13	"	2100:20:100			Bend test--1200
	-14	"	Ditto			Bend test--1600
	-15	"	"			Bend test--1400
	-16	"	"			Bend test--1200
	-17	"	"			(Not tested)
	-18	"	"			Ditto
5	V-1	"	Defected 2100:10:10			Metallography
	-2	"	Defected 2100:10/40:50			"
	-3	"	2100:2/20:200			"
	-4	"	2100:2:100			"
	-5	"	2100:2/20:200			(Not tested)
	-6	"	2300:2:100			Metallography
	-7	"	2300:2/20:200			"
	-8	"	2300:2:10			"
	-9	"	None			"
	-10	"	2100:20:100			Bend test--1500
	-11	"	Ditto			Bend test--1600
	-12	"	"			Bend test--1400

TABLE A-2. (continued)

System	Sample Number	Sample Size	Oxidation Exposure Temp., F	Oxidation Exposure Time, hr Cycle	Oxidation Exposure Time, hr Total	Examined for
5 (cont.)	V-13	3/4 x 3-1/2	2100:20:100			(Not tested)
	-14	"	Ditto			Ditto
	-15	"	"			"
6	VI-1	1 x 1	2100:2/20:200			Metallography
	-2	"	2100:2:100			"
	-3	3/4 x 3-1/2	None			"
	-4	"	2100:2:40			(Not tested)
	-5	"	2300:2:2			Metallography
	-6	"	2300:2:6			"
	-7	"	Ditto			(Not tested)
	-8	"	2100:20:100			Bend test--1600
	-9	"	Ditto			Bend test--1400
	-10	"	"			(Not tested)
	-11	"	"			Ditto
	-12	"	"			"
	-13	"	"			"
7	VII-1	"	2100:2/20:200			Metallography
	-2	"	2300:2/20:200			"
	-3	"	2100:2:50			"
	-4	"	2100:2:90			"
	-5	"	2300:2:10			(Not tested)
	-6	"	2300:2:100			Metallography
	-7	"	None			"
8	VIII-1	"	2100:2:100			"
	-2	"	2100:2/100:200			"
	-3	"	2100:2/20:200			(Not tested)
	-4	"	2300:2/20:140			Metallography
	-5	"	2300:2:100			"
	-6	"	2300:2:200			(Not tested)
	-7	"	None			Metallography
9	IX-1	"	2300:2:2			"
	-2	"	None			Bend test--1000
	-3	"	2100:2:10			Metallography
	-4	"	None			Bend test--1200
	-5	"	None			Bend test--800
10	X-1	"	2300:20:80			(Not tested)
	-2	"	2300:20:100			Bend test--1400
	-3	"	Ditto			Metallography
	-4	"	2100:2:100			"
	-5	"	2300:20:100			Bend test--1600
11	XI-1	"	2100:2:100			Metallography
	-2	"	2300:2:100			"
	-3	"	2300:20:100			Bend test--1600

TABLE A-2. (continued)

System	Sample Number	Sample Size	Oxidation Exposure Temp., F	Time, hr Cycle	Time, hr Total	Examined for
11 (cont.)	XI-4	3/4 x 3-1/2	2300:20:100			Bend test--1200
	-5	"	Ditto			(Not tested)(2)
12	XII-1	"	"			Bend test--1400
	-2	"	"			Bend test--1600
	-3	"	"			(Not tested)
	-4	"	2100:2:100			Metallography
	-5	"	2300:2:100			"
13	13-1	"	2100:2:10(1)			Bend test--1200
	-2	"	Ditto			Bend test--800
	-3	"	"			Bend test--600
	-4	"	"			Bend test--700
	-5	"	"			(Not tested)
	-6	"	"			Ditto
	-7	"	2100:20:100(1)			Bend test--1200
	-8	"	Ditto			Bend test--800
	-9	"	"			Bend test--600
	-10	"	"			Bend test--700
	-11	"	"			Metallography
	-12	"	"			(Not tested)
	-13	"	None			Bend test--1200
	-14	"	None			Bend test--800
	-15	"	None			Bend test--700
	-16	"	None			Bend test--600
	-17	"	None			(Not tested)
14	14-1	"	2100:20:100			Bend test--1600
	-2	"	Ditto			Bend test--1200
	-3	"	"			Bend test--1400
	-4	"	"			Bend test--1500
	-5	"	"			(Not tested)
	-6	"	"			Metallography
	-7	"	None			"
15	15-1	"	2100:100:100			Bend test--1200
	-2	"	None			Metallography
	-3	"	2100:100:100			Bend test--1400
	-4	"	Ditto			Bend test--1500
	-5	"	"			Bend test--1600
	-6	"	"			Metallography
	-7	"	2100:20:100			"
	-8	"	Ditto			Bend test--1600
	-9	"	"			Bend test--1500
	-10	"	"			Bend test--1200
	-11	"	"			Bend test--1400
	-12	"	"			(Not tested)

TABLE A-2. (continued)

System	Sample Number	Sample Size	Oxidation Exposure Temp., F	Time, hr Cycle	Time, hr Total	Examined for
16	16-1	3/4 x 3-1/2	None			Bend test--1200
	-2	"	None			Bend test--1400
	-3	"	None			Bend test--1300
	-4	"	None			(Not tested)
	-5	"	None			Ditto
	-6	"	None			"
17	17-1	"	None			Surface analysis
	-2	"	None			(Not tested)
	-3	"	None			Ditto
	-4	"	None			"
	-5	"	None			"
	-6	"	None			"
	-7	"	2100:20:20			"
	-8	"	Ditto			"
	-9	"	"			"
	-10	"	"			"
	-11	"	"			"
	-12	"	"			"

(1) Exposed in high-purity argon atmospheres.

(2) These samples subsequently used in decladding studies designed to detect interdiffusion

DISTRIBUTION LIST FOR SUMMARY REPORT

Contract NAS 3-7612

	Addressee		Number of Copies
(1)	NASA Headquarters 600 Independence Avenue, S.W. Washington, D.C. 20546		
	Attention: N. F. Rekos (RAP)		1
	R. H. Raring (RRM)		1
	G. Deutsch (RRM)		1
(2)	NASA-Lewis Research Center 21000 Brookpark Road Cleveland, Ohio 44135		
	Attention: Technology Utilization Office	M.S. 3-19	1
	Report Control Office	M.S. 5-5	1
	Fluid System Components Division		
	I. I. Pinkel	M.S. 5-3	1
	P. T. Hacker	M.S. 5-3	1
	Air-Breathing Engine Division		
	J. Howard Childs	M.S. 60-4	1
	Dr. W. H. Roudebush	M.S. 60-6	1
	A. Anglin	M.S. 60-6	1
	Air-Breathing Engine Procurement Section		
	John H. DeFord	M.S. 60-5	1
	Materials & Stresses Division		
	S. J. Grisaffe	M.S. 49-1	2
	G. M. Ault	M.S. 105-1	1
	R. W. Hall	M.S. 105-1	1
	J. W. Weeton	M.S. 49-1	1
	J. Freche	M.S. 49-1	1
	H. B. Probst	M.S. 49-1	1
	R. E. Oldrieve		5
	Patent Counsel	M.S. 501-3	1
	Library	M.S. 60-3	2
(3)	FAA Headquarters 800 Independence Avenue, S.W. Washington, D.C. 20553		
	Attention: F. B. Howard/SS-210		1
	Brig. Gen. J. C. Maxwell		1
(4)	Supersonic Transport Office Wright-Patterson AFB, Ohio 45433		
	Attention: SESHS, J. L. Wilkins		2

	Addressee	Number of Copies
(5)	NASA Scientific & Technical Information Facility P. O. Box 3300 College Park, Maryland 20740 Attention: NASA Representative RQT-2448	6
(6)	Aerospace Corporation P. O. Box 95085 Los Angeles, California 90045 Attention: Reports Acquisitions	1
(7)	Air Force Flight Dynamics Laboratory (FDTS) Wright-Patterson AFB, Ohio 45433 Attention: SM Sgt. Jesse C. Ingram, Jr.	1
(8)	AiResearch Manufacturing Company 9851-9951 Sepulveda Blvd. Los Angeles, California 90009 Attention: H. H. Block, Senior Metallurgist	1
(9)	Alloy Surfaces, Inc. 100 South Justison Street Wilmington, Delaware 19899 Attention: George H. Cook	1
(10)	AVCO Space Systems Division Lowell Industrial Park Lowell, Massachusetts 01851 Attention: Allan S. Bufferd	1
(11)	American Society for Metals Metals Park Novelty, Ohio 44073 Attention: Dr. Taylor Lyman	1
(12)	U. S. Army Materials Research Agency Watertown, Massachusetts 02172 Attention: M. Levy	1
(13)	Bendix Corporation Research Laboratory Division Southfield, Michigan 48075 Attention: W. M. Spurgeon, Head, M & P Dept.	1
(14)	Boeing Company P. O. Box 733 Renton, Washington 98055 Attention: W. E. Binz, Jr., SST Unit Chief	1
(15)	Bureau of Naval Weapons Department of the Navy Washington, D.C. 20025 Attention: I. Machlin C. Gilmore RRMA23	1 1

	Addressee	Number of Copies
(16)	Consolidated Controls Corporation 15 Durant Avenue Bethel, Connecticut 06801 Attention: R. Engdahl	1
(17)	Corning Glass Works Corning, New York 14830 Attention: James E. Durham	1
(18)	Chromalloy Corporation 169 Western Highway West Nyack, New York 10994 Attention: L. Maisel	1
(19)	Chromizing Corporation 12536 Chardon Avenue Hawthorne, California 90250 Attention: M. R. Commandy	1
(20)	City College of the City University of New York School of Engineering & Architecture Department of Chemical Engineering New York, New York 10031 Attention: M. Kolodney R. A. Graff	1 1
(21)	Curtiss-Wright Corporation Metals Processing Division 760 Northland Avenue Buffalo, New York 14215 Attention: B. Triffleman	1
(22)	Denver Research Institute University Park Denver, Colorado 80210 Attention: Dwight G. Moore	1
(23)	Douglas Aircraft Company, Inc. Astropower Laboratory Santa Monica, California 90406 Attention: Dr. N. A. Tiner	1
(24)	Fansteel Metallurgical Corporation Number One Tantalum Place North Chicago, Illinois 60064 Attention: Dr. D. K. Priest L. M. Raring	1 1
(25)	Materials Development Department Turbine Operations Ford Motor Company 20000 Rotunda Drive P. O. Box 2053 Dearborn, Michigan 48123 Attention: J. A. Petrusha (RM. E-1166)	1

	Addressee	Number of Copies
(26)	General Dynamics Corporation General Dynamics/Convair P. O. Box 1950 San Diego, California 92112 Attention: Dr. J. Kerr	1
(27)	General Electric Company Advanced Technology Laboratories Schenectady, New York 12305	1
(28)	Ganeral Electric Company Lamp Metals & Components Department Cleveland, Ohio 44117 Attention: A. Hegedus	1
(29)	General Electric Company Materials Development Lab. Oper. Advanced Engine & Technology Dept. Cincinnati, Ohio 45215 Attention: L. P. Jahnke W. Chang D. Levine M. Levinstein	1 1 1 1
(30)	General Technologies Corporation 708 North West Street Alexandria, Virginia 22314 Attention: James C. Withers	1
(31)	Howmet Corporation Misco Divisinn One Misco Drive Whitehall, Michigan 49461 Attention: S. Wolosin	1
(32)	Hughes Research Laboratories 3011 Malibu Canyon Road Malibu, California 90265 Attention: Rodger Turk	1
(33)	IIT Research Institute Technology Center Chicago, Illinois 60616 Attention: V. Hill	1
(34)	International Nickel Company Paul D. Merica Research Laboratory Sterling Forest Suffern, New York 10901 Attention: Dr. F. Decker	1

	Addressee	Number of Copies
(35)	Lockheed Missiles & Space Division Dept. 52-30 Palo Alto, California 94304 Attention: R. A. Perkins	1
(36)	Massachusetts Institute of Technology Department of Metallurgy, RM. 8-305 77 Massachusetts Avenue Cambridge, Massachusetts 02138 Attention: Prof. N. J. Grant	1
(37)	McDonnell Aircraft Corporation Lambert-St. Louis Municipal Airport St. Louis, Missouri 63166	1
(38)	Narmco Research & Development Division Whittaker Corporation 3540 Aero Court San Diego, California 92123 Attention: Dr. F. J. Riel, Technical Director	1
(39)	North American Aviation, Inc. Rocketdyne Division 6633 Canoga Avenue Canoga Park, California 91303 Attention: Dr. S. D. Brown	1
(40)	North Star Research & Development Institute 3100 - 38th Avenue, South Minneapolis, Minnesota 55406 Attention: M. Browning	1
(41)	Ohio State University Columbus, Ohio 43210 Attention: Prof. M. G. Fontana Chairman, Dept. of Metallurgical Engineering	1
(42)	Pratt & Whitney Aircraft Division United Aircraft Corporation 400 Main Street East Hartford, Connecticut 06108 Attention: E. F. Bradley F. Talboom/G. Andreini	1 1
(43)	Solar, A Division of International Harvester 2200 Pacific Highway San Diego, California 92112 Attention: A. R. Stetson J. V. Long	1 1
(44)	Sylvania Electric Products Sylcor Division Cantiague Road Hicksville, Long Island, New York 11802 Attention: L. Sama	1

	Addressee	Number of Copies
(45)	Texas Instruments P. O. Box 5303 Dallas, Texas 75222 Attention: Materials R & D Lab	1
(46)	TRW Inc. TRW Electromechanical Division 23555 Euclid Avenue Cleveland, Ohio 44117 Attention: J. Gadd Dr. R. Quigg	1 1
(47)	Union Carbide Corporation Stellite Division P. O. Box 746 Kokomo, Indiana 46901 Attention: Reference Librarian	1
(48)	Universal-Cyclops Steel Corporation Bridgeville, Pennsylvania 15017 Attention: C. P. Mueller	1
(49)	University of California at Los Angeles Los Angeles, California 90024 Attention: Dr. G. Hoffman	1
(50)	University of Dayton Research Institute 300 College Park Avenue Dayton, Ohio 45409 Attention: John Wurst	1
(51)	University of Pittsburgh Metallurgical Department Pittsburgh, Pennsylvania 14213 Attention: Dr. G. R. Fitterer	1
(52)	University of Washington Ceramics Department Seattle, Washington 98101 Attention: Dr. J. Mueller	1
(53)	Vitro Laboratories 200 Pleasant Valley Way West Orange, New Jersey 07052 Attention: M. Ortner	1
(54)	Westinghouse Electric Corporation Research Laboratories Pittsburgh, Pennsylvania 15235 Attention: R. Grekila	1

	Addressee	Number of Copies
(55)	Whitfield Laboratories P. O. Box 287 Bethel, Connecticut 06801	1
(56)	U. S. Atomic Energy Commission Washington, D.C. 20545 Attention: William C. Gough	1
(57)	Headquarters, USAF Air Force Office of Scientific Research Propulsion Research Division Washington, D.C. 20025 Attention: Dr. M. Slawsky	1
(58)	Defense Documentation Center (DDC) Cameron Station 5010 Duke Street Alexandria, Virginia 22314	1
(59)	AFML Wright-Patterson AFB, Ohio 45433 Attention: N. Geyer (MAMP) Dr. A. M. Lovelace, Director (MAG) E. Beardslee (MAAE) R. O. Hughes (MAAM)	1 1 1 1
(60)	Department of the Navy ONR Code 429 Washington, D.C. 20025 Attention: Dr. R. Roberts	1
(61)	Chief, Bureau of Naval Weapons Department of the Navy Washington, D.C. 20025 Attention: RRMA-2	1
(62)	NASA-Langley Research Center Langley Station Hampton, Virginia 23365 Attention: Technical Library E. E. Mathauser Irvin Miller, M.S. 214	1 1 1
(63)	NASA-Manned Spacecraft Center Structures & Mechanics Division 2101 Webster-Seabrook Road Houston, Texas 77058 Attention: Branch Chief (ES441)	1
(64)	Union Carbide Technical Center 12900 Snow Road P. O. Box 6116 Cleveland, Ohio 44101 Attention: Library	1